

Guide for the Design and Construction of Concrete Reinforced with FRP Bars

Reported by ACI Committee 440

*ACI encourages the development and appropriate use of new and emerging technologies through the publication of the **Emerging Technology Series**. This series presents information and recommendations based on available test data, technical reports, limited experience with field applications, and the opinions of committee members. The presented information and recommendations, and their basis, may be less fully developed and tested than those for more mature technologies. This report identifies areas in which information is believed to be less fully developed, and describes research needs. The professional using this document should understand the limitations of this document and exercise judgment as to the appropriate application of this emerging technology.*

	Sami H. Rizkalla Chair	John P. Busel Secretary	
Charles E. Bakis	Duane J. Gee	Damian I. Kachlakev	Max L. Porter
P. N. Balaguru	Russell T. Gentry	Vistasp M. Karbhari	Morris Schupack
Craig A. Ballinger	Arie Gerritse	Howard S. Kliger	David W. Scott
Lawrence C. Bank	Karl Gillette	James G. Korff	Rajan Sen
Abdeldjelil Belarbi	William J. Gold	Michael W. Lee	Mohsen A. Shahawy
Brahim Benmokrane	Charles H. Goodspeed, III	Ibrahim Mahfouz	Carol K. Shield
Gregg J. Blaszak	Nabil F. Grace	Henry N. Marsh, Jr.	Khaled A. Soudki
Gordon L. Brown, Jr.	Mark F. Green	Orange S. Marshall	Luc R. Taerwe
Vicki L. Brown	Mark E. Greenwood	Amir Mirmiran	Jay Thomas
Thomas I. Campbell	Doug D. Gremel	Steve Morton	Houssam A. Toutanji
Charles W. Dolan	Michael S. Guglielmo	Ayman S. Mosallam	Taketo Uomoto
Dat Duthinh	Issam E. Harik	Antoine E. Naaman	Miroslav Vadovic
Rami M. El Hassan	Mark P. Henderson	Antonio Nanni*	Milan Vatovec
Salem S. Faza*	Bohdan N. Horeczko	Kenneth Neale	Stephanie L. Walkup
Edward R. Fyfe	Srinivasa L. Iyer	Edward F. O'Neil, III	David White
David M. Gale			

*Co-Chairs of Subcommittee that prepared this document.
Note: The committee acknowledges the contribution of associate member Tarek Alkhrdaji.

Fiber-reinforced polymer (FRP) materials have emerged as a practical alternative material for producing reinforcing bars for concrete structures. FRP reinforcing bars offer advantages over steel reinforcement in that FRP bars are noncorrosive, and some FRP bars are nonconductive. Due to other differences in the physical and mechanical behavior of FRP materials versus steel, unique guidance on the engineering and construction of concrete structures reinforced with FRP bars is needed. Several countries, such as Japan and Canada, have already established design and construction guidelines specifically for the use of FRP bars as concrete reinforcement. This document

offers general information on the history and use of FRP reinforcement, a description of the unique material properties of FRP, and committee recommendations on the engineering and construction of concrete reinforced with FRP bars. The proposed guidelines are based on the knowledge gained from worldwide experimental research, analytical work, and field applications of FRP reinforcement.

Keywords: aramid fibers; carbon fibers; concrete; development length; fiber-reinforced polymers; flexure; glass fibers; moment; reinforced concrete; reinforcement; shear; slab; strength.

ACI Committee Reports, Guides, Standard Practices, and Commentaries are intended for guidance in planning, designing, executing, and inspecting construction. This document is intended for the use of individuals who are competent to evaluate the significance and limitations of its content and recommendations and who will accept responsibility for the application of the material it contains. The American Concrete Institute disclaims any and all responsibility for the stated principles. The Institute shall not be liable for any loss or damage arising therefrom.

Reference to this document shall not be made in contract documents. If items found in this document are desired by the Architect/Engineer to be a part of the contract documents, they shall be restated in mandatory language for incorporation by the Architect/Engineer.

CONTENTS

PART 1—GENERAL, p. 440.1R-2 **Chapter 1—Introduction, p. 440.1R-2**

- 1.1—Scope
- 1.2—Definitions

ACI 440.1R-03 supersedes ACI 440.1R-01 and became effective March 27, 2003.
Copyright © 2003, American Concrete Institute.

All rights reserved including rights of reproduction and use in any form or by any means, including the making of copies by any photo process, or by electronic or mechanical device, printed, written, or oral, or recording for sound or visual reproduction or for use in any knowledge or retrieval system or device, unless permission in writing is obtained from the copyright proprietors.

- 1.3—Notation
- 1.4—Applications and use

Chapter 2—Background information, p. 440.1R-6

- 2.1—Historical development
- 2.2—Commercially available FRP reinforcing bars
- 2.3—History of use

PART 2—FRP BAR MATERIALS, p. 440.1R-8

Chapter 3—Material characteristics, p. 440.1R-8

- 3.1—Physical properties
- 3.2—Mechanical properties and behavior
- 3.3—Time-dependent behavior

Chapter 4—Durability, p. 440.1R-12

PART 3—RECOMMENDED MATERIALS REQUIREMENTS AND CONSTRUCTION PRACTICES, p. 440.1R-13

Chapter 5—Material requirements and testing, p. 440.1R-13

- 5.1—Strength and modulus grades of FRP bars
- 5.2—Surface geometry
- 5.3—Bar sizes
- 5.4—Bar identification
- 5.5—Straight bars
- 5.6—Bent bars

Chapter 6—Construction practices, p. 440.1R-15

- 6.1—Handling and storage of materials
- 6.2—Placement and assembly of materials
- 6.3—Quality control and inspection

PART 4—DESIGN RECOMMENDATIONS, p. 440.1R-16

Chapter 7—General design considerations, p. 440.1R-16

- 7.1—Design philosophy
- 7.2—Design material properties

Chapter 8—Flexure, p. 440.1R-17

- 8.1—General considerations
- 8.2—Flexural strength
- 8.3—Serviceability
- 8.4—Creep rupture and fatigue

Chapter 9—Shear, p. 440.1R-23

- 9.1—General considerations
- 9.2—Shear strength of FRP-reinforced members
- 9.3—Detailing of shear stirrups

Chapter 10—Temperature and shrinkage reinforcement, p. 440.1R-25

Chapter 11—Development and splices of reinforcement, p. 440.1R-25

- 11.1—Development length of a straight bar
- 11.2—Development length of a bent bar
- 11.3—Tension lap splice

Chapter 12—Slabs on ground, p. 440.1R-28

- 12.1—Design of plain concrete slabs
- 12.2—Design of slabs with shrinkage and temperature reinforcement

Chapter 13—References, p. 440.1R-28

- 13.1—Referenced standards and reports
- 13.2—Cited references

PART 5—DESIGN EXAMPLES, p. 440.1R-35

Appendix A—Test method for tensile strength and modulus of FRP bars, p. 440.1R-40

Appendix B—Areas of future research, p. 440.1R-42

PART 1—GENERAL

CHAPTER 1—INTRODUCTION

Conventional concrete structures are reinforced with nonprestressed and prestressed steel. The steel is initially protected against corrosion by the alkalinity of the concrete, usually resulting in durable and serviceable construction. For many structures subjected to aggressive environments, such as marine structures and bridges and parking garages exposed to deicing salts, combinations of moisture, temperature, and chlorides reduce the alkalinity of the concrete and result in the corrosion of reinforcing and prestressing steel. The corrosion process ultimately causes concrete deterioration and loss of serviceability. To address corrosion problems, professionals have turned to alternative metallic reinforcement, such as epoxy-coated steel bars. While effective in some situations, such remedies may still be unable to completely eliminate the problems of steel corrosion (Keesler and Powers 1988).

Recently, composite materials made of fibers embedded in a polymeric resin, also known as fiber-reinforced polymers (FRP), have become an alternative to steel reinforcement for concrete structures. Because FRP materials are nonmagnetic and noncorrosive, the problems of electromagnetic interference and steel corrosion can be avoided with FRP reinforcement. Additionally, FRP materials exhibit several properties, such as high tensile strength, that make them suitable for use as structural reinforcement (Iyer and Sen 1991; JSCE 1992; Neale and Labossiere 1992; White 1992; Nanni 1993a; Nanni and Dolan 1993; Taerwe 1995; ACI Committee 440; El-Badry 1996; JSCE 1997a; Benmokrane and Rahman 1998; Saadatmanesh and Ehsani 1998; Dolan, Rizkalla, and Nanni 1999).

The mechanical behavior of FRP reinforcement differs from the behavior of steel reinforcement. Therefore, changes in the design philosophy of concrete structures using FRP reinforcement are needed. FRP materials are anisotropic and are characterized by high tensile strength only in the direction of the reinforcing fibers. This anisotropic behavior affects the shear strength and dowel action of FRP bars, as well as the bond performance of FRP bars to concrete. Furthermore, FRP materials do not exhibit yielding; rather, they are elastic until failure. Design procedures should account for a lack of ductility in concrete reinforced with FRP bars.

Several countries, such as Japan (JSCE 1997b) and Canada (Canadian Standards Association 1996), have established design procedures specifically for the use of FRP reinforcement for concrete structures. In North America, the analytical and experimental phases are sufficiently complete, and efforts are being made to establish recommendations for design with FRP reinforcement.

1.1—Scope

This document provides recommendations for the design and construction of FRP reinforced concrete structures as an emerging technology. The document only addresses nonprestressed FRP reinforcement. The basis for this document is the knowledge gained from worldwide experimental research, analytical work, and field applications of FRP reinforcement. The recommendations in this document are intended to be conservative. Areas where further research is needed are highlighted in this document and compiled in Appendix B.

Design recommendations are based on the current knowledge and intended to supplement existing codes and guidelines for reinforced concrete structures and provide engineers and building officials with assistance in the specification, design, and construction of concrete reinforced with FRP bars.

In North America, comprehensive test methods and material specifications to support design and construction guidelines have not yet been approved by the organizations of competence. As an example, Appendix A reports a proposed test method for the case of tensile characterization of FRP bars. The users of this guide are therefore directed to test methods proposed in other countries (JSCE 1997b) or procedures used by researchers as reported/cited in the literature (ACI 440R; Iyer and Sen 1991; JSCE 1992; Neale and Labossiere 1992; White 1992; Nanni 1993a; Nanni and Dolan 1993; Taerwe 1995; El-Badry 1996; JSCE 1997a; Benmokrane and Rahman 1998; and Saadatmanesh and Ehsani 1998; Dolan, Rizkalla, and Nanni 1999).

Guidance on the use of FRP reinforcement in combination with steel reinforcement is not given in this document.

1.2—Definitions

The following definitions clarify terms pertaining to FRP that are not commonly used in reinforced concrete practice.

-A-

AFRP—Aramid-fiber-reinforced polymer.

Aging—The process of exposing materials to an environment for an interval of time.

Alkalinity — The condition of having or containing hydroxyl (OH⁻) ions; containing alkaline substances. In concrete, the alkaline environment has a pH above 12.

-B-

Balanced FRP reinforcement ratio—The reinforcement ratio in a flexural member that causes the ultimate strain of FRP bars and the ultimate compressive strain of concrete (assumed to be 0.003) to be simultaneously attained.

Bar, FRP—A composite material formed into a long, slender structural shape suitable for the internal reinforcement of concrete and consisting of primarily longitudinal unidirectional fibers bound and shaped by a rigid polymer resin material. The bar may have a cross section of variable shape (commonly circular or rectangular) and may have a deformed or roughened surface to enhance bonding with concrete.

Braiding—A process whereby two or more systems of yarns are intertwined in the bias direction to form an integrated structure. Braided material differs from woven and knitted fabrics in the method of yarn introduction into the fabric and the manner by which the yarns are interlaced.

-C-

CFRP—Carbon-fiber-reinforced polymer.

Composite—A combination of one or more materials differing in form or composition on a macroscale. Note: The constituents retain their identities; that is, they do not dissolve or merge completely into one another, although they act in concert. Normally, the components can be physically identified and exhibit an interface between one another.

Cross-link—A chemical bond between polymer molecules. Note: An increased number of cross-links per polymer molecule increases strength and modulus at the expense of ductility.

Curing of FRP bars—A process that irreversibly changes the properties of a thermosetting resin by chemical reaction, such as condensation, ring closure, or addition. Note: Curing can be accomplished by the adding of cross-linking (curing) agents with or without heat and pressure.

-D-

Deformability factor—The ratio of energy absorption (area under the moment-curvature curve) at ultimate strength of the section to the energy absorption at service level.

Degradation—A decline in the quality of the mechanical properties of a material.

-E-

E-glass—A family of glass with a calcium alumina borosilicate composition and a maximum alkali content of 2.0%. A general-purpose fiber that is used in reinforced polymers.

Endurance limit—The number of cycles of deformation or load required to bring about failure of a material, test specimen, or structural member.

-F-

Fatigue strength—The greatest stress that can be sustained for a given number of load cycles without failure.

Fiber—Any fine thread-like natural or synthetic object of mineral or organic origin. Note: This term is generally used for materials whose length is at least 100 times its diameter.

Fiber, aramid—Highly oriented organic fiber derived from polyamide incorporating into an aromatic ring structure.

Fiber, carbon—Fiber produced by heating organic precursor materials containing a substantial amount of carbon,

such as rayon, polyacrylonitrile (PAN), or pitch in an inert environment.

Fiber, glass—Fiber drawn from an inorganic product of fusion that has cooled without crystallizing.

Fiber content—The amount of fiber present in a composite. Note: This usually is expressed as a percentage volume fraction or weight fraction of the composite.

Fiber-reinforced polymer (FRP)—Composite material consisting of continuous fibers impregnated with a fiber-binding polymer then molded and hardened in the intended shape.

Fiber volume fraction—The ratio of the volume of fibers to the volume of the composite.

Fiber weight fraction—The ratio of the weight of fibers to the weight of the composite.

-G-

GFRP—Glass-fiber-reinforced polymer.

Grid—A two-dimensional (planar) or three-dimensional (spatial) rigid array of interconnected FRP bars that form a contiguous lattice that can be used to reinforce concrete. The lattice can be manufactured with integrally connected bars or made of mechanically connected individual bars.

-H-

Hybrid—A combination of two or more different fibers, such as carbon and glass or carbon and aramid, into a structure.

-I-

Impregnate—In fiber-reinforced polymers, to saturate the fibers with resin.

-M-

Matrix—In the case of fiber-reinforced polymers, the materials that serve to bind the fibers together, transfer load to the fibers, and protect them against environmental attack and damage due to handling.

-P-

Pitch—A black residue from the distillation of petroleum.

Polymer—A high molecular weight organic compound, natural or synthetic, containing repeating units.

Precursor—The rayon, PAN, or pitch fibers from which carbon fibers are derived.

Pultrusion—A continuous process for manufacturing composites that have a uniform cross-sectional shape. The process consists of pulling a fiber-reinforcing material through a resin impregnation bath then through a shaping die where the resin is subsequently cured.

-R-

Resin—Polymeric material that is rigid or semirigid at room temperature, usually with a melting point or glass transition temperature above room temperature.

-S-

Stress concentration—The magnification of the local stresses in the region of a bend, notch, void, hole, or inclusion, in comparison to the stresses predicted by the ordinary formulas of mechanics without consideration of such irregularities.

Sustained stress—stress caused by unfactored sustained loads including dead loads and the sustained portion of the live load.

-T-

Thermoplastic—Resin that is not cross-linked; it generally can be remelted and recycled.

Thermoset—Resin that is formed by cross-linking polymer chains. Note: A thermoset cannot be melted and recycled, because the polymer chains form a three-dimensional network.

-V-

Vinyl esters—A class of thermosetting resins containing ester of acrylic, methacrylic acids, or both, many of which have been made from epoxy resin.

-W-

Weaving—A multidirectional arrangement of fibers. For example, polar weaves have reinforcement yarns in the circumferential, radial, and axial (longitudinal) directions; orthogonal weaves have reinforcement yarns arranged in the orthogonal (Cartesian) geometry, with all yarns intersecting at 90 degrees.

1.3—Notation

a	=	depth of equivalent rectangular stress block, in.
A	=	the effective tension area of concrete, defined as the area of concrete having the same centroid as that of tensile reinforcement, divided by the number of bars, in. ²
A_f	=	area of FRP reinforcement, in. ²
$A_{f,bar}$	=	area of one FRP bar, in. ²
$A_{f,min}$	=	minimum area of FRP reinforcement needed to prevent failure of flexural members upon cracking, in. ²
A_{fv}	=	amount of FRP shear reinforcement within spacing s , in. ²
$A_{fv,min}$	=	minimum amount of FRP shear reinforcement within spacing s , in. ²
$A_{f,sh}$	=	area of shrinkage and temperature FRP reinforcement per linear foot, in. ²
A_s	=	area of tension steel reinforcement, in. ²
b	=	width of rectangular cross section, in.
b_f	=	width of the flange, in.
b_w	=	width of the web, in.
c	=	distance from extreme compression fiber to the neutral axis, in.
	=	clear concrete cover, in.
c_b	=	distance from extreme compression fiber to neutral axis at balanced strain condition, in.
C_E	=	environmental reduction factor for various fiber type and exposure conditions, given in Table 7.1
d	=	distance from extreme compression fiber to centroid of tension reinforcement, in.
d_b	=	diameter of reinforcing bar, in.
d_c	=	thickness of the concrete cover measured from extreme tension fiber to center of bar or wire location closest thereto, in.
E_c	=	modulus of elasticity of concrete, psi
E_f	=	guaranteed modulus of elasticity of FRP

	defined as the mean modulus of a sample of test specimens ($E_f = E_{f,ave}$), psi	V_n	= nominal shear strength at section
E_s	= modulus of elasticity of steel, psi	V_s	= shear resistance provided by steel stirrups
f_c	= compressive stress in concrete, psi	V_f	= shear resistance provided by FRP stirrups
f'_c	= specified compressive strength of concrete, psi	V_u	= factored shear force at section
$\sqrt{f'_c}$	= square root of specified compressive strength of concrete, psi	w	= crack width, mils ($\times 10^{-3}$ in.)
f_f	= stress in the FRP reinforcement in tension, psi	α	= angle of inclination of stirrups or spirals (Chapter 9), and slope of the load-displacement curve of FRP bar between 20% and 60% of the ultimate tensile capacity (Appendix A), lb/in.
f_{fb}	= strength of a bent portion of FRP bar, psi	α_1	= ratio of the average stress of the equivalent rectangular stress block to f'_c
$f_{f,s}$	= stress level induced in the FRP by sustained loads, psi	α_b	= bond dependent coefficient used in calculating deflection, taken as 0.5 (Chapter 8)
f^*_{fu}	= guaranteed tensile strength of an FRP bar, defined as the mean tensile strength of a sample of test specimens minus three times the standard deviation ($f^*_{fu} = f_{fu,ave} - 3\sigma$), psi	α_L	= longitudinal coefficient of thermal expansion, 1/F
f_{fu}	= design tensile strength of FRP, considering reductions for service environment, psi	α_T	= transverse coefficient of thermal expansion, 1/F
f_{fv}	= tensile strength of FRP for shear design, taken as the smallest of the design tensile strength f_{fu} , the strength of the bent portion of the FRP stirrups f_{fb} , or the stress corresponding to 0.002 E_f , psi	β	= ratio of the distance from the neutral axis to extreme tension fiber to the distance from the neutral axis to the center of the tensile reinforcement (Section 8.3.1)
f_r	= rupture strength of concrete	β_d	= reduction coefficient used in calculating deflection (Section 8.3.2)
$f_{u,ave}$	= mean tensile strength of a sample of test specimens, psi	β_1	= factor taken as 0.85 for concrete strength f_c up to and including 4000 psi. For strength above 4000 psi, this factor is reduced continuously at a rate of 0.05 per each 1000 psi of strength in excess of 4000 psi, but is not taken less than 0.65
f_y	= specified yield stress of nonprestressed steel reinforcement, psi	$\Delta_{(cp+sh)}$	= additional deflection due to creep and shrinkage under sustained loads, in.
h	= overall height of a flexural member, in.	Δ_i	= immediate deflection, in.
I	= moment of inertia, in. ⁴	$(\Delta_i)_d$	= immediate deflection due to dead load, in.
I_{cr}	= moment of inertia of transformed cracked section, in. ⁴	$(\Delta_i)_{d+l}$	= immediate deflection due to dead plus live loads, in.
I_e	= effective moment of inertia, in. ⁴	$(\Delta_i)_l$	= immediate deflection due to live load, in.
I_g	= gross moment of inertia, in. ⁴	$(\Delta_i)_{sus}$	= immediate deflection due to sustained loads, in.
k	= ratio of the depth of the neutral axis to the reinforcement depth	ϵ_c	= strain in concrete
k_b	= bond-dependent coefficient	ϵ_{cu}	= ultimate strain in concrete
k_m	= modifier of basic development length	ϵ_f	= strain in FRP reinforcement
l	= span length of member, ft	ϵ^*_{fu}	= guaranteed rupture strain of FRP reinforcement defined as the mean tensile strain at failure of a sample of test specimens minus three times the standard deviation ($\epsilon^*_{fu} = \epsilon_{u,ave} - 3\sigma$), in./in.
L	= distance between joints in a slab on grade, ft	ϵ_{fu}	= design rupture strain of FRP reinforcement
l_a	= additional embedment length at support or at point of inflection, in.	ϵ_s	= strain in steel reinforcement
l_{bf}	= basic development length of an FRP bar, in.	$\epsilon_{u,ave}$	= mean tensile strength at rupture of a sample of test specimens
l_{df}	= development length of an FRP bar, in.	λ	= multiplier for additional long-term deflection
l_{dhf}	= development length of an FRP standard hook in tension, measured from critical section to the outside end of the hook, in.	μ	= coefficient of subgrade friction for calculation of shrinkage and temperature reinforcement
l_{bhf}	= basic development length of an FRP standard hook in tension, in.	μ_f	= average bond stress acting on the surface of FRP bar, ksi
l_{thf}	= length of tail beyond a hook in an FRP bar, in.	ξ	= time-dependent factor for sustained load
M_a	= maximum moment in a member at a stage deflection is computed, lb-in.	ρ'	= ratio of steel compression reinforcement, $\rho' = A'_s/bd$
M_{cr}	= cracking moment, lb-in.	ρ_f	= FRP reinforcement ratio
M_n	= nominal moment capacity, lb-in.	ρ_{fb}	= FRP reinforcement ratio producing balanced strain conditions
M_s	= moment due to sustained load, lb-in.	$\rho_{f,t,s}$	= reinforcement ratio for temperature and shrinkage FRP reinforcement
M_u	= factored moment at section, lb-in.	ρ_b	= steel reinforcement ratio producing balanced strain conditions
n_f	= ratio of the modulus of elasticity of FRP bars to the modulus of elasticity of concrete	ρ_s	= steel reinforcement ratio
r_b	= internal radius of bend in FRP reinforcement, in.	$\rho_{s,max}$	= maximum steel reinforcement ratio
s	= stirrup spacing or pitch of continuous spirals, in.	σ	= standard deviation
T_g	= glass transition temperature, F		
V_c	= nominal shear strength provided by concrete with steel flexural reinforcement		
V_{cf}	= nominal shear strength provided by concrete with FRP flexural reinforcement		

Table 1.1—Advantages and disadvantages of FRP reinforcement

Advantages of FRP reinforcement	Disadvantages of FRP reinforcement
High longitudinal strength (varies with sign and direction of loading relative to fibers)	No yielding before brittle rupture
Corrosion resistance (not dependent on a coating)	Low transverse strength (varies with sign and direction of loading relative to fibers)
Nonmagnetic	Low modulus of elasticity (varies with type of reinforcing fiber)
High fatigue endurance (varies with type of reinforcing fiber)	Susceptibility of damage to polymeric resins and fibers under ultraviolet radiation exposure
Lightweight (about 1/5 to 1/4 the density of steel)	Durability of glass fibers in a moist environment
Low thermal and electric conductivity (for glass and aramid fibers)	Durability of some glass and aramid fibers in an alkaline environment
—	High coefficient of thermal expansion perpendicular to the fibers, relative to concrete
—	May be susceptible to fire depending on matrix type and concrete cover thickness

1.4—Applications and use

The material characteristics of FRP reinforcement need to be considered when determining whether FRP reinforcement is suitable or necessary in a particular structure. The material characteristics are described in detail in [Chapter 3](#); [Table 1.1](#) lists some of the advantages and disadvantages of FRP reinforcement for concrete structures.

The corrosion-resistant nature of FRP reinforcement is a significant benefit for structures in highly corrosive environments such as seawalls and other marine structures, bridge decks and superstructures exposed to deicing salts, and pavements treated with deicing salts. In structures supporting magnetic resonance imaging (MRI) units or other equipment sensitive to electromagnetic fields, the nonmagnetic properties of FRP reinforcement are significantly beneficial. Because FRP reinforcement has a nonductile behavior, the use of FRP reinforcement should be limited to structures that will significantly benefit from other properties such as the noncorrosive or nonconductive behavior of its materials. Due to lack of experience in its use, FRP reinforcement is not recommended for moment frames or zones where moment redistribution is required.

FRP reinforcement should not be relied upon to resist compression. Available data indicate that the compressive modulus of FRP bars is lower than its tensile modulus (see discussion in [Section 3.2.2](#)). Due to the combined effect of this behavior and the relatively lower modulus of FRP compared to steel, the maximum contribution of compression FRP reinforcement calculated at crushing of concrete (typically at $\epsilon_{cu} = 0.003$) is small. Therefore, FRP reinforcement should not be used as reinforcement in columns or other compression members, nor should it be used as compression reinforcement in flexural members. It is acceptable for FRP tension reinforcement to experience compression due to moment reversals or changes in load pattern. The compressive strength of the FRP reinforcement should, however, be neglected. Further research is needed in this area.

CHAPTER 2—BACKGROUND INFORMATION

2.1—Historical development

The development of FRP reinforcement can be traced to the expanded use of composites after World War II. The aerospace industry had long recognized the advantages of the high strength and lightweight of composite materials, and during the Cold War the advancements in the aerospace and defense industry increased the use of composites. Furthermore, the United States' rapidly expanding economy demanded inexpensive materials to meet consumer demands. Pultrusion offered a fast and economical method of forming constant profile parts, and pultruded composites were being used to make golf clubs and fishing poles. It was not until the 1960s, however, that these materials were seriously considered for use as reinforcement in concrete.

The expansion of the national highway systems in the 1950s increased the need to provide year-round maintenance. It became common to apply deicing salts on highway bridges. As a result, reinforcing steel in these structures and those subject to marine salt experienced extensive corrosion and thus became a major concern. Various solutions were investigated, including galvanized coatings, electro-static-spray fusion-bonded (powder resin) coatings, polymer-impregnated concrete, epoxy coatings, and glass FRP (GFRP) reinforcing bars (ACI 440R). Of these options, epoxy-coated steel reinforcement appeared to be the best solution and was implemented in aggressive corrosion environments. The FRP reinforcing bar was not considered a viable solution or commercially available until the late 1970s. In 1983, the first project funded by the United States Department of Transportation (USDOT) was on "Transfer of Composite Technology to Design and Construction of Bridges" (Plecnik and Ahmad 1988).

Marshall-Vega Inc. led the initial development of GFRP reinforcing bars in the United States. Initially, GFRP bars were considered a viable alternative to steel as reinforcement for polymer concrete due to the incompatibility of the coefficients of thermal expansion between polymer concrete and steel. In the late 1970s, International Grating Inc. entered the North American FRP reinforcement market. Marshall-Vega and International Grating led the research and development of FRP reinforcing bars into the 1980s.

The 1980s market demanded nonmetallic reinforcement for specific advanced technology. The largest demand for electrically nonconductive reinforcement was in facilities for MRI medical equipment. FRP reinforcement became the standard in this type of construction. Other uses began to develop as the advantages of FRP reinforcing became better known and desired, specifically in seawall construction, substation reactor bases, airport runways, and electronics laboratories (Brown and Bartholomew 1996).

During the 1990s, concern for the deterioration of aging bridges in the United States due to corrosion became more apparent (Boyle and Karbhari 1994). Additionally, detection of corrosion in the commonly used epoxy-coated reinforcing bars increased interest in alternative methods of avoiding corrosion. Once again, FRP reinforcement began to be considered as a general solution to address problems of

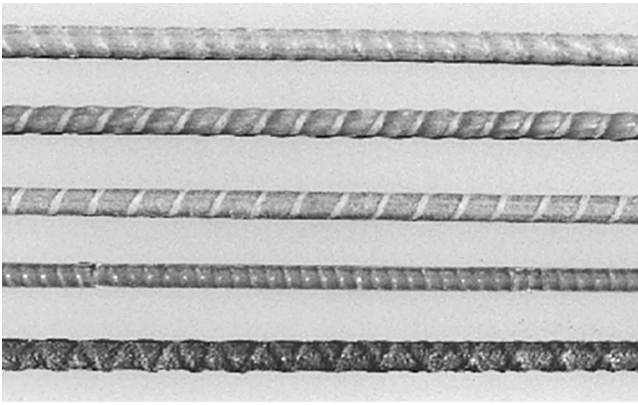


Fig. 1.1—Commercially available GFRP reinforcing bars.

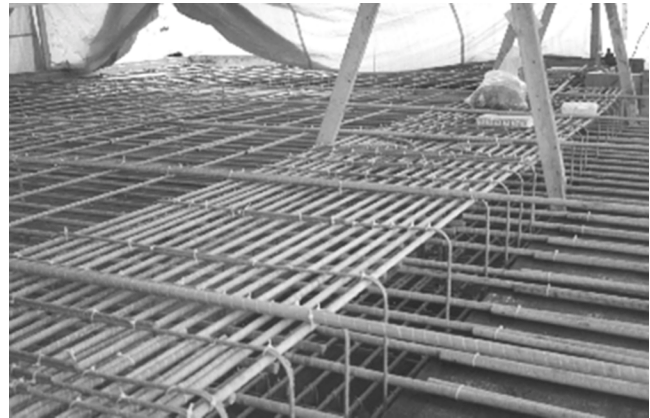


Fig. 1.3—GFRP bars used in a winery in British Columbia in 1998.



Fig. 1.2—GFRP bars installed during the construction of the Crowchild bridge deck in Calgary, Alberta, in 1997.



Fig. 1.4—FRP-reinforced deck constructed in Lima, Ohio (Pierce Street Bridge), in 1999.

corrosion in bridge decks and other structures (Benmokrane, Chaallal, and Masmoudi 1996).

2.2—Commercially available FRP reinforcing bars

Commercially available FRP reinforcing materials are made of continuous aramid (AFRP), carbon (CFRP), or glass (GFRP) fibers embedded in a resin matrix (ACI 440R). Typical FRP reinforcement products are grids, bars, fabrics, and ropes. The bars have various types of cross-sectional shapes (square, round, solid, and hollow) and deformation systems (exterior wound fibers, sand coatings, and separately formed deformations). A sample of five distinctly different GFRP reinforcing bars is shown in Fig. 1.1.

2.3—History of use

The Japanese have the most FRP reinforcement applications with more than 100 demonstration or commercial projects. FRP design provisions were included in the design and construction recommendations of the Japan Society of Civil Engineers (1997b).

The use of FRP reinforcement in Europe began in Germany with the construction of a prestressed FRP highway bridge in 1986 (Meier 1992). Since the construction of this bridge, programs have been implemented to increase the research and use of FRP reinforcement in Europe. The European BRITE/EURAM Project, “Fiber Composite Elements and Techniques as Nonmetallic Reinforcement,” conducted extensive testing and analysis of the FRP mate-

rials from 1991 to 1996 (Taerwe 1997). More recently, EUROCRETE has headed the European effort with research and demonstration projects.

Canadian civil engineers are continuing to develop provisions for FRP reinforcement in the Canadian Highway Bridge Design Code and have constructed a number of demonstration projects. The Headingley Bridge in Manitoba included both CFRP and GFRP reinforcement (Rizkalla 1997). Additionally, the Kent County Road No. 10 Bridge used CFRP grids to reinforce the negative moment regions (Tadros, Tromposch, and Mufti 1998). The Joffre Bridge, located over the St-François River in Sherbrooke, Quebec, included CFRP grids in its deck slab and GFRP reinforcing bars in the traffic barrier and sidewalk. The bridge, which was opened to traffic in December 1997, included fiber-optic sensors that were structurally integrated into the FRP reinforcement for remotely monitoring strains (Benmokrane, Tighiouart, and Chaallal 1996). Photographs of two applications (bridge and building) are shown in Fig. 1.2 and 1.3.

In the United States, typical uses of FRP reinforcement have been previously reported (ACI 440R). The photographs shown in Fig. 1.4 and 1.5 show recent applications in bridge deck construction.



Fig. 1.5—GFRP bars used in the redecking of Dayton, Ohio's Salem Avenue bridge in 1999.

Table 3.1—Typical densities of reinforcing bars, lb/ft³ (g/cm³)

Steel	GFRP	CFRP	AFRP
493.00 (7.90)	77.8 to 131.00 (1.25 to 2.10)	93.3 to 100.00 (1.50 to 1.60)	77.80 to 88.10 (1.25 to 1.40)

Table 3.2—Typical coefficients of thermal expansion for reinforcing bars*

Direction	CTE, $\times 10^{-6}/F$ ($\times 10^{-6}/C$)			
	Steel	GFRP	CFRP	AFRP
Longitudinal, α_L	6.5 (11.7)	3.3 to 5.6 (6.0 to 10.0)	-4.0 to 0.0 (-9.0 to 0.0)	-3.3 to -1.1 (-6 to -2)
Transverse, α_T	6.5 (11.7)	11.7 to 12.8 (21.0 to 23.0)	41 to 58 (74.0 to 104.0)	33.3 to 44.4 (60.0 to 80.0)

*Typical values for fiber volume fraction ranging from 0.5 to 0.7.

PART 2—FRP BAR MATERIALS

CHAPTER 3—MATERIAL CHARACTERISTICS

The physical and mechanical properties of FRP reinforcing bars are presented in this chapter to develop a fundamental understanding of the behavior of these bars and the properties that affect their use in concrete structures. Furthermore, the effects of factors, such as loading history and duration, temperature, and moisture, on the properties of FRP bars are discussed.

It is important to note that FRP bars are anisotropic in nature and can be manufactured using a variety of techniques such as pultrusion, braiding, and weaving (Bank 1993 and Bakis 1993). Factors such as fiber volume, type of fiber, type of resin, fiber orientation, dimensional effects, and quality control during manufacturing all play a major role in establishing the characteristics of an FRP bar. The material characteristics described in this chapter should be considered as generalizations and may not apply to all products commercially available.

Several agencies are developing consensus-based test methods for FRP reinforcement. Appendix A summarizes a tensile test method used by researchers. While this Appendix is not a detailed consensus document, it does provide insight into testing and reporting issues associated with FRP reinforcement.

3.1—Physical properties

3.1.1 Density—FRP bars have a density ranging from 77.8 to 131.3 lb/ft³ (1.25 to 2.1 g/cm³), one-sixth to one-fourth that of steel (Table 3.1). The reduced weight leads to lower transportation costs and may ease handling of the bars on the project site.

3.1.2 Coefficient of thermal expansion—The coefficients of thermal expansion of FRP bars vary in the longitudinal and transverse directions depending on the types of fiber, resin, and volume fraction of fiber. The longitudinal coefficient of thermal expansion is dominated by the properties of the fibers, while the transverse coefficient is dominated by the resin (Bank 1993). Table 3.2 lists the longitudinal and transverse coefficients of thermal expansion for typical FRP bars and steel bars. Note that a negative coefficient of thermal expansion indicates that the material contracts with increased temperature and expands with decreased temperature. For reference, concrete has a coefficient of thermal expansion that varies from 4×10^{-6} to $6 \times 10^{-6}/F$ (7.2×10^{-6} to $10.8 \times 10^{-6}/C$) and is usually assumed to be isotropic (Mindess and Young 1981).

3.1.3 Effects of high temperatures—The use of FRP reinforcement is not recommended for structures in which fire resistance is essential to maintain structural integrity. Because FRP reinforcement is embedded in concrete, the reinforcement cannot burn due to a lack of oxygen; however, the polymers will soften due to the excessive heat. The temperature at which a polymer will soften is known as the glass-transition temperature, T_g . Beyond the T_g , the elastic modulus of a polymer is significantly reduced due to changes in its molecular structure. The value of T_g depends on the type of resin but is normally in the region of 150 to 250 F (65 to 120 C). In a composite material, the fibers, which exhibit better thermal properties than the resin, can continue to support some load in the longitudinal direction; however, the tensile properties of the overall composite are reduced due to a reduction in force transfer between fibers through bond to the resin. Test results have indicated that temperatures of 480 F (250 C), much higher than the T_g , will reduce the tensile strength of GFRP and CFRP bars in excess of 20% (Kumahara, Masuda, and Tanano 1993). Other properties more directly affected by the shear transfer through the resin, such as shear and bending strength, are reduced significantly at temperatures above the T_g (Wang and Evans 1995).

For FRP reinforced concrete, the properties of the polymer at the surface of the bar are essential in maintaining bond between FRP and concrete. At a temperature close to its T_g , however, the mechanical properties of the polymer are significantly reduced, and the polymer is not able to transfer stresses from the concrete to the fibers. One study carried out with bars having a T_g of 140 to 255 F (60 to 124 C) reports a reduction in pullout (bond) strength of 20 to 40% at a temperature of approximately 210 F (100 C), and a reduction of 80 to 90% at a temperature of 390 F (200 C) (Katz, Berman, and Bank 1998 and 1999). In a study on flexural behavior of beams with partial pretensioning with AFRP tendons and reinforcement with either AFRP or CFRP bars, beams were subjected to elevated temperatures under a sustained load. Failure of the beams occurred when the

temperature of the reinforcement reached approximately 390 F (200 C) and 572 F (300 C) in the carbon and aramid bars, respectively (Okamoto et al. 1993). Another study involving FRP reinforced beams reported reinforcement tensile failures when the reinforcement reached temperatures of 480 to 660 F (250 to 350 C) (Sakashita et al. 1997).

Locally such behavior can result in increased crack widths and deflections. Structural collapse can be avoided if high temperatures are not experienced at the end regions of FRP bars allowing anchorage to be maintained. Structural collapse can occur if all anchorage is lost due to softening of the polymer or if the temperature rises above the temperature threshold of the fibers themselves. The latter can occur at temperatures near 1800 F (980 C) for glass fibers and 350 F (175 C) for aramid fibers. Carbon fibers are capable of resisting temperatures in excess of 3000 F (1600 C). The behavior and endurance of FRP reinforced concrete structures under exposure to fire and high heat is still not well understood and further research in this area is required. ACI 216R may be used for an estimation of temperatures at various depths of a concrete section. Further research is needed in this area.

3.2—Mechanical properties and behavior

3.2.1 Tensile behavior—When loaded in tension, FRP bars do not exhibit any plastic behavior (yielding) before rupture. The tensile behavior of FRP bars consisting of one type of fiber material is characterized by a linearly elastic stress-strain relationship until failure. The tensile properties of some commonly used FRP bars are summarized in **Table 3.3**.

The tensile strength and stiffness of an FRP bar are dependent on several factors. Because the fibers in an FRP bar are the main load-carrying constituent, the ratio of the volume of fiber to the overall volume of the FRP (fiber-volume fraction) significantly affects the tensile properties of an FRP bar. Strength and stiffness variations will occur in bars with various fiber-volume fractions, even in bars with the same diameter, appearance, and constituents. The rate of curing, the manufacturing process, and the manufacturing quality control also affect the mechanical characteristics of the bar (Wu 1990).

Unlike steel bars, some FRP bars exhibit a substantial effect of cross-sectional area on tensile strength. For example, GFRP bars from three different manufacturers show tensile strength reductions of up to 40% as the diameter increases proportionally from 0.375 to 0.875 in. (9.5 to 22.2 mm) (Faza and GangaRao 1993b). On the other hand, similar cross-section changes do not seem to affect the strength of twisted CFRP strands (Santoh 1993). The sensitivity of AFRP bars to cross-section size has been shown to vary from one commercial product to another. For example, in braided AFRP bars, there is a less than 2% strength reduction as bars increase in diameter from 0.28 to 0.58 in. (7.3 to 14.7 mm) (Tamura 1993). The strength reduction in a unidirectionally pultruded AFRP bar with added aramid fiber surface wraps is approximately 7% for diameters increasing from 0.12 to 0.32 in. (3 to 8 mm) (Noritake et al. 1993). The FRP bar manufacturer should be contacted for particular strength values of differently sized FRP bars.

Table 3.3—Usual tensile properties of reinforcing bars*

	Steel	GFRP	CFRP	AFRP
Nominal yield stress, ksi (MPa)	40 to 75 (276 to 517)	N/A	N/A	N/A
Tensile strength, ksi (MPa)	70 to 100 (483 to 690)	70 to 230 (483 to 1600)	87 to 535 (600 to 3690)	250 to 368 (1720 to 2540)
Elastic modulus, ×10 ³ ksi (GPa)	29.0 (200.0)	5.1 to 7.4 (35.0 to 51.0)	15.9 to 84.0 (120.0 to 580.0)	6.0 to 18.2 (41.0 to 125.0)
Yield strain, %	1.4 to 2.5	N/A	N/A	N/A
Rupture strain, %	6.0 to 12.0	1.2 to 3.1	0.5 to 1.7	1.9 to 4.4

*Typical values for fiber volume fractions ranging from 0.5 to 0.7.

Determination of FRP bar strength by testing is complicated because stress concentrations in and around anchorage points on the test specimen can lead to premature failure. An adequate testing grip should allow failure to occur in the middle of the test specimen. Proposed test methods for determining the tensile strength and stiffness of FRP bars are available in the literature, but are not yet established by any standards-producing organizations (see **Appendix A**).

The tensile properties of a particular FRP bar should be obtained from the bar manufacturer. Usually, a normal (Gaussian) distribution is assumed to represent the strength of a population of bar specimens; although, at this time additional research is needed to determine the most generally appropriate distribution for FRP bars. Manufacturers should report a guaranteed tensile strength, f_{fu}^* , defined by this guide as the mean tensile strength of a sample of test specimens minus three times the standard deviation ($f_{fu}^* = f_{u,ave} - 3\sigma$), and similarly report a guaranteed rupture strain, ϵ_{fu}^* ($\epsilon_{fu}^* = \epsilon_{u,ave} - 3\sigma$) and a specified tensile modulus, E_f ($E_f = E_{f,ave}$). These guaranteed values of strength and strain provide a 99.87% probability that the indicated values are exceeded by similar FRP bars, provided at least 25 specimens are tested (Dally and Riley 1991; Mutsuyoshi, Uehara, and Machida 1990). If less specimens are tested or a different distribution is used, texts and manuals on statistical analysis should be consulted to determine the confidence level of the distribution parameters (MIL-17 1999). In any case, the manufacturer should provide a description of the method used to obtain the reported tensile properties.

An FRP bar cannot be bent once it has been manufactured (an exception to this would be an FRP bar with a thermoplastic resin that could be reshaped with the addition of heat and pressure). FRP bars, however, can be fabricated with bends. In FRP bars produced with bends, a strength reduction of 40 to 50% compared to the tensile strength of a straight bar can occur in the bend portion due to fiber bending and stress concentrations (Nanni et al. 1998).

3.2.2 Compressive behavior—While it is not recommended to rely on FRP bars to resist compressive stresses, the following section is presented to characterize fully the behavior of FRP bars.

Tests on FRP bars with a length to diameter ratio from 1:1 to 2:1 have shown that the compressive strength is lower

than the tensile strength (Wu 1990). The mode of failure for FRP bars subjected to longitudinal compression can include transverse tensile failure, fiber microbuckling, or shear failure. The mode of failure depends on the type of fiber, the fiber-volume fraction, and the type of resin. Compressive strengths of 55, 78, and 20% of the tensile strength have been reported for GFRP, CFRP, and AFRP, respectively (Mallick 1988; Wu 1990). In general, compressive strengths are higher for bars with higher tensile strengths, except in the case of AFRP where the fibers exhibit nonlinear behavior in compression at a relatively low level of stress.

The compressive modulus of elasticity of FRP reinforcing bars appears to be smaller than its tensile modulus of elasticity. Test reports on samples containing 55 to 60% volume fraction of continuous E-glass fibers in a matrix of vinyl ester or isophthalic polyester resin indicate a compressive modulus of elasticity of 5000 to 7000 ksi (35 to 48 GPa) (Wu 1990). According to reports, the compressive modulus of elasticity is approximately 80% for GFRP, 85% for CFRP, and 100% for AFRP of the tensile modulus of elasticity for the same product (Mallick 1988; Ehsani 1993). The slightly lower values of modulus of elasticity in the reports may be attributed to the premature failure in the test resulting from end brooming and internal fiber microbuckling under compressive loading.

Standard test methods are not yet established to characterize the compressive behavior of FRP bars. If the compressive properties of a particular FRP bar are needed, these should be obtained from the bar manufacturer. The manufacturer should provide a description of the test method used to obtain the reported compression properties.

3.2.3 Shear behavior—Most FRP bar composites are relatively weak in interlaminar shear where layers of unreinforced resin lie between layers of fibers. Because there is usually no reinforcement across layers, the interlaminar shear strength is governed by the relatively weak polymer matrix. Orientation of the fibers in an off-axis direction across the layers of fiber will increase the shear resistance, depending upon the degree of offset. For FRP bars this can be accomplished by braiding or winding fibers transverse to the main fibers. Off-axis fibers can also be placed in the pultrusion process by introducing a continuous strand mat in the roving/mat creel. Standard test methods are not yet established to characterize the shear behavior of FRP bars. If the shear properties of a particular FRP bar are needed, these should be obtained from the bar manufacturer. The manufacturer should provide a description of the test method used to obtain the reported shear values.

3.2.4 Bond behavior—Bond performance of an FRP bar is dependent on the design, manufacturing process, mechanical properties of the bar itself, and the environmental conditions (Al-Dulaijan et al. 1996; Nanni et al. 1997; Bakis et al. 1998; Bank, Puterman, and Katz 1998; Freimanis et al. 1998). When anchoring a reinforcing bar in concrete, the bond force can be transferred by:

- Adhesion resistance of the interface, also known as chemical bond;
- Frictional resistance of the interface against slip; and

- Mechanical interlock due to irregularity of the interface.

In FRP bars, it is postulated that bond force is transferred through the resin to the reinforcement fibers, and a bond-shear failure in the resin is also possible. When a bonded deformed bar is subjected to increasing tension, the adhesion between the bar and the surrounding concrete breaks down, and deformations on the surface of the bar cause inclined contact forces between the bar and the surrounding concrete. The stress at the surface of the bar resulting from the force component in the direction of the bar can be considered the bond stress between the bar and the concrete. Unlike reinforcing steel, the bond of FRP rebars appears not to be significantly influenced by the concrete compressive strength provided adequate concrete cover exists to prevent longitudinal splitting (Nanni et al. 1995; Benmokrane, Tighiouart, and Chaallal 1996; Kachlakev and Lundy 1998).

The bond properties of FRP bars have been extensively investigated by numerous researchers through different types of tests, such as pullout tests, splice tests, and cantilever beams, to determine an empirical equation for embedment length (Faza and GangaRao 1990, Ehsani et al. 1996, Benmokrane 1997). The bond stress of a particular FRP bar should be based on test data provided by the manufacturer using standard test procedures that are still under development at this time.

With regard to bond characteristics of FRP bars, the designer is referred to the standard test methods cited in the literature. The designer should always consult with the bar manufacturer to obtain bond values.

3.3—Time-dependent behavior

3.3.1 Creep rupture—FRP reinforcing bars subjected to a constant load over time can suddenly fail after a time period called the endurance time. This phenomenon is known as creep rupture (or static fatigue). Creep rupture is not an issue with steel bars in reinforced concrete except in extremely high temperatures, such as those encountered in a fire. As the ratio of the sustained tensile stress to the short-term strength of the FRP bar increases, endurance time decreases. The creep rupture endurance time can also irreversibly decrease under sufficiently adverse environmental conditions such as high temperature, ultraviolet radiation exposure, high alkalinity, wet and dry cycles, or freezing-thawing cycles. Literature on the effects of such environments exists; although, the extraction of precise design laws is hindered by a lack of standard creep test methods and reporting, and the diversity of constituents and processes used to make proprietary FRP products. In addition, little data are currently available for endurance times beyond 100 h. Design conservatism is advised until more research has been done on this subject. Several representative examples of endurance times for bar and bar-like materials follow. No creep strain data are available in these cases.

In general, carbon fibers are the least susceptible to creep rupture, whereas aramid fibers are moderately susceptible, and glass fibers are the most susceptible. A comprehensive series of creep rupture tests was conducted on 0.25 in. (6 mm) diameter smooth FRP bars reinforced with glass, aramid, and carbon fibers (Yamaguchi et al. 1997). The bars were tested

at different load levels in room temperature, laboratory conditions using split conical anchors. Results indicated that a linear relationship exists between creep rupture strength and the logarithm of time for times up to nearly 100 h. The ratios of stress level at creep rupture to the initial strength of the GFRP, AFRP, and CFRP bars after 500,000 h (more than 50 years) were linearly extrapolated to be 0.29, 0.47, and 0.93, respectively.

In another extensive investigation, endurance times were determined for braided AFRP bars and twisted CFRP bars, both utilizing epoxy resin as the matrix material (Ando et al. 1997). These commercial bars were tested at room temperature in laboratory conditions and were anchored with an expansive cementitious grout inside of friction-type grips. Bar diameters ranged from 0.26 to 0.6 in. (5 to 15 mm) but were not found to affect the results. The percentage of stress at creep rupture versus the initial strength after 50 years calculated using a linear relationship extrapolated from data available to 100 h was found to be 79% for CFRP, and 66% for AFRP.

An investigation of creep rupture in GFRP bars in room temperature laboratory conditions was reported by Seki, Sekijima, and Konno (1997). The molded E-glass/vinyl ester bars had a small (0.0068 in.² [4.4 mm²]) rectangular cross-section and integral GFRP tabs. The percentage of initial tensile strength retained followed a linear relationship with logarithmic time, reaching a value of 55% at an extrapolated 50-year endurance time.

Creep rupture data characteristics of a 0.5 in. diameter (12.5 mm) commercial CFRP twisted strand in an indoor environment is available from the manufacturer (Tokyo Rope 2000). The rupture strength at a projected 100-year endurance time is reported to be 85% of the initial strength.

An extensive investigation of creep deformation (not rupture) in one commercial AFRP and two commercial CFRP bars tested to 3000 h has been reported (Saadatmanesh and Tannous 1999a,b). The bars were tested in laboratory air and in room-temperature solutions with a pH equal to 3 and 12. The bars had diameters between 0.313 to 0.375 in. (8 to 10 mm) and the applied stress was fixed at 40% of initial strength. The results indicated a slight trend towards higher creep strain in the larger-diameter bars and in the bars immersed in the acidic solution. Bars tested in air had the lowest creep strains of the three environments. Considering all environments and materials, the range of strains recorded after 3000 h was 0.002 to 0.037%. Creep strains were slightly higher in the AFRP bar than in the CFRP bars.

For experimental characterization of creep rupture, the designer can refer to the test method currently proposed by the committee of Japan Society of Civil Engineers (1997b), "Test Method on Tensile Creep-Rupture of Fiber Reinforced Materials, JSCE-E533-1995." Creep characteristics of FRP bars can also be determined from pullout test methods cited in the literature. Recommendations on sustained stress limits imposed to avoid creep rupture are provided in the design section of this guide.

3.3.2 Fatigue—A substantial amount of data for fatigue behavior and life prediction of stand-alone FRP materials

has been generated in the last 30 years (National Research Council 1991). During most of this time period, the focus of research investigations was on materials suitable for aerospace applications. Some general observations on the fatigue behavior of FRP materials can be made, even though the bulk of the data is obtained from FRP specimens intended for aerospace applications rather than construction. Unless stated otherwise, the cases that follow are based on flat, unidirectional coupons with approximately 60% fiber-volume fraction and subjected to tension-tension sinusoidal cyclic loading at:

- A frequency low enough not to cause self-heating;
- Ambient laboratory environments;
- A stress ratio (ratio of minimum applied stress to maximum applied stress) of 0.1; and
- A direction parallel to the principal fiber alignment.

Test conditions that raise the temperature and moisture content of FRP materials generally degrade the ambient environment fatigue behavior.

Of all types of current FRP composites for infrastructure applications, CFRP is generally thought to be the least prone to fatigue failure. On a plot of stress versus the logarithm of the number of cycles at failure (S-N curve), the average downward slope of CFRP data is usually about 5 to 8% of initial static strength per decade of logarithmic life. At 1 million cycles, the fatigue strength is generally between 50 and 70% of initial static strength and is relatively unaffected by realistic moisture and temperature exposures of concrete structures unless the resin or fiber/resin interface is substantially degraded by the environment. Some specific reports of data to 10 million cycles indicated a continued downward trend of 5 to 8% decade in the S-N curve (Curtis 1989).

Individual glass fibers, such as E-glass and S-glass, are generally not prone to fatigue failure. Individual glass fibers, however, have demonstrated delayed rupture caused by the stress corrosion induced by the growth of surface flaws in the presence of even minute quantities of moisture in ambient laboratory environment tests (Mandell and Meier 1983). When many glass fibers are embedded into a matrix to form an FRP composite, a cyclic tensile fatigue effect of approximately 10% loss in the initial static capacity per decade of logarithmic lifetime has been observed (Mandell 1982). This fatigue effect is thought to be due to fiber-fiber interactions and not dependent on the stress corrosion mechanism described for individual fibers. No clear fatigue limit can usually be defined. Environmental factors play an important role in the fatigue behavior of glass fibers due to their susceptibility to moisture, alkaline, and acidic solutions.

Aramid fibers, for which substantial durability data are available, appear to behave similarly to carbon and glass fibers in fatigue. Neglecting in this context the rather poor durability of all aramid fibers in compression, the tension-tension fatigue behavior of an impregnated aramid fiber bar is excellent. Strength degradation per decade of logarithmic lifetime is approximately 5 to 6% (Roylance and Roylance 1981). While no distinct endurance limit is known for AFRP, 2 million cycle fatigue strengths of commercial AFRP bars for concrete applications have been reported in the range of

54 to 73% of initial bar strengths (Odagiri, Matsumoto, and Nakai 1997). Based on these findings, Odagiri suggested that the maximum stress be set to 54 to 73% of the initial tensile strength. Because the slope of the applied stress versus logarithmic creep-rupture time of AFRP is similar to the slope of the stress versus logarithmic cyclic lifetime data, the individual fibers appear to fail by a strain-limited creep-rupture process. This failure condition in commercial AFRP bars was noted to be accelerated by exposure to moisture and elevated temperature (Roylance and Roylance 1981; Rostasy 1997).

The influence of moisture on the fatigue behavior of unidirectional FRP materials, while generally thought to be detrimental if the resin or fiber/matrix interface is degraded, is also inconclusive because the results depend on fiber and matrix types, preconditioning methods, solution content, and the environmental condition during fatigue (Hayes et al. 1998, Rahman, Adimi, and Crimi 1997). In addition, factors such as gripping and presence of concrete surrounding the bar during the fatigue test need to be considered.

Fatigue strength of CFRP bars encased in concrete has been observed to decrease when the environmental temperature increases from 68 to 104 F (20 to 40 C) (Adimi et al. 1998). In this same investigation, endurance limit was found to be inversely proportional to loading frequency. It was also found that higher cyclic loading frequencies in the 0.5 to 8 Hz range corresponded to higher bar temperatures due to sliding friction. Thus, endurance limit at 1 Hz could be more than 10 times higher than that at 5 Hz. In the cited investigation, a stress ratio (minimum stress divided by maximum stress) of 0.1 and a maximum stress of 50% of initial strength resulted in runouts of greater than 400,000 cycles when the loading frequency was 0.5 Hz. These runout specimens had no loss of residual tensile strength.

It has also been found with CFRP bars that the endurance limit depends also on the mean stress and the ratio of maximum-to-minimum cyclic stress. Higher mean stress or a lower stress ratio (minimum divided by maximum) will cause a reduction in the endurance limit (Rahman and Kingsley 1996; Saadatmanesh and Tannous 1999a).

Fatigue tests on unbonded GFRP dowel bars have shown that fatigue behavior similar to that of steel dowel bars can be achieved for cyclic transverse shear loading of up to 10 million cycles. The test results and the stiffness calculations have shown that an equivalent performance can be achieved between FRP and steel bars subjected to transverse shear by changing some of the parameters, such as diameter, spacing, or both (Porter et al. 1993; Hughes and Porter 1996).

The addition of ribs, wraps, and other types of deformations improve the bond behavior of FRP bars. Such deformations, however, has been shown to induce local stress concentrations that significantly affect the performance of a GFRP bar under fatigue loading situations (Katz 1998). Local stress concentrations degrade fatigue performance by imposing multiaxial stresses that serve to increase matrix-dominated damage mechanisms normally suppressed in fiber-dominated composite materials. Additional fiber-dominated damage mechanisms can be also activated near deformations, depending on the construction of the bar.

The effect of fatigue on the bond of deformed GFRP bars embedded in concrete has been investigated in detail using specialized bond tests (Sippel and Mayer 1996; Bakis et al. 1998, Katz 2000). Different GFRP materials, environments, and test methods were followed in each cited case, and the results indicated that bond strength can either increase, decrease, or remain the same following cyclic loading. Bond fatigue behavior has not been sufficiently investigated to date and conservative design criteria based on specific materials and experimental conditions are recommended.

Design limitations on fatigue stress ranges for FRP bars ultimately depend on the manufacturing process of the FRP bar, environmental conditions, and the type of fatigue load being applied. Given the ongoing development in the manufacturing process of FRP bars, conservative design criteria should be used for all commercially available FRP bars. Design criteria are given in [Section 8.4.2](#).

With regard to the fatigue characteristics of FRP bars, the designer is referred to the provisional standard test methods cited in the literature. The designer should always consult with the bar manufacturer for fatigue response properties.

CHAPTER 4—DURABILITY

FRP bars are susceptible to varying amounts of strength and stiffness changes in the presence of environments prior to, during, and after construction. These environments can include water, ultraviolet exposure, elevated temperature, alkaline or acidic solutions, and saline solutions. Strength and stiffness may increase, decrease, or remain the same, depending on the particular material and exposure conditions. Tensile and bond properties of FRP bars are the primary parameters of interest for reinforced concrete construction.

The environmental condition that has attracted the most interest by investigators concerned with FRP bars is the highly alkaline pore water found in outdoor concrete structures (Gerritse 1992; Takewaka and Khin 1996; Rostasy 1997; and Yamaguchi et al. 1997). Methods for systematically accelerating the strength degradation of bare, unstressed, glass filaments in concrete using temperature have been successful (Litherland, Oakley, and Proctor 1981) and have also been often applied to GFRP materials to predict long-term performance in alkaline solutions. There is no substantiation to-date, however, that acceleration methods for bare glass (where only one chemical reaction controls degradation) applies to GFRP composites (where multiple reactions and degradation mechanisms may be activated at once or sequentially). Furthermore, the effect of applied stress during exposure needs to be factored into the situation as well. Due to insufficient data on combined weathering and applied stress, the discussions of weathering, creep, and fatigue are kept separate in this document. Hence, while short-term experiments using aggressive environments certainly enable quick comparisons of materials, extrapolation of the results to field conditions and expected lifetimes are not possible in the absence of real-time data (Gentry et al. 1998; Clarke and Sheard 1998). In most cases available to date, bare bars were subjected to the aggressive environment

under no load. The relationships between data on bare bars and data on bars embedded in concrete are affected by additional variables such as the degree of protection offered to the bars by the concrete (Clarke and Sheard 1998; Scheibe and Rostasy 1998; Sen et al. 1998). Test times included in this review are typically in the 10- to 30-month range. Due to the large amount of literature on the subject (Benmokrane and Rahman 1998) and the limited space here, some generalizations must be made at the expense of presenting particular quantitative results. With these cautions in mind, representative experimental results for a range of FRP bar materials and test conditions are reviewed as follows. Conservatism is advised in applying these results in design until additional long-term durability data are available.

Aqueous solutions with high values of pH are known to degrade the tensile strength and stiffness of GFRP bars (Porter and Barnes 1998), although particular results vary tremendously according to differences in test methods. Higher temperatures and longer exposure times exasperate the problem. Most data have been generated using temperatures as low as slightly subfreezing and as high as a few degrees below the T_g of the resin. The degree to which the resin protects the glass fibers from the diffusion of deleterious hydroxyl (OH⁻) ions figures prominently in the alkali resistance of GFRP bars (Bank and Puterman 1997; Coomarasamy and Goodman 1997; GangaRao and Vijay 1997b; Porter et al. 1997; Bakis et al. 1998; Tannous and Saadatmanesh 1999; Uomoto 2000). Most researchers are of the opinion that vinyl ester resins have superior resistance to moisture ingress in comparison with other commodity resins. The type of glass fiber also appears to be an important factor in the alkali resistance of GFRP bars (Devalapura et al. 1996). Tensile strength reductions in GFRP bars ranging from zero to 75% of initial values have been reported in the cited literature. Tensile stiffness reductions in GFRP bars range between zero and 20% in many cases. Tensile strength and stiffness of AFRP rods in elevated temperature alkaline solutions either with and without tensile stress applied have been reported to decrease between 10 to 50% and 0 to 20% of initial values, respectively (Takewaka and Khin 1996; Rostasy 1997; Sen et al. 1998). In the case of CFRP, strength and stiffness have been reported to each decrease between 0 to 20% (Takewaka and Khin 1996).

Extended exposure of FRP bars to ultraviolet rays and moisture before their placement in concrete could adversely affect their tensile strength due to degradation of the polymer constituents, including aramid fibers and all resins. Proper construction practices and resin additives can ameliorate this type of weathering problem significantly. Some results from combined ultraviolet and moisture exposure tests with and without applied stress applied to the bars have shown tensile strength reductions of 0 to 20% of initial values in CFRP, 0 to 30% in AFRP and 0 to 40% in GFRP (Sasaki et al. 1997, Uomoto 2000). An extensive study of GFRP, AFRP, and CFRP bars kept outdoors in a rack by the ocean showed no significant change of tensile strength or modulus of any of the bars (Tomosowa and Nakatsuji 1996, 1997).

Adding various types of salts to the solutions in which FRP bars are immersed has been shown to not necessarily make a significant difference in the strength and stiffness of many FRP bars, in comparison to the same solution without salt (Rahman, Kingsley, and Crimi 1996). Most studies do not separate the effects of water and salt added to water, however. One study found a 0 to 20% reduction of initial tensile strength in GFRP bars subjected to a saline solution at room-temperature and cyclic freezing-thawing temperatures (Vijay and GangaRao 1999) and another has found a 15% reduction in the strength of AFRP bars in a marine environment (Sen et al. 1998).

Studies of the durability of bond between FRP and concrete have been mostly concerned with the moist, alkaline environment found in concrete. Bond of FRP reinforcement relies upon the transfer of shear and transverse forces at the interface between bar and concrete, and between individual fibers within the bar. These resin-dominated mechanisms are in contrast to the fiber-dominated mechanisms that control properties such as longitudinal strength and stiffness of FRP bars. Environments that degrade the polymer resin or fiber/resin interface are thus also likely to degrade the bond strength of an FRP bar. Numerous bond test methods have been proposed for FRP bars, although the direct pullout test remains rather popular due to its simplicity and low cost (Nanni, Bakis, and Boothby 1995). Pullout specimens with CFRP and GFRP bars have been subjected to natural environmental exposures and have not indicated significant decreases in bond strength over periods of time between 1 and 2 years (Clarke and Sheard 1998 and Sen et al. 1998a). Positive and negative trends in pullout strength with respect to shorter periods of time have been obtained with GFRP bars subjected to wet elevated-temperature environments in concrete, with or without artificially added alkalinity (Al-Dulaijan et al. 1996; Bakis et al. 1998; Bank, Puterman, and Katz 1998; Porter and Barnes 1998). Similar observations on such accelerated pullout tests carry over to AFRP and CFRP bars (Conrad et al. 1998). Longitudinal cracking in the concrete cover can seriously degrade the apparent bond capability of FRP bars and sufficient measures must be taken to prevent such cracking in laboratory tests and field applications (Sen et al. 1998a). The ability of chemical agents to pass through the concrete to the FRP bar is another important factor thought to affect bond strength (Porter and Barnes 1998). Specific recommendations on bond-related parameters, such as development and splice lengths, are provided in [Chapter 11](#).

With regard to the durability characterization of FRP bars, refer to the provisional test methods cited in the literature. The designer should always consult with the bar manufacturer to obtain durability factors.

PART 3—RECOMMENDED MATERIALS REQUIREMENTS AND CONSTRUCTION PRACTICES

CHAPTER 5—MATERIAL REQUIREMENTS AND TESTING

FRP bars made of continuous fibers (aramid, carbon, glass, or any combination) should conform to quality standards as

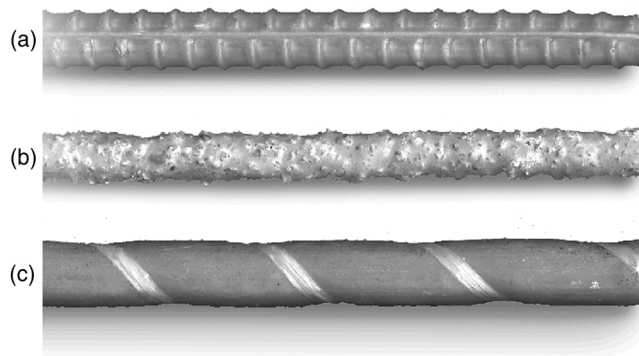


Fig. 5.1—Surface deformation patterns for commercially available FRP bars: (a) ribbed; (b) sand-coated; and (c) wrapped and sand-coated.

Table 5.1—Minimum modulus of elasticity, by fiber type, for reinforcing bars

	Modulus grade, $\times 10^3$ ksi (GPa)
GFRP bars	E5.7 (39.3)
AFRP bars	E10.0 (68.9)
CFRP bars	E16.0 (110.3)

described in Section 5.1. FRP bars are anisotropic, with the longitudinal axis being the major axis. Their mechanical properties vary significantly from one manufacturer to another. Factors, such as volume fraction and type of fiber, resin, fiber orientation, dimensional effects, quality control, and manufacturing process, have a significant effect on the physical and mechanical characteristics of the FRP bars.

FRP bars should be designated with different grades according to their engineering characteristics (such as tensile strength and modulus of elasticity). Bar designation should correspond to tensile properties, which should be uniquely marked so that the proper FRP bar is used.

5.1—Strength and modulus grades of FRP bars

FRP reinforcing bars are available in different grades of tensile strength and modulus of elasticity. The tensile strength grades are based on the tensile strength of the bar, with the lowest grade being 60,000 psi (414 MPa). Finite strength increments of 10,000 psi (69 MPa) are recognized according to the following designation:

Grade F60: corresponds to a $f_{fu}^* \geq 60,000$ psi (414 MPa)

Grade F70: corresponds to a $f_{fu}^* \geq 70,000$ psi (483 MPa)

↓

Grade F300: corresponds to a $f_{fu}^* \geq 300,000$ psi (2069 MPa).

For design purposes, the engineer can select any FRP strength grade between F60 and F300 without having to choose a specific commercial FRP bar type.

A modulus of elasticity grade is established similar to the strength grade. For the modulus of elasticity grade, the minimum value is prescribed depending on the fiber type. For design purposes, the engineer can select the minimum modulus of elasticity grade that corresponds to the chosen fiber type for the member or project. For example, an FRP bar specified with a modulus grade of E5.7 indicates that the

modulus of the bar should be at least 5700 ksi (39.3 GPa). Manufacturers producing FRP bars with a modulus of elasticity in excess of the minimum specified will have superior FRP bars that can result in savings on the amount of FRP reinforcement used for a particular application.

The modulus of elasticity grades for different types of FRP bars are summarized in Table 5.1. For all these FRP bars, rupture strain should not be less than 0.005 in./in.

5.2—Surface geometry

FRP reinforcing bars are produced through a variety of manufacturing processes. Each manufacturing method produces a different surface condition. The physical characteristics of the surface of the FRP bar is an important property for mechanical bond with concrete. Three types of surface deformation patterns for FRP bars that are commercially available are shown in Fig. 5.1.

Presently, there is no standardized classification of surface deformation patterns. Research is in progress to produce a bond grade similar to the strength and modulus grades.

5.3—Bar sizes

FRP bar sizes are designated by a number corresponding to the approximate nominal diameter in eighths of an inch, similar to standard ASTM steel reinforcing bars. There are 12 standard sizes, as illustrated in Table 5.2, which also includes the corresponding metric conversion.

The nominal diameter of a deformed FRP bar is equivalent to that of a plain round bar having the same area as the deformed bar. When the FRP bar is not of the conventional solid round shape (that is, rectangular or hollow), the outside diameter of the bar or the maximum outside dimension of the bar will be provided in addition to the equivalent nominal diameter. The nominal diameter of these unconventional bars would be equivalent to that of a solid plain round bar having the same area.

5.4—Bar identification

With the various grades, sizes, and types of FRP bars available, it is necessary to provide some means of easy identification. Each bar producer should label the bars, container/packaging, or both, with the following information:

- A symbol to identify the producer;
- A letter to indicate the type of fiber (that is, g for glass, c for carbon, a for aramid, or h for a hybrid) followed by the number corresponding to the nominal bar size designation according to the ASTM standard;
- A marking to designate the strength grade;
- A marking to designate the modulus of elasticity of the bar in thousands of ksi; and
- In the case of an unconventional bar (a bar with a cross section that is not uniformly circular or solid), the outside diameter or the maximum outside dimension.

A bond grade will be added when a classification is available. Example of identification symbols are shown below

Table 5.2—ASTM standard reinforcing bars

Bar size designation		Nominal diameter, in. (mm)	Area, in. ² (mm ²)
Standard	Metric conversion		
No. 2	No. 6	0.250 (6.4)	0.05 (31.6)
No. 3	No. 10	0.375 (9.5)	0.11 (71)
No. 4	No. 13	0.500 (12.7)	0.20 (129)
No. 5	No. 16	0.625 (15.9)	0.31 (199)
No. 6	No. 19	0.750 (19.1)	0.44 (284)
No. 7	No. 22	0.875 (22.2)	0.60 (387)
No. 8	No. 25	1.000 (25.4)	0.79 (510)
No. 9	No. 29	1.128 (28.7)	1.00 (645)
No. 10	No. 32	1.270 (32.3)	1.27 (819)
No. 11	No. 36	1.410 (35.8)	1.56 (1006)
No. 14	No. 43	1.693 (43.0)	2.25 (1452)
No. 18	No. 57	2.257 (57.3)	4.00 (2581)

where

XXX = manufacturer's symbol or name;

G#4 = glass FRP bar No. 4 (nominal diameter of 1/2 in.);

F100 = strength grade of at least 100 ksi ($f_{fu}^* \geq 100$ ksi);

E6.0 = modulus grade of at least 6,000,000 psi.

In the case of a hollow or unconventionally shaped bar, an extra identification should be added to the identification symbol as shown below:

XXX - G#4 - F100 - E6.0 - 0.63

where:

0.63 = maximum outside dimension is 5/8 in.

Markings should be used at the construction site to verify that the specified type, grades, and bar sizes are being used.

5.5—Straight bars

Straight bars are cut to a specified length from longer stock lengths in a fabricator's shop or at the manufacturing plant.

5.6—Bent bars

Bending FRP rebars made of thermoset resin should be carried out before the resin is fully cured. After the bars have cured, bending or alteration is not possible due to the inflexibility or rigid nature of a cured FRP bar. Because thermoset polymers are highly cross-linked, heating the bar is not allowed as it would lead to a decomposition of the resin, thus a loss of strength in the FRP.

The strength of bent bars varies greatly for the same type of fiber, depending on the bending technique and type of resin used. Therefore, the strength of the bent portion generally should be determined based on suitable tests performed in accordance with recommended test methods cited in the literature. Bars in which the resin has not yet fully cured can be bent, but only according to the manufacturer's specifications and with a gradual transition, avoiding sharp angles that damage the fibers.

CHAPTER 6—CONSTRUCTION PRACTICES

FRP reinforcing bars are ordered for specific parts of a structure and are delivered to a job site storage area. Construction operations should be performed in a manner

designed to minimize damage to the bars. Similarly to epoxy-coated steel bars, FRP bars should be handled, stored, and placed more carefully than uncoated steel reinforcing bars.

6.1—Handling and storage of materials

FRP reinforcing bars are susceptible to surface damage. Puncturing their surface can significantly reduce the strength of the FRP bars. In the case of glass FRP bars, the surface damage can cause a loss of durability due to infiltration of alkalis. The following handling guidelines are recommended to minimize damage to both the bars and the bar handlers:

- FRP reinforcing bars should be handled with work gloves to avoid personal injuries from either exposed fibers or sharp edges;
- FRP bars should not be stored on the ground. Pallets should be placed under the bars to keep them clean and to provide easy handling;
- High temperatures, ultraviolet rays, and chemical substances should be avoided because they can damage FRP bars;
- Occasionally, bars become contaminated with form releasing agents or other substances. Substances that decrease bond should be removed by wiping the bars with solvents before placing FRP bars in concrete form;
- It may be necessary to use a spreader bar so that the FRP bars can be hoisted without excessive bending; and
- When necessary, cutting should be performed with a high-speed grinding cutter or a fine-blade saw. FRP bars should never be sheared. Dust masks, gloves, and glasses for eye protection are recommended when cutting. There is insufficient research available to make any recommendation on treatment of saw-cut bar ends.

6.2—Placement and assembly of materials

In general, placing FRP bars is similar to placing steel bars, and common practices should apply with some exceptions for the specifications prepared by the engineer as noted:

- FRP reinforcement should be placed and supported using chairs (preferably plastic or noncorrosive). The requirements for support chairs should be included in the project specifications;
- FRP reinforcement should be secured against displacement while the concrete is being placed. Coated tie wire, plastic or nylon ties, and plastic snap ties can be used in tying the bars. The requirement for ties should be included in the project specifications;
- Bending of cured thermoset FRP bars on site should not be permitted. For other FRP systems, manufacturer's specifications should be followed; and
- Whenever reinforcement continuity is required, lapped splices should be used. The length of lap splices varies with concrete strength, type of concrete, bar grades, size, surface geometry, spacing, and concrete cover. Details of lapped splices should be in accordance with the project specifications. Mechanical connections are not yet available.

6.3—Quality control and inspection

Quality control should be carried out by lot testing of FRP bars. The manufacturer should supply adequate lot or production run traceability. Tests conducted by the manufacturer or a third-party independent testing agency can be used.

All tests should be performed using the recommended test methods cited in the literature. Material characterization tests that include the following properties should be performed at least once before and after any change in manufacturing process, procedure, or materials:

- Tensile strength, tensile modulus of elasticity, and ultimate strain;
- Fatigue strength;
- Bond strength;
- Coefficient of thermal expansion; and
- Durability in alkaline environment.

To assess quality control of an individual lot of FRP bars, it is recommended to determine tensile strength, tensile modulus of elasticity, and ultimate strain. The manufacturer should furnish upon request a certificate of conformance for any given lot of FRP bars with a description of the test protocol.

PART 4—DESIGN RECOMMENDATIONS

CHAPTER 7—GENERAL DESIGN CONSIDERATIONS

The general design recommendations for flexural concrete elements reinforced with FRP bars are presented in this chapter. The recommendations presented are based on principles of equilibrium and compatibility and the constitutive laws of the materials. Furthermore, the brittle behavior of both FRP reinforcement and concrete allows consideration to be given to either FRP rupture or concrete crushing as the mechanisms that control failure.

7.1—Design philosophy

Both strength and working stress design approaches were considered by this committee. The committee opted for the strength design approach of reinforced concrete members reinforced with FRP bars to ensure consistency with other ACI documents. In particular, this guide makes reference to provisions as per ACI 318-95, “Building Code Requirements for Structural Concrete and Commentary.” These design recommendations are based on limit states design principles in that an FRP reinforced concrete member is designed based on its required strength and then checked for fatigue endurance, creep rupture endurance, and serviceability criteria. In many instances, serviceability criteria or fatigue and creep rupture endurance limits may control the design of concrete members reinforced for flexure with FRP bars (especially aramid and glass FRP that exhibit low stiffness).

The load factors given in ACI 318 are used to determine the required strength of a reinforced concrete member.

7.2—Design material properties

The material properties provided by the manufacturer, such as the guaranteed tensile strength, should be considered as initial properties that do not include the effects of long-term exposure to the environment. Because long-term exposure to

various types of environments can reduce the tensile strength and creep rupture and fatigue endurance of FRP bars, the material properties used in design equations should be reduced based on the type and level of environmental exposure.

Equations (7-1) through (7-3) give the tensile properties that should be used in all design equations. The design tensile strength should be determined by

$$f_{fu} = C_E f_{fu}^* \quad (7-1)$$

where

- f_{fu} = design tensile strength of FRP, considering reductions for service environment, psi;
 C_E = environmental reduction factor, given in Table 7.1 for various fiber type and exposure conditions; and
 f_{fu}^* = guaranteed tensile strength of an FRP bar defined as the mean tensile strength of a sample of test specimens minus three times the standard deviation ($f_{fu}^* = f_{u,ave} - 3\sigma$), psi.

The design rupture strain should be determined as

$$\epsilon_{fu} = C_E \epsilon_{fu}^* \quad (7-2)$$

where

- ϵ_{fu}^* = design rupture strain of FRP reinforcement; and
 ϵ_{fu}^* = guaranteed rupture strain of FRP reinforcement defined as the mean tensile strain at failure of a sample of test specimens minus three times the standard deviation ($\epsilon_{fu}^* = \epsilon_{u,ave} - 3\sigma$).

The design modulus of elasticity will be the same as the value reported by the manufacturer ($E_f = E_{f,ave}$).

The environmental reduction factors given in Table 7.1 are conservative estimates depending on the durability of each fiber type and are based on the consensus of Committee 440. Temperature effects are included in the C_E values. FRP bars, however, should not be used in environments with a service temperature higher than the T_g of the resin used for their manufacturing. It is expected that with continued research, these values will become more reflective of actual effects of environment. The methodology regarding the use of these factors, however, is not expected to change.

7.2.1 Tensile strength of FRP bars at bends—The design tensile strength of FRP bars at a bend portion can be determined as

$$f_{fb} = \left(0.05 \cdot \frac{r_b}{d_b} + 0.3 \right) f_{fu} \leq f_{fu} \quad (7-3)$$

where

- f_{fb} = design tensile strength of the bend of FRP bar, psi;
 r_b = radius of the bend, in.;
- d_b = diameter of reinforcing bar, in.; and
 f_{fu} = design tensile strength of FRP, considering reductions for service environment, psi.

Equation (7-3) is adapted from design recommendations by the Japan Society of Civil Engineers (1997b). Limited

Table 7.1—Environmental reduction factor for various fibers and exposure conditions

Exposure condition	Fiber type	Environmental reduction factor C_E
Concrete not exposed to earth and weather	Carbon	1.0
	Glass	0.8
	Aramid	0.9
Concrete exposed to earth and weather	Carbon	0.9
	Glass	0.7
	Aramid	0.8

research on FRP hooks (Ehsani, Saadatmanesh, and Tao 1995) indicates that the tensile force developed by the bent portion of a GFRP bar is mainly influenced by the ratio of the bend radius to the bar diameter, r_b/d_b , the tail length, and to a lesser extent, the concrete strength.

For an alternative determination of the reduction in tensile strength due to bending, manufacturers of bent bars may provide test results based on test methodologies cited in the literature.

CHAPTER 8—FLEXURE

The design of FRP reinforced concrete members for flexure is analogous to the design of steel-reinforced concrete members. Experimental data on concrete members reinforced with FRP bars show that flexural capacity can be calculated based on assumptions similar to those made for members reinforced with steel bars (Faza and GangaRao 1993; Nanni 1993b; GangaRao and Vijay 1997a). The design of members reinforced with FRP bars should take into account the mechanical behavior of FRP materials.

8.1—General considerations

The recommendations given in this chapter are only for rectangular sections, as the experimental work has almost exclusively considered members with this shape. In addition, this chapter refers only to cases of rectangular sections with a single layer of one type of FRP reinforcement. The concepts described here, however, can also be applied to the analysis and design of members with different geometry and multiple types, multiple layers, or both, of FRP reinforcement. Although there is no evidence that the flexural theory, as developed here, does not apply equally well to nonrectangular sections, the behavior of nonrectangular sections has yet to be confirmed by experimental results.

8.1.1 Flexural design philosophy—Steel-reinforced concrete sections are commonly under-reinforced to ensure yielding of steel before the crushing of concrete. The yielding of the steel provides ductility and a warning of failure of the member. The nonductile behavior of FRP reinforcement necessitates a reconsideration of this approach.

If FRP reinforcement ruptures, failure of the member is sudden and catastrophic. There would be limited warning of impending failure in the form of extensive cracking and large deflection due to the significant elongation that FRP reinforcement experiences before rupture. In any case, the member would not exhibit ductility as is commonly

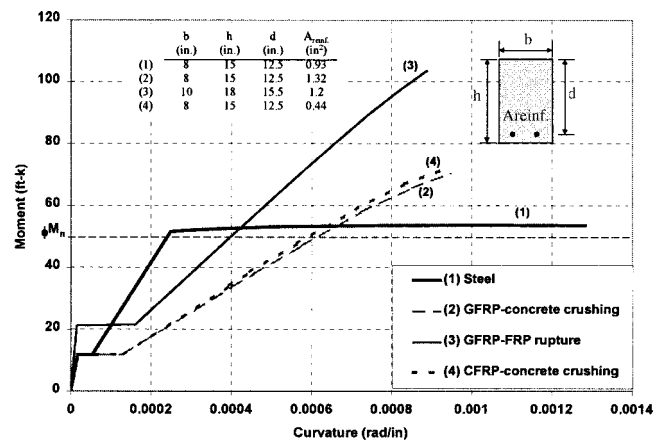


Fig. 8.1—Theoretical moment-curvature relationships for reinforced concrete sections using steel and FRP bars.

observed for under-reinforced concrete beams reinforced with steel rebars.

The concrete crushing failure mode is marginally more desirable for flexural members reinforced with FRP bars (Nanni 1993b). By experiencing concrete crushing, a flexural member does exhibit some plastic behavior before failure.

In conclusion, both failure modes (FRP rupture and concrete crushing) are acceptable in governing the design of flexural members reinforced with FRP bars provided that strength and serviceability criteria are satisfied. To compensate for the lack of ductility, the member should possess a higher reserve of strength. The suggested margin of safety against failure is therefore higher than that used in traditional steel-reinforced concrete design.

Experimental results (Nanni 1993b; Jaeger, Mufti, and Tadros 1997; GangaRao and Vijay 1997a; Theriault and Benmokrane 1998) indicated that when FRP reinforcing bars ruptured in tension, the failure was sudden and led to the collapse of the member. A more progressive, less catastrophic failure with a higher deformability factor was observed when the member failed due to the crushing of concrete. The use of high-strength concrete allows for better use of the high-strength properties of FRP bars and can increase the stiffness of the cracked section, but the brittleness of high-strength concrete, as compared to normal-strength concrete, can reduce the overall deformability of the flexural member.

Figure 8.1 shows a comparison of the theoretical moment-curvature behavior of beam cross sections designed for the same strength ϕM_n following the design approach of ACI 318 and that described in this chapter (including the recommended strength reduction factors). Three cases are presented in addition to the steel reinforced cross section: two sections reinforced with GFRP bars and one reinforced with CFRP bars. For the section experiencing GFRP bars rupture, the concrete dimensions are larger than for the other beams to attain the same design capacity.

8.1.2 Assumptions—Computations of the strength of cross sections should be performed based on of the following assumptions:

- Strain in the concrete and the FRP reinforcement is

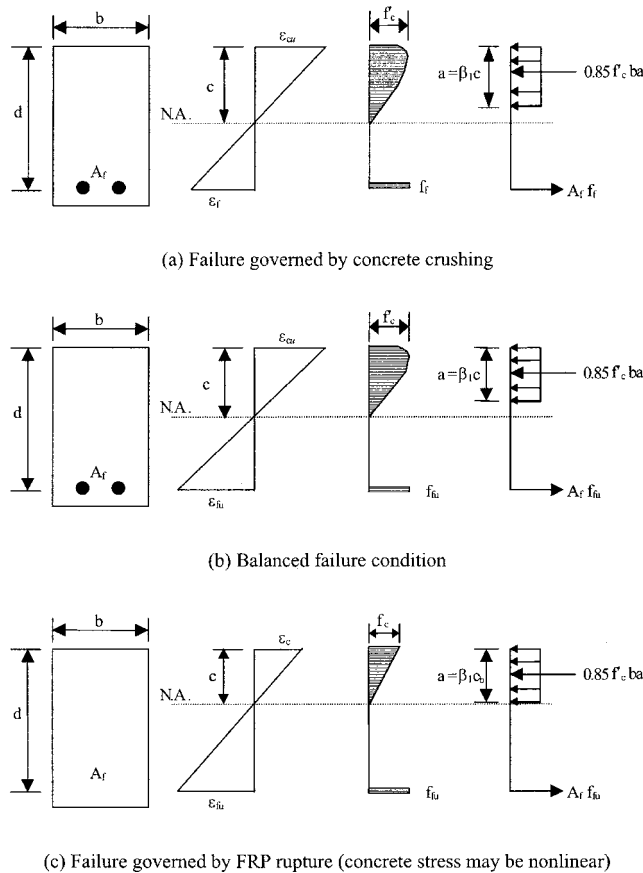


Fig. 8.2—Strain and stress distribution at ultimate conditions.

proportional to the distance from the neutral axis (that is, a plane section before loading remains plane after loading);

- The maximum usable compressive strain in the concrete is assumed to be 0.003;
- The tensile strength of concrete is ignored;
- The tensile behavior of the FRP reinforcement is linearly elastic until failure; and
- Perfect bond exists between concrete and FRP reinforcement.

8.2—Flexural strength

The strength design philosophy states that the design flexural capacity of a member must exceed the flexural demand (Eq. (8-1)). Design capacity refers to the nominal strength of the member multiplied by a strength-reduction factor (Φ , to be discussed in Section 8.2.3), and the demand refers to the load effects calculated from factored loads (for example, $1.4D + 1.7L + \dots$). This guide recommends that the flexural demand on an FRP reinforced concrete member be computed with the load factors required by ACI 318.

$$\phi M_n \geq M_u \tag{8-1}$$

The nominal flexural strength of an FRP reinforced concrete member can be determined based on strain compatibility, internal force equilibrium, and the controlling mode of failure. Figure 8.2 illustrates the stress, strain, and internal

Table 8.1—Typical values for the balanced reinforcement ratio for a rectangular section with $f'_c = 5000$ psi (34.5 MPa)

Bar type	Tensile strength, f_y or f_{fu} , ksi (MPa)	Modulus of elasticity, ksi (GPa)	ρ_b or ρ_{fb}
Steel	60 (414)	29,000 (200)	0.0335
GFRP	80 (552)	6000 (41.4)	0.0078
AFRP	170 (1172)	12,000 (82.7)	0.0035
CFRP	300 (2070)	22,000 (152)	0.0020

forces for the three possible cases of a rectangular section reinforced with FRP bars.

8.2.1 Failure mode—The flexural capacity of an FRP reinforced flexural member is dependent on whether the failure is governed by concrete crushing or FRP rupture. The failure mode can be determined by comparing the FRP reinforcement ratio to the balanced reinforcement ratio (that is, a ratio where concrete crushing and FRP rupture occur simultaneously). Because FRP does not yield, the balanced ratio of FRP reinforcement is computed using its design tensile strength. The FRP reinforcement ratio can be computed from Eq. (8-2), and the balanced FRP reinforcement ratio can be computed from Eq. (8-3).

$$\rho_f = \frac{A_f}{bd} \tag{8-2}$$

$$\rho_{fb} = 0.85\beta_1 \frac{f'_c}{f_{fu} E_f \epsilon_{cu} + f_{fu}} \frac{E_f \epsilon_{cu}}{E_f \epsilon_{cu} + f_{fu}} \tag{8-3}$$

If the reinforcement ratio is below the balanced ratio ($\rho_f < \rho_{fb}$), FRP rupture failure mode governs. Otherwise, ($\rho_f > \rho_{fb}$) concrete crushing governs.

Table 8.1 reports some typical values for the balanced reinforcement ratio, showing that the balanced ratio for FRP reinforcement ρ_{fb} , is much lower than the balanced ratio for steel reinforcement, ρ_b . In fact, the balanced ratio for FRP reinforcement can be even lower than the minimum reinforcement ratio for steel ($\rho_{min} = 0.0035$ for Grade 60 steel and $f'_c = 5000$ psi).

8.2.2 Nominal flexural capacity—When $\rho_f > 1.4\rho_{fb}$, the failure of the member is initiated by crushing of the concrete, and the stress distribution in the concrete can be approximated with the ACI rectangular stress block. Based on the equilibrium of forces and strain compatibility (shown in Fig. 8.2), the following can be derived

$$M_n = A_f f_f \left(d - \frac{a}{2} \right) \tag{8-4a}$$

$$a = \frac{A_f f_f}{0.85 f'_c b} \tag{8-4b}$$

$$f_f = E_f \epsilon_{cu} \frac{\beta_1 d - a}{a} \tag{8-4c}$$

substituting a from Eq. (8-4b) into Eq. (8-4c) and solving for f_f gives

$$f_f = \left(\sqrt{\frac{(E_f \epsilon_{cu})^2}{4} + \frac{0.85 \beta_1 f'_c}{\rho_f} E_f \epsilon_{cu} - 0.5 E_f \epsilon_{cu}} \right) \leq f_{fu} \quad (8-4d)$$

The nominal flexural strength can be determined from Eq. (8-4a), (8-4b), and (8-4d). FRP reinforcement is linearly elastic at concrete crushing failure mode so the stress level in the FRP can be found from Eq. (8-4c) because it is less than f_{fu} .

Alternatively, the nominal flexural capacity can be expressed in terms of the FRP reinforcement ratio as given in Eq. (8-5) to replace Eq. (8-4a).

$$M_n = \rho_f f_f \left(1 - 0.59 \frac{\rho_f f_f}{f'_c} \right) b d^2 \quad (8-5)$$

When $\rho_f < \rho_{fb}$, the failure of the member is initiated by rupture of FRP bar, and the ACI stress block is not applicable because the maximum concrete strain (0.003) may not be attained. In this case, an equivalent stress block would need to be used that approximates the stress distribution in the concrete at the particular strain level reached. The analysis incorporates two unknowns: the concrete compressive strain at failure, ϵ_c , and the depth to the neutral axis, c . In addition, the rectangular stress block factors, α_1 and β_1 , are unknown. The factor, α_1 , is the ratio of the average concrete stress to the concrete strength. β_1 is the ratio of the depth of the equivalent rectangular stress block to the depth of the neutral axis. The analysis involving all these unknowns becomes complex. Flexural capacity can be computed as shown in Eq. (8-6a)

$$M_n = A_f f_{fu} \left(d - \frac{\beta_1 c}{2} \right) \quad (8-6a)$$

For a given section, the product of $\beta_1 c$ in Eq. (8-6a) varies depending on material properties and FRP reinforcement ratio. The maximum value for this product is equal to $\beta_1 c_b$ and is achieved when the maximum concrete strain (0.003) is attained. A simplified and conservative calculation of the nominal flexural capacity of the member can be based on Eq. (8-6b) and (8-6c) as follows

$$M_n = 0.8 A_f f_{fu} \left(d - \frac{\beta_1 c_b}{2} \right) \quad (8-6b)$$

$$c_b = \left(\frac{\epsilon_{cu}}{\epsilon_{cu} + \epsilon_{fu}} \right) d \quad (8-6c)$$

The committee feels that the coefficient of 0.8 used in Eq. (8-6b) provides a conservative and yet meaningful approximation of the nominal moment.

8.2.3 Strength reduction factor for flexure—Because FRP members do not exhibit ductile behavior, a conservative strength reduction factor should be adopted to provide a higher reserve of strength in the member. The Japanese recommendations for design of flexural members using FRP suggest a strength-reduction factor equal to 1/1.3 (JSCE 1997). Other researchers (Benmokrane et al. 1996) suggest a value of 0.75 determined based on probabilistic concepts.

Based on the provisions of ACI 318 Appendix B, a steel-reinforced concrete member with failure controlled by concrete crushing has a strength reduction factor of 0.70. This philosophy (strength reduction factors of 0.7 for concrete crushing failures) should be used for FRP reinforced concrete members. Because a member that experiences an FRP rupture exhibits less plasticity than one that experiences concrete crushing, a strength reduction factor of 0.50 is recommended for rupture-controlled failures.

While a concrete crushing failure mode can be predicted based on calculations, the member as constructed may not fail accordingly. For example, if the concrete strength is higher than specified, the member can fail due to FRP rupture. For this reason and to establish a transition between the two values of ϕ , a section controlled by concrete crushing is defined as a section in which $\rho_f \geq 1.4 \rho_{fb}$, and a section controlled by FRP rupture is defined as one in which $\rho_f < \rho_{fb}$.

The strength reduction factor for flexure can be computed by Eq. (8-7). This equation is represented graphically by Fig. 8.3 and gives a factor of 0.70 for sections controlled by concrete crushing, 0.50 for sections controlled by FRP rupture, and provides a linear transition between the two.

$$\phi = \begin{cases} 0.50 & \text{for } \rho_f \leq \rho_{fb} \\ \frac{\rho_f}{2\rho_{fb}} & \text{for } \rho_{fb} < \rho_f < 1.4\rho_{fb} \\ 0.70 & \text{for } \rho_f \geq 1.4\rho_{fb} \end{cases} \quad (8-7)$$

8.2.4 Minimum FRP reinforcement—If a member is designed to fail by FRP rupture, $\rho_f < \rho_{fb}$, a minimum amount of reinforcement should be provided to prevent failure upon concrete cracking (that is, $\phi M_n \geq M_{cr}$ where M_{cr} is the cracking moment). The provisions in ACI 318 for minimum reinforcement are based on this concept and, with modifications, are applicable to FRP reinforced members. The modifications result from a different strength reduction factor (that is, 0.5 for tension-controlled sections, instead of 0.9). The minimum reinforcement area for FRP reinforced members is obtained by multiplying the existing ACI equation for steel limit by 1.8 ($1.8 = 0.90/0.50$). This results in Eq. (8-8).

$$A_{f,min} = \frac{5.4 \sqrt{f'_c}}{f_{fu}} b_w d \geq \frac{360}{f_{fu}} b_w d \quad (8-8)$$

If failure of a member is not controlled by FRP rupture, $\rho_f > \rho_{fb}$, the minimum amount of reinforcement to prevent

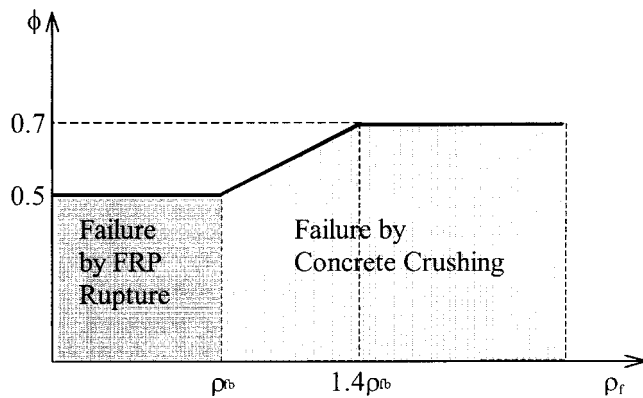


Fig. 8.3—Strength reduction factor as a function of the reinforcement ratio.

failure upon cracking is automatically achieved. Therefore, Eq. (8-8) is required as a check only if $\rho_f < \rho_{fb}$.

8.2.5 Special considerations

8.2.5.1 Multiple layers of reinforcement and combinations of different FRP types—All steel tension reinforcement is assumed to yield at ultimate when using the strength design method to calculate the capacity of members with steel reinforcement arranged in multiple layers. Therefore, the tension force is assumed to act at the centroid of the reinforcement with a magnitude equal to the area of tension reinforcement times the yield strength of steel. Because FRP materials have no plastic region, the stress in each reinforcement layer will vary depending on its distance from the neutral axis. Similarly, if different types of FRP bars are used to reinforce the same member, the variation in the stress level in each bar type should be considered when calculating the flexural capacity. In these cases, failure of the outermost layer controls overall reinforcement failure, and the analysis of the flexural capacity should be based on a strain-compatibility approach.

8.2.5.2 Moment redistribution—The failure mechanism of FRP reinforced flexural members should not be based on the formation of plastic hinges, because FRP materials demonstrate a linear-elastic behavior up to failure. Moment redistribution in continuous beams or other statically indeterminate structures should not be considered for FRP reinforced concrete.

8.2.5.3 Compression reinforcement—FRP reinforcement has a significantly lower compressive strength than tensile strength and is subject to significant variation (Kobayashi and Fujisaki 1995; JSCE 1997). Therefore, the strength of any FRP bar in compression should be ignored in design calculations (Almusallam et al. 1997).

This guide does not recommend using FRP bars as longitudinal reinforcement in columns or as compression reinforcement in flexural members. Placing FRP bars in the compression zone of flexural members, however, cannot be avoided in some cases. Examples include the supports of continuous beams or where bars secure the stirrups in place. In these cases, confinement should be considered for the FRP bars in compression regions to prevent their instability

and to minimize the effect of the relatively high transverse expansion of some types of FRP bars.

8.3—Serviceability

FRP reinforced concrete members have a relatively small stiffness after cracking. Consequently, permissible deflections under service loads can control the design. In general, designing FRP reinforced cross sections for concrete crushing failure satisfies serviceability criteria for deflection and crack width (Nanni 1993a; GangaRao and Vijay 1997a; Theriault and Benmokrane 1998).

Serviceability can be defined as satisfactory performance under service load conditions. This in turn can be described in terms of two parameters:

- **Cracking**—Excessive crack width is undesirable for aesthetic and other reasons (for example, to prevent water leakage) that can damage or deteriorate the structural concrete; and
- **Deflection**—Deflections should be within acceptable limits imposed by the use of the structure (for example, supporting attached nonstructural elements without damage).

The serviceability provisions given in ACI 318 need to be modified for FRP reinforced members due to differences in properties of steel and FRP, such as lower stiffness, bond strength, and corrosion resistance. The substitution of FRP for steel on an equal area basis, for example, would typically result in larger deflections and wider crack widths (Gao, Benmokrane, and Masmoudi 1998a; Tighiouart, Benmokrane, and Gao 1998).

8.3.1 Cracking—FRP rods are corrosion resistant, therefore the maximum crack-width limitation can be relaxed when corrosion of reinforcement is the primary reason for crack-width limitations. If steel is to be used in conjunction with FRP reinforcement, however, ACI 318 provisions should be used.

The Japan Society of Civil Engineers (1997b) takes into account the aesthetic point of view only to set the maximum allowable crack width of 0.020 in. (0.5 mm). The Canadian Highways Bridge Design Code (Canadian Standards Association 1996) allows crack widths of 0.020 in. (0.5 mm) for exterior exposure and 0.028 in. (0.7 mm) for interior exposure when FRP reinforcement is used. ACI 318 provisions for allowable crack-width limits in steel-reinforced structures correspond to 0.013 in. (0.3 mm) for exterior exposure and 0.016 in. (0.4 mm) for interior exposure.

It is recommended that the Canadian Standards Association (1996) limits be used for most cases. These limitations may not be sufficiently restrictive for structures exposed to aggressive environments or designed to be watertight. Therefore, additional caution is recommended for such cases. Conversely, for structures with short life-cycle requirements or those for which aesthetics is not a concern, crack-width requirements can be disregarded (unless steel reinforcement is also present).

Crack widths in FRP reinforced members are expected to be larger than those in steel-reinforced members. Experimental and theoretical research on crack width (Faza and

GangaRao 1993; Masmoudi, Benmokrane, and Challal 1996; Gao, Benmokrane, and Masmoudi 1998a) has indicated that the well-known Gergely-Lutz equation can be modified to give a reasonable estimate of the crack width of FRP reinforced members. The original Gergely-Lutz (1973) equation is given as follows

$$w = 0.076\beta(E_s \varepsilon_s)^3 \sqrt{d_c A} \quad (8-9a)$$

in which E_s is in ksi, and w is in mils (10^{-3} in.). The crack width is proportional to the strain in the tensile reinforcement rather than the stress (Wang and Salmon 1992). Therefore, the Gergely-Lutz equation can be adjusted to predict the crack width of FRP reinforced flexural members by replacing the steel strain, ε_s , with the FRP strain, $\varepsilon_f = f_f/E_f$ and by substituting 29,000 ksi for the modulus of elasticity for steel as follows

$$w = 0.076\beta \frac{E_s}{E_f} f_f^3 \sqrt{d_c A} \quad (8-9b)$$

When used with FRP deformed bars having a bond strength similar to that of steel, this equation estimates crack width accurately (Faza and GangaRao 1993). This equation can overestimate crack width when applied to a bar with a higher bond strength than that of steel and underestimate crack width when applied to a bar with a lower bond strength than that of steel. Therefore, to make the expression more generic, it is necessary to introduce a corrective coefficient for the bond quality. For FRP reinforced members, crack width can be calculated from Eq. (8-9c).

$$w = \frac{2200}{E_f} \beta k_b f_f^3 \sqrt{d_c A} \quad (8-9c)$$

For SI units,

$$w = \frac{2.2}{E_f} \beta k_b f_f^3 \sqrt{d_c A}$$

with f_f and E_f in MPa, d_c in mm, and A in mm^2 .

The k_b term is a coefficient that accounts for the degree of bond between FRP bar and surrounding concrete. For FRP bars having bond behavior similar to steel bars, the bond coefficient k_b is assumed equal to one. For FRP bars having bond behavior inferior to steel, k_b is larger than 1.0, and for FRP bars having bond behavior superior to steel, k_b is smaller than 1.0. Gao, Benmokrane, and Masmoudi (1998a) introduced a similar formula based on test results. Using the test results from Gao, Benmokrane, and Masmoudi (1998a), the calculated values of k_b for three types of GFRP rods were found to be 0.71, 1.00, and 1.83. These values indicate that bond characteristics of GFRP bars can vary from that of steel. Further research is needed to verify the effect of surface characteristics of FRP bars on the bond behavior and

on crack widths. Data should be obtained for commercially available FRP bars. Based on this committee consensus, when k_b is not known, a value of 1.2 is suggested for deformed FRP bars.

8.3.2 Deflections—In general, the ACI 318 provisions for deflection control are concerned with deflections that occur at service levels under immediate and sustained static loads and do not apply to dynamic loads such as earthquakes, transient winds, or vibration of machinery. Two methods are presently given in ACI 318 for control of deflections of one-way flexural members:

- The indirect method of mandating the minimum thickness of the member (Table 9.5(a) in ACI 318); and
- The direct method of limiting computed deflections (Table 9.5(b) in ACI 318).

8.3.2.1 Minimum thickness for deflection control (indirect method)—The values of minimum thickness, as given by ACI 318, Table 9.5(a), are not conservative for FRP reinforced one-way systems and should only be used as first trial values in the design of a member.

Further studies are required before this committee can provide guidance on design of minimum thickness without having to check deflections.

8.3.2.2 Effective moment of inertia—When a section is uncracked, its moment of inertia is equal to the gross moment of inertia, I_g . When the applied moment, M_a , exceeds the cracking moment, M_{cr} , cracking occurs, which causes a reduction in the stiffness; and the moment of inertia is based on the cracked section, I_{cr} . For a rectangular section, the gross moment of inertia is calculated as $I_g = bh^3/12$, while I_{cr} can be calculated using an elastic analysis. The elastic analysis for FRP reinforced concrete is similar to the analysis used for steel reinforced concrete (that is, concrete in tension is neglected) and is given by Eq. (8-10) and (8-11) with n_f as the modular ratio between the FRP reinforcement and the concrete.

$$I_{cr} = \frac{bd^3}{3} k^3 + n_f A_f d^2 (1 - k)^2 \quad (8-10)$$

$$k = \sqrt{2\rho_f n_f + (\rho_f n_f)^2} - \rho_f n_f \quad (8-11)$$

The overall flexural stiffness, $E_c I$, of a flexural member that has experienced cracking at service varies between $E_c I_g$ and $E_c I_{cr}$, depending on the magnitude of the applied moment. Branson (1977) derived an equation to express the transition from I_g to I_{cr} . Branson's equation was adopted by the ACI 318 as the following expression for the effective moment of inertia, I_e :

$$I_e = \left(\frac{M_{cr}}{M_a}\right)^3 I_g + \left[1 - \left(\frac{M_{cr}}{M_a}\right)^3\right] I_{cr} \leq I_g$$

Branson's equation reflects two different phenomena: the variation of EI stiffness along the member and the effect of concrete tension stiffening.

This equation was based on the behavior of steel-reinforced beams at service load levels. Because FRP bars exhibit linear behavior up to failure, the equation offers a close approximation for FRP reinforced beams (Zhao, Pilakouras, and Waldron 1997). Research on deflection of FRP reinforced beams (Benmokrane, Chaallal, and Masmoudi 1996; Brown and Bartholomew 1996) indicates that on a plot of load versus maximum deflection of simply supported beams, the experimental curves are parallel to those predicted by the equation. Because the bond characteristics of FRP bars also affect the deflection of a member, Branson's equation can overestimate the effective moment of inertia of FRP reinforced beams (Benmokrane, Chaallal, and Masmoudi 1996). Gao, Benmokrane, and Masmoudi (1998a) concluded that to account for the lower modulus of elasticity of FRP bars and the different bond behavior of the FRP, a modified expression for the effective moment of inertia is required. This expression is recommended and is given by Eq. (8-12a) and (8-12b).

$$I_e = \left(\frac{M_{cr}}{M_a}\right)^3 \beta_d I_g + \left[1 - \left(\frac{M_{cr}}{M_a}\right)^3\right] I_{cr} \leq I_g \quad (8-12a)$$

$$\beta_d = \alpha_b \left[\frac{E_f}{E_s} + 1 \right] \quad (8-12b)$$

Eq. (8-12a) is only valid for $M_a > M_{cr}$. In Eq. (8-12b), α_b is a bond-dependent coefficient. According to test results of simply supported beams, the value of α_b for a given GFRP bar was found to be 0.5, which is the same as steel bars (Gao, Benmokrane, and Masmoudi 1998a). Further research studies are required to investigate the value of α_b for other FRP bar types. Until more data become available, it is recommended to take the value of $\alpha_b = 0.5$ for all FRP bar types.

8.3.2.3 Calculation of deflection (direct method)—The short-term deflections (instantaneous deflection under service loads) of an FRP one-way flexural member can be calculated using the effective moment of inertia of the FRP reinforced beam and the usual structural analysis techniques.

Long-term deflection can be two to three times the short-term deflection, and both short-term and long-term deflections under service loads should be considered in the design. The long-term increase in deflection is a function of member geometry (reinforcement area and member size), load characteristics (age of concrete at the time of loading, and magnitude and duration of sustained load), and material characteristics (creep and shrinkage of concrete, formation of new cracks, and widening of existing cracks).

Limited data on long-term deflections of FRP reinforced members (Kage et al. 1995; Brown 1997) indicate creep behavior in FRP reinforced members is similar to that of steel-reinforced members. The time-versus-deflection curves of FRP reinforced and steel-reinforced members have the same shape, indicating that the same approach for estimating the long-term deflection can be used. Experiments have shown that initial short-term deflections of FRP reinforced members are three to four times greater than those of steel-reinforced members for the same design strength. In

addition, after one year, FRP reinforced members deflected 1.2 to 1.8 times that for the steel reinforced members, depending on the type of the FRP bar (Kage et al. 1995).

According to ACI 318, Section 9.5.2.5, the long-term deflection due to creep and shrinkage, $\Delta_{(cp+sh)}$, can be computed according to the equations given below:

$$\Delta_{(cp+sh)} = \lambda (\Delta_i)_{sus} \quad (8-13a)$$

$$\lambda = \frac{\xi}{1 + 50\rho'} \quad (8-13b)$$

These equations can be used for FRP reinforcement with modifications to account for the differences in concrete compressive stress levels, lower elastic modulus, and different bond characteristics of FRP bars. Because compression reinforcement is not considered for FRP reinforced members ($\rho_f' = 0$), λ is equal to ξ .

Brown (1997) indicated that long-term deflection varies with the compressive stress in the concrete. This issue is not addressed by the equations in ACI 318, which only multiplies the initial deflection by the time dependent factor, ξ . Brown concluded that the creep coefficient should be adjusted twice; first, to account for the compressive stress in concrete, and second, to account for the larger initial deflection.

From available data (Kage et al. 1995; Brown 1997), the modification factor for ξ (ratio of ξ_{FRP}/ξ_{steel}) varies from 0.46 for AFRP and GFRP to 0.53 for CFRP. In another study, the modification factor for ξ based on a failure controlled by concrete crushing varied from 0.75 after one year to 0.58 after 5 years (Vijay and GangaRao 1998). Based on the above results, a modification factor of 0.6 is recommended. The long-term deflection of FRP reinforced members can, therefore, be determined from Eq. (8-14). Further parametric studies and experimental work are necessary to validate Eq. (8-14).

$$\Delta_{(cp+sh)} = 0.6\xi(\Delta_i)_{sus} \quad (8-14)$$

8.4—Creep rupture and fatigue

To avoid creep rupture of the FRP reinforcement under sustained stresses or failure due to cyclic stresses and fatigue of the FRP reinforcement, the stress levels in the FRP reinforcement under these stress conditions should be limited. Because these stress levels will be within the elastic range of the member, the stresses can be computed through an elastic analysis as depicted in Fig. 8.4.

8.4.1 Creep rupture stress limits—To avoid failure of an FRP reinforced member due to creep rupture of the FRP, stress limits should be imposed on the FRP reinforcement. The stress level in the FRP reinforcement can be computed using Eq. (8-15) with M_s equal to the unfactored moment due to all sustained loads (dead loads and the sustained portion of the live load).

$$f_{f,s} = M_s \frac{n_f d(1-k)}{I_{cr}} \quad (8-15)$$

The cracked moment of inertia, I_{cr} , and the ratio of the effective depth to the depth of the elastic neutral axis, k , are computed using Eq. (8-10) and (8-11).

Values for safe sustained stress levels are given in Table 8.2. These values are based on the creep rupture stress limits previously stated in Section 3.3.1 with an imposed safety factor of 1/0.60.

8.4.2 Fatigue stress limits—If the structure is subjected to fatigue regimes, the FRP stress should be limited to the values stated in Table 8.2. The FRP stress can be calculated using Eq. (8-15) with M_s equal to the moment due to all sustained loads plus the maximum moment induced in a fatigue loading cycle.

CHAPTER 9—SHEAR

In this document, FRP stirrups and continuous rectangular spirals are considered for shear reinforcement. Because of their location as an outer reinforcement, stirrups are more susceptible to severe environmental conditions and may be subject to related deterioration, reducing the service life of the structure. Available research results, however, are sufficient to develop a conservative design guideline for FRP shear reinforcement. Due to limited experience, this chapter does not address the use of FRP bars for punching shear reinforcement. Further research is needed in this area.

9.1—General considerations

Several issues need to be addressed when using FRP as shear reinforcement, namely:

- FRP has a relatively low modulus of elasticity;
- FRP has a high tensile strength and no yield point;
- Tensile strength of the bent portion of an FRP bar is significantly lower than the straight portion; and
- FRP has low dowel resistance.

9.1.1 Shear design philosophy—The design of FRP shear reinforcement is based on the strength design method. The strength reduction factor given by ACI 318 for reducing nominal shear capacity of steel-reinforced concrete members should be used for FRP reinforcement as well.

9.2—Shear strength of FRP-reinforced members

According to ACI 318, the nominal shear strength of a reinforced concrete cross section, V_n , is the sum of the shear resistance provided by concrete, V_c , and the steel shear reinforcement, V_s .

Compared to a steel-reinforced section of equal flexural capacity, a cross section using FRP flexural reinforcement after cracking has a smaller depth to the neutral axis because of the lower axial stiffness (that is, product of reinforcement area times modulus of elasticity). The compression region of the cross section is reduced and the crack widths are wider. As a result, the shear resistance provided by both the aggregate interlock and the compressed concrete, V_{cf} , is smaller. Research on the shear capacity of flexural members without shear reinforcement has indicated that the concrete shear strength is influenced by the stiffness of the tensile (flexural) reinforcement (Nagasaka, Fukuyama, and Tanigaki 1993;

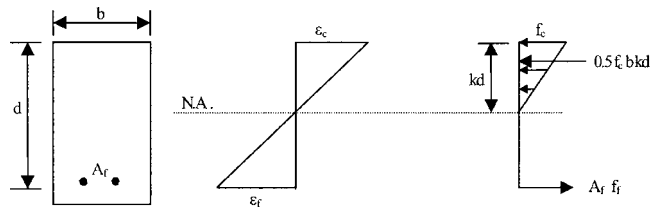


Fig. 8.4—Elastic stress and strain distribution.

Table 8.2—Creep rupture stress limits in FRP reinforcement

Fiber type	GFRP	AFRP	CFRP
Creep rupture stress limit $F_{f,s}$	$0.20f_{ju}$	$0.30f_{ju}$	$0.55f_{ju}$

Zhao, Maruyama, and Suzuki 1995; JSCE 1997; Sonobe et al. 1997; Michaluk et al. 1998).

The contribution of longitudinal FRP reinforcement in terms of dowel action has not been determined. Because of the lower strength and stiffness of FRP bars in the transverse direction, however, it is assumed that their dowel action contribution is less than that of an equivalent steel area. Further research is needed to determine the effect of FRP reinforcement dowel action and in shear friction.

The concrete shear capacity $V_{c,f}$ of flexural members using FRP as main reinforcement can be evaluated as shown below. The proposed equation accounts for the axial stiffness of the FRP reinforcement ($A_f E_f$) as compared to that of steel reinforcement ($A_s E_s$).

$$V_{c,f} = \frac{A_f E_f}{A_s E_s} V_c$$

or

$$V_{c,f} = \frac{\rho_f E_f}{\rho_s E_s} V_c$$

A_s and ρ_s in the equations above represent area of steel and corresponding steel reinforcement ratio for a reinforced concrete section having the same ϕM_n of the FRP reinforced concrete section.

For practical design purposes, the value of ρ_s can be taken as $0.5\rho_{s,max}$ or $0.375\rho_b$. Considering a typical steel yield strength of 60 ksi (420 MPa) for flexural reinforcement, the equation for $V_{c,f}$ proposed by this committee can be expressed as follows

$$V_{c,f} = \frac{\rho_f E_f}{90\beta_1 f'_c} V_c \tag{9-1}$$

The value of $V_{c,f}$ computed in Equation (9-1) cannot be larger than V_c .

The ACI 318 method used to calculate the shear contribution of steel stirrups is applicable when using FRP as shear reinforcement. The shear resistance provided by FRP stir-

rups perpendicular to the axis of the member V_f can be written as:

$$V_f = \frac{A_{fv}f_{fv}d}{s} \quad (9-2)$$

The stress level in the FRP shear reinforcement should be limited to control shear crack widths and maintain shear integrity of the concrete and to avoid failure at the bent portion of the FRP stirrup (see Eq. (7-3)). Equation (9-3) gives the stress level in the FRP shear reinforcement at ultimate for use in design.

$$f_{fv} = 0.004E_f \leq f_{fb} \quad (9-3)$$

When using shear reinforcement perpendicular to the axis of the member, the required spacing and area of shear reinforcement can be computed from Eq. (9-4).

$$\frac{A_{fv}}{s} = \frac{(V_u - \phi V_{cf})}{\phi f_{fv} d} \quad (9-4)$$

When inclined FRP stirrups are used as shear reinforcement, Eq. (9-5) is used to calculate the contribution of the FRP stirrups.

$$V_f = \frac{A_{fv}f_{fv}d}{s}(\sin \alpha + \cos \alpha) \quad (9-5)$$

When continuous FRP rectangular spirals are used as shear reinforcement (in this case s is the pitch and α is the angle of inclination of the spiral), Eq. (9-6) gives the contribution of the FRP spirals.

$$V_f = \frac{A_{fv}f_{fv}d}{s}(\sin \alpha) \quad (9-6)$$

Shear failure modes of members with FRP as shear reinforcement can be classified into two types (Nagasaka, Fukuyama, and Tanigaki 1993): shear-tension failure mode (controlled by the rupture of FRP shear reinforcement) and shear-compression failure mode (controlled by the crushing of the concrete web). The first mode is more brittle, and the latter results in larger deflections. Experimental results have shown that the modes of failure depend on the shear reinforcement index $\rho_{fv}E_f$, where ρ_{fv} is the ratio of FRP shear reinforcement, $A_{fv}/b_w s$. As the value of $\rho_{fv}E_f$ increases, the shear capacity in shear tension increases and the mode of failure changes from shear tension to shear compression.

9.2.1 Limits on tensile strain of shear reinforcement—The design assumption that concrete and reinforcement capacities are added is accurate when shear cracks are adequately controlled. Therefore, the tensile strain in FRP shear reinforcement should be limited to ensure that the ACI design approach is applicable.

The Canadian Highway Bridge Design Code (Canadian Standards Association 2000) limits the tensile strain in FRP shear reinforcement to 0.002 in./in. It is recognized that this strain value (corresponding to the yield strain of Grade 60 steel) may be very conservative. Experimental evidence shows the attainment of higher strain values (Wang 1998; Zhao, Maruyama, and Suzuki 1995; Okamoto, Nagasaka, and Tanigaki 1994). The Eurocrete Project provisions limit the value of the shear strain in FRP reinforcement to 0.0025 in./in. (Dowden and Dolan 1997). Given the high strain to failure of FRP, the engineer could consider using 0.00275 as implicitly allowed by 318-95 for welded wire fabric (Section R11.5.2). In no case should effective strain in FRP shear reinforcement exceed 0.004 nor should the design strength exceed the strength of the bent portion of the stirrup f_{fb} . The value of 0.004 is justified as the strain that prevents degradation of aggregate interlock and corresponding concrete shear (Priestley, Seible, and Calvi 1996).

9.2.2 Minimum amount of shear reinforcement—ACI 318 requires a minimum amount of shear reinforcement when V_u exceeds $\phi V_c/2$. This requirement is to prevent or restrain shear failure in members where the sudden formation of cracks can lead to excessive distress (ACI/ASCE 426-74). To prevent brittle shear failure, adequate reserve strength should be provided to ensure a factor of safety similar to ACI 318 provisions for steel reinforcement. Eq. (9-7) gives the recommended minimum amount of FRP shear reinforcement.

$$A_{fv, min} = \frac{50b_w s}{f_{fv}} \quad (9-7)$$

for SI units

$$A_{fv, min} = 0.35 \frac{b_w s}{f_{fv}}$$

with b_w and s in mm, and f_{fv} in MPa.

The minimum amount of reinforcement given by Eq. (9-7) is independent of the strength of concrete. If steel stirrups are used, the minimum amount of reinforcement provides a shear strength that varies from 1.50 V_c when f'_c is 2500 psi (17 MPa) to 1.25 V_c when f'_c is 10,000 psi (69 MPa). Equation (9-7), which was derived for steel-reinforced members, is more conservative when used with FRP reinforced members. For example, when applied to a flexural member having GFRP as longitudinal reinforcement, the shear strength provided by Eq. (9-7) could exceed 3 V_c . The ratio of the shear strength provided by Eq. (9-7) to V_c will decrease as the stiffness of longitudinal reinforcement increases or as the strength of concrete increases.

9.2.3 Shear failure due to crushing of the web—Studies by Nagasaka, Fukuyama, and Tanigaki (1993) indicate that for FRP reinforced sections, the transition from rupture to crushing failure mode occurs at an average value of 0.3 $f'_c b_w d$ for V_{cf} but can be as low as 0.18 $f'_c b_w d$. When V_{cf} is smaller than 0.18 $f'_c b_w d$, shear-tension can be expected, whereas when V_{cf} exceeds 0.3 $f'_c b_w d$, crushing failure is expected.

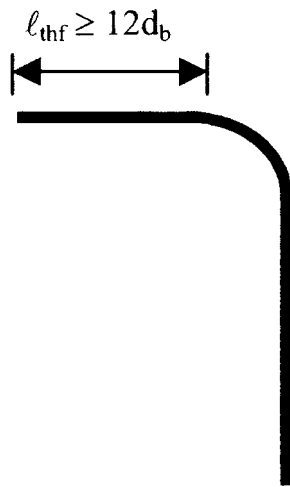


Fig. 9.1—Required tail length for FRP stirrups.

The correlation between rupture and the crushing failure is not fully understood, and it is more conservative to use the ACI 318 limit of $8\sqrt{f'_c} b_w d$ rather than $0.3f'_c b_w d$. It is therefore recommended to use the ACI 318 limit.

9.3—Detailing of shear stirrups

The maximum spacing of vertical steel stirrups given in ACI 318 as the smaller of $d/2$ or 24 in. is used for vertical FRP shear reinforcement. This limit ensures that each shear crack is intercepted by at least one stirrup.

Tests by Ehsani, Saadatmanesh, and Tao (1995) indicated that for specimens with r_b/d_b of zero, the reinforcing bars failed in shear at very low load levels at the bends. Therefore, although manufacturing of FRP bars with sharp bends is possible, such details should be avoided. A minimum r_b/d_b ratio of three is recommended. In addition, FRP stirrups should be closed with 90-degree hooks.

ACI 318 provisions for bond of hooked steel bars cannot be applied directly to FRP reinforcing bars because of their different mechanical properties. The tensile force in a vertical stirrup leg is transferred to the concrete through the tail beyond the hook, as shown in Fig. 9.1. Ehsani, Saadatmanesh, and Tao (1995) found that for a tail length, l_{thf} , beyond $12d_b$, there is no significant slippage and no influence on the tensile strength of the stirrup leg. Therefore, it is recommended that a minimum tail length of $12d_b$ be used.

CHAPTER 10—TEMPERATURE AND SHRINKAGE REINFORCEMENT

Shrinkage and temperature reinforcement is intended to limit crack width. The stiffness and strength of reinforcing bars control this behavior. Shrinkage cracks perpendicular to the member span are restricted by flexural reinforcement; thus, shrinkage and temperature reinforcement are only required in the direction perpendicular to the span. ACI 318 requires a minimum steel reinforcement ratio of 0.0020 when using Grade 40 or 50 deformed steel bars and 0.0018 when using Grade 60 deformed bars or welded fabric (deformed or smooth). ACI 318 also requires that the spacing of shrinkage and temperature reinforcement not exceed five times the member thickness or 18 in. (500 mm).

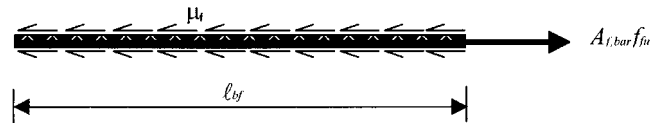


Fig. 11.1—Transfer of force through the development length.

No experimental data are available for the minimum FRP reinforcement ratio for shrinkage and temperature. ACI 318, Section 7.12.2, states that for slabs with steel reinforcement having a yield stress exceeding 60 ksi (414 MPa) measured at a yield strain of 0.0035, the ratio of reinforcement to gross area of concrete should be at least $0.0018 \times 60/f_y$, where f_y is in ksi, but not less than 0.0014. The stiffness and the strength of shrinkage and temperature FRP reinforcement can be incorporated in this formula. Therefore, when deformed FRP shrinkage and temperature reinforcement is used, the amount of reinforcement should be determined by using Eq. (10-1).

$$\rho_{f,ts} = 0.0018 \times \frac{60,000 E_s}{f_{fu} E_f} \text{ (US)} \quad (10-1)$$

$$\rho_{f,ts} = 0.0018 \times \frac{414 E_s}{f_{fu} E_f} \text{ (SI)}$$

Due to limited experience, it is recommended that the ratio of temperature and shrinkage reinforcement given by Eq. (10-1) be taken not less than 0.0014, the minimum value specified by ACI 318 for steel shrinkage and temperature reinforcement. The engineer may consider an upper limit for the ratio of temperature and shrinkage reinforcement equal to 0.0036, or compute the ratio based on calculated strain levels corresponding to the nominal flexural capacity rather than the strains calculated using Eq. (10-1). Spacing of shrinkage and temperature FRP reinforcement should not exceed three times the slab thickness or 12 in. (300 mm), whichever is less.

CHAPTER 11—DEVELOPMENT AND SPLICES OF REINFORCEMENT

In a reinforced concrete flexural member, the tension force carried by the reinforcement balances the compression force in the concrete. The tension force is transferred to the reinforcement through the bond between the reinforcement and the surrounding concrete. Bond stresses exist whenever the force in the tensile reinforcement changes. Bond between FRP reinforcement and concrete is developed through a mechanism similar to that of steel reinforcement and depends on FRP type, elastic modulus, surface deformation, and the shape of the FRP bar (Al-Zahrani et al. 1996; Uppuluri et al. 1996; Gao, Benmokrane, and Tighiouart 1998b).

11.1—Development length of a straight bar

Figure 11.1 shows the equilibrium condition of an FRP bar with a length equal to its basic development length, l_{bf} . The force in the bar is resisted by an average bond stress, μ_f , acting on the surface of the bar. Equilibrium of forces can be written as follows

$$l_{bf}\pi d\mu_f = A_{f,bar}f_{fu} \quad (11-1)$$

in which $A_{f,bar}$ is the area of one bar.

Rearranging Eq. (11-1), the basic development length can be expressed as

$$l_{bf} = \frac{A_{f,bar}f_{fu}}{\pi d\mu_f} \quad (11-2)$$

or

$$l_{bf} = \frac{d_b f_{fu}}{4\mu_f} \quad (11-3)$$

Research in development length (Orangun, Jirsa, and Breen 1977) has illustrated that the bond stress of steel bars is a function of the concrete strength and the bar diameter. A general expression for the average bond stress can be expressed as follows

$$\mu = \frac{K_1 \sqrt{f'_c}}{d_b} \quad (11-4)$$

where K_1 is a constant. By substituting Eq. (11-4) into Eq. (11-1), the basic development length of FRP reinforcement can be expressed as

$$l_{bf} = K_2 \frac{d_b^2 f_{fu}}{\sqrt{f'_c}} \quad (11-5)$$

where K_2 is a new constant.

For FRP reinforcement several investigators have attempted to determine experimentally the K_2 factor for given bar types. Pleimann (1987, 1991) conducted pullout tests with No. 2, 3, and 4 FRP bars. Two types of FRP bars were used in these tests: glass and aramid FRP bars. The proposed K_2 factors were 1/19.4 and 1/18 for GFRP and AFRP, respectively. Faza and GangaRao (1990) investigated the bond behavior of FRP bars by testing cantilever beams and pullout specimens. They proposed a K_2 factor equal to 1/16.7. Ehsani, Saadatmanesh, and Tao (1996a) tested 48 beam specimens and 18 pullout specimens with No. 3, 6, and 9 GFRP bars. Based on the test results, they proposed a K_2 factor equal to 1/21.3. Tighiouart, Benmokrane, and Gao (1998) tested 45 beam specimens using two types of No. 4, 5, 6, and 8 GFRP bars. They suggested that the K_2 factor is equal to 1/5.6.

For pullout controlled failure rather than concrete splitting, Ehsani, Saadatmanesh, and Tao (1996a) and Gao, Benmokrane, and Tighiouart (1998b) proposed the following equation

$$l_{bf} = \frac{d_b f_{fu}}{K_3} \quad (11-6)$$

where K_3 had a numerical value of approximately 2850.

In light of the above findings, a conservative estimate of the basic development length of FRP bars controlled by pullout failure is given by

$$l_{bf} = \frac{d_b f_{fu}}{2700} \quad (11-7a)$$

For SI units,

$$l_{bf} = \frac{d_b f_{fu}}{18.5}$$

with l_{bf} in mm, f_{fu} in MPa, and d_b in mm.

Splitting of concrete is prevented by imposing a modification to the basic development length computed by Eq. (11-7a) based on concrete cover (see Section 11.1.2). Manufacturers can furnish alternative values of the required basic development length based on substantiated tests conducted in accordance with available testing procedures. Reinforcement should be deformed or surface-treated to enhance bond characteristics with concrete.

11.1.1 Bar location modification factor—While placing concrete, air, water, and fine particles migrate upwards through the concrete. This can cause a significant drop in bond strength under the horizontal reinforcement. The term top reinforcement usually refers to horizontal reinforcement with more than 12 in. (305 mm) of concrete below it at the time of embedment. Challal and Benmokrane (1993) investigated the top bar modification factors for three different bar diameters (No. 4, 5, and 6). The modification factor varied from 1.08 to 1.38 for normal-strength concrete and from 1.11 to 1.22 for high-strength concrete. In another experiment (Ehsani, Saadatmanesh, and Tao 1996b), No. 4 and 6 GFRP bars were placed at the top, middle, and bottom of a concrete wall (48 x 30 x 16 in. [1.22 x 0.76 x 0.41 m]) with an equal spacing of 16 in. (0.41 cm). The modification factor varied from 1.09 to 1.14 for middle to top bars and 1.26 to 1.32 for bottom to top bars. Based on the available data, the use of a modification factor of 1.3 is recommended when calculating the development length of top FRP bars, as shown in Eq. (11-7b).

11.1.2 Concrete cover modification factor—The concrete cover has a significant impact on the failure mechanism. When the concrete cover is less than or equal to two bar diameters, $2d_b$, a splitting failure can occur; if the concrete cover exceeds two bar diameters, a pullout failure is more likely (Ehsani, Saadatmanesh, and Tao 1996a). Experimental investigation on the effect of concrete cover (Ehsani, Saadatmanesh, and Tao 1996b) through pullout tests indicated that the ratio of the nominal tensile strength of the bar to the measured strength with concrete covers of $2d_b$ to d_b varied between 1.2 and 1.5.

In this document, it is recommended that the concrete cover for FRP reinforcement be not less than d_b . The modification factor of 1.5 should be used as a multiplier of the basic development length when the concrete cover or the reinforcement

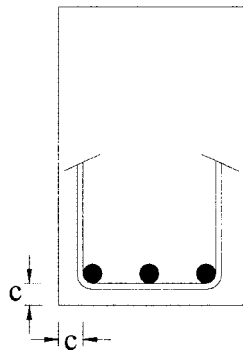


Fig. 11.2—Clear concrete cover.

spacing is equal to d_b . For concrete cover or reinforcement spacing larger than $2d_b$, a modification factor of 1.0 should be applied. Linear interpolation of these factors is allowed for concrete cover or reinforcement spacing between d_b and $2d_b$, as shown in Eq. (11-7c).

The development length l_{df} shall be expressed as a function of the basic development length l_{bf}

$$l_{df} = k_m l_{bf} \tag{11-7b}$$

where $k_m = 1.3$ for top bars, and for bottom bars (see Fig. 11.1)

$$k_m = \begin{cases} 1.0 & \text{if } c > 2d_b \\ \frac{4d_b - c}{2d_b} & \text{if } d_b \leq c \leq 2d_b \end{cases} \tag{11-7c}$$

where c is as shown in Fig. 11.2.

11.2—Development length of a bent bar

Limited experimental data are available on the bond behavior of hooked FRP reinforcing bars. ACI 318 provisions for development length of hooked steel bars are not applicable to FRP bars due to the differences in material characteristics.

Ehsani, Saadatmanesh, and Tao (1996b) tested 36 specimens with hooked GFRP bars. Based on the results of the study, the expression for the development length of a 90-degree hooked bar, l_{bhf} , was proposed as follows

$$l_{bhf} = K_4 \frac{d_b}{\sqrt{f'_c}} \tag{11-8}$$

The K_4 factor for the calculation of the development length in this equation is 1820 for bars with f_{fu} less than 75,000 psi (517 MPa). This factor should be multiplied by $f_{fu}/75,000$ for bars having a tensile strength between 75,000 psi (517 MPa) and 150,000 psi (1034 MPa).

When the side cover (normal to the plane of hook) is more than 2-1/2 in. (6.4 cm) and the cover extension beyond hook is not less than 2 in. (5 cm), another multiplier of 0.7 can be applied (Ehsani, Saadatmanesh, and Tao 1996b). These modification factors are similar to those in ACI 318, Section 12.5.3, for steel hooked bars. To account for the lack of experimental data,

Table 11.1—Type of tension lap splice required

		Maximum percentage of A_f spliced within required lap length	
		50%	100%
$\frac{A_{f,provided}}{A_{f,required}}$	Equivalent to	f_f/f_{fu}	
		2 or more	
Less than 2		0.5 or less	Class A
		More than 0.5	Class B

the use of Eq. (11-9) in calculating the development length of hooked bars is recommended by the committee.

$$l_{bhf} = \begin{cases} 2000 \frac{d_b}{\sqrt{f'_c}} & \text{for } f_{fu} \leq 75,000 \text{ psi} \\ \frac{f_{fu}}{37.5} \frac{d_b}{\sqrt{f'_c}} & \text{for } 75,000 < f_{fu} < 150,000 \text{ psi} \\ 4000 \frac{d_b}{\sqrt{f'_c}} & \text{for } f_{fu} \geq 150,000 \text{ psi} \end{cases} \tag{11-9}$$

For SI units,

$$l_{bhf} = \begin{cases} 165 \frac{d_b}{\sqrt{f'_c}} & \text{for } f_{fu} \leq 520 \text{ MPa} \\ 3.1 \frac{f_{fu}}{\sqrt{f'_c}} \frac{d_b}{\sqrt{f'_c}} & \text{for } 520 < f_{fu} < 1040 \text{ MPa} \\ 330 \frac{d_b}{\sqrt{f'_c}} & \text{for } f_{fu} \geq 1040 \text{ MPa} \end{cases}$$

with l_{bhf} in mm, f_{fu} and f'_c in MPa, and d_b in mm.

The value calculated using Eq. (11-9) should not be less than $12d_b$ or 9 in. (23 cm). These values are based on test results reported by Ehsani, Saadatmanesh, and Tao (1995), in which the tensile force and slippage of a hooked bar stabilized in the neighborhood of $12d_b$. The tail length of a hooked bar, l_{thf} (see Fig. 9.1), should not be less than $12d_b$. Longer tail lengths were found to have an insignificant influence on the ultimate tensile force and slippage of the hook. To avoid shear failure at the bend, the radius of the bend should not be less than $3d_b$ (Ehsani, Saadatmanesh, and Tao 1995).

11.3—Tension lap splice

ACI 318, Section 12.15, distinguishes between two types of tension lap splices depending on the fraction of the bars spliced in a given length and on the reinforcement stress in the splice. Table 11.1 is a reproduction of Table R12.15.2 given in ACI 318, with modifications applicable to FRP reinforcement. For steel reinforcement, the splice length for a Class A splice is $1.0l_d$ and for Class B splice is $1.3l_d$.

Limited data are available for the minimum development length of FRP tension lap splices. For Class B, available research has indicated that the ultimate capacity of the FRP

bar is achieved at $1.6l_{df}$ (Benmokrane 1997). Because the stress level for Class A splices is not to exceed 50% of the tensile strength of the bar, using the value of $1.3l_{df}$ should be conservative. Further research is required in this area; however, the values of 1.3 and $1.6l_{df}$ are recommended at this time for Class A and B.

CHAPTER 12—SLABS ON GROUND

Normally, slabs on ground impart a pressure to the grade or soil that is less than 50% of its allowable bearing capacity. Two of the most common types of construction for slabs on ground are discussed in this chapter: these are plain concrete slabs and slabs reinforced with temperature and shrinkage reinforcement.

12.1—Design of plain concrete slabs

Plain concrete slabs on ground transmit loads to the subgrade with minimal distress and are designed to remain uncracked under service loads. To reduce shrinkage crack effects, the spacing of construction or contraction joints, or both, is usually limited. For details of design methods of plain concrete slabs on ground, refer to ACI 360R.

12.2—Design of slabs with shrinkage and temperature reinforcement

When designing a slab with shrinkage and temperature reinforcement, it should be considered a plain concrete slab without reinforcement to determine its thickness. The slab is assumed to remain uncracked when loads are placed on its surface. Shrinkage crack width and spacing are limited by a nominal amount of distributed FRP reinforcement placed in the upper half of the slab. The primary purpose of shrinkage reinforcement is to control the width of any crack that forms between joints. Shrinkage reinforcement does not prevent cracking nor does it significantly add to the flexural capacity of the slab. Increasing the thickness of the slab can increase the flexural capacity.

Even though the slab is intended to remain uncracked under service loading, the reinforcement is used to limit crack spacing and width, permit the use of wider joint spacing, increase the ability to transfer load at joints, and provide a reserve strength after shrinkage or temperature cracking has occurred.

The subgrade drag method is frequently used to determine the amount of nonprestressed shrinkage and temperature reinforcement that is needed but does not apply when prestressing or randomly distributed fibers are used (PCA 1990). When using steel reinforcement, the drag equation is as follows

$$A_s = \frac{\mu L w}{2f_s}$$

where

A_s = cross-sectional area of steel per linear foot, in.²;

f_s = allowable stress in steel reinforcement, psi, commonly taken as 2/3 to 3/4 of f_y ;

μ = coefficient of subgrade friction; (1.5 is recommended for floors on ground, [PCA 1990])

L = distance between joints, ft; and

w = dead weight of the slab, psf, usually assumed to be 12.5 psf per in. of slab thickness.

Because of the lower modulus of the FRP reinforcement, the governing equation should be based on the strain rather than the stress level when designing shrinkage and temperature FRP reinforcement. At the allowable stress, the strain in steel reinforcement is about 0.0012; implementing the same strain for FRP will result in a stress of $0.0012 E_f$, and Eq. (12-1) can be written.

$$A_{f,sh} = \frac{\mu L w}{2(0.0012 E_f)} \quad (12-1)$$

where $A_{f,sh}$ is the cross-sectional area of FRP reinforcement (in.²) per linear foot.

Equation (12-1) can also be used to determine joint spacing, L , for a set amount of reinforcement. No experimental data have been reported on FRP slab-on-ground applications; research is required to validate this approach.

CHAPTER 13—REFERENCES

13.1—Referenced standards and reports

The standards and reports listed below were the latest editions at the time this document was prepared. Because these documents are revised frequently, the reader is advised to contact the proper sponsoring organization for the latest edition.

American Concrete Institute (ACI)

- 117 Standard Tolerance for Concrete Construction and Materials
- 318-95 Building Code Requirements for Structural Concrete and Commentary
- 360R Design of Slabs on Ground
- 426-74 The Shear Strength of Reinforced Concrete Members (Joint ACI-ASCE)
- 440R State-of-the-Art Report on FRP for Concrete Structures

These publications may be obtained from:

American Concrete Institute
P. O. Box 9094
Farmington Hills, Mich. 48333-9094

13.2—Cited references

Adimi, R.; Rahman, H.; Benmokrane, B.; and Kobayashi, K., 1998, "Effect of Temperature and Loading Frequency on the Fatigue Life of a CFRP Bar in Concrete," *Proceedings of the Second International Conference on Composites in Infrastructure (ICCI-98)*, Tucson, Ariz., V. 2, pp. 203-210.

Al-Dulaijan, S. U.; Nanni, A.; Al-Zahrani, M. M.; and Bakis, C. E., 1996, "Bond Evaluation of Environmentally Conditioned GFRP/Concrete System," *Proceedings of the Second International Conference on Advanced Composite Materials in Bridges and Structures (ACMBS-2)*, M. M. El-Badry, ed., Canadian Society for Civil Engineering, Montreal, Quebec, pp. 845-852.

Almusallam, T. H.; Al-Salloum, Y.; Alsayed, S.; and Amjad, M., 1997, "Behavior of Concrete Beams Doubly Reinforced by FRP Bars," *Proceedings of the Third International Symposium on Non-Metallic (FRP) Reinforcement for Concrete Structures (FRPRCS-3)*, Japan Concrete Institute, Sapporo, Japan, V. 2, pp. 471-478.

Al-Zahrani, M. M.; A. Nanni; Al-Dulaijan, S. U.; and Bakis, C. E., 1996, "Bond of FRP to Concrete for Rods with Axisymmetric Deformations," *Proceedings of the Second International Conference on Advanced Composite Materials in Bridges and Structures (ACMBS-II)*, Montreal, Canada, pp. 853-860.

Ando, N.; Matsukawa, H.; Hattori, A.; and Mashima, A., 1997, "Experimental Studies on the Long-Term Tensile Properties of FRP Tendons," *Proceedings of the Third International Symposium on Non-Metallic (FRP) Reinforcement for Concrete Structures (FRPRCS-3)*, Japan Concrete Institute, Sapporo, Japan, V. 2, pp. 203-210.

Arrhenius, S. A., 1925, *Chemistry in Modern Life*, D. Van Nostrand Company, New York, N.Y.

Bakis, C. E., 1993, "FRP Composites: Materials and Manufacturing," *Fiber-Reinforced-Plastic for Concrete Structures: Properties and Applications*, A. Nanni, ed., Elsevier, Amsterdam, pp. 13-58.

Bakis, C. E.; Al-Dulaijan, S. U.; Nanni, A.; Boothby, T. E. and Al-Zahrani, M. M., 1998a, "Effect of Cyclic Loading on Bond Behavior of GFRP Rods Embedded in Concrete Beams," *Journal of Composites Technology and Research*, V. 20, No. 1, pp. 29-37.

Bakis, C. E.; Freimanis, A. J.; Gremel, D.; and Nanni, A., 1998b, "Effect of Resin Material on Bond and Tensile Properties of Unconditioned and Conditioned FRP Reinforcement Rods," *Proceedings of the First International Conference on Durability of Composites for Construction*, B. Benmokrane, and H. Rahman, eds., Sherbrooke, Quebec, pp. 525-535.

Bank, L. C., 1993, "Properties of FRP Reinforcement for Concrete," *Fiber-Reinforced-Plastic (FRP) Reinforcement for Concrete Structures: Properties and Applications, Developments in Civil Engineering*, V. 42, A. Nanni, ed., Elsevier, Amsterdam, pp. 59-86.

Bank, L. C., and Puterman, M., 1997, "Microscopic Study of Surface Degradation of Glass Fiber-Reinforced Polymer Rods Embedded in Concrete Castings Subjected to Environmental Conditioning," *High Temperature and Environmental Effects on Polymeric Composites*, V. 2, ASTM STP 1302, T. S. Gates and A.-H. Zureick, eds., American Society for Testing and Materials, West Conshohocken, Pa., pp. 191-205.

Bank, L. C.; Puterman, M.; and Katz, A., 1998, "The Effect of Material Degradation on Bond Properties of FRP Reinforcing Bars in Concrete," *ACI Materials Journal*, V. 95, No. 3, May-June, pp. 232-243.

Benmokrane, B., 1997, "Bond Strength of FRP Rebar Splices," *Proceedings of the Third International Symposium on Non-Metallic (FRP) Reinforcement for Concrete Structures (FRPRCS-3)*, Japan Concrete Institute, Sapporo, Japan, V. 2, pp. 405-412.

Benmokrane, B.; Chaallal, O.; and Masmoudi, R., 1996, "Flexural Response of Concrete Beams Reinforced with FRP Reinforcing Bars," *ACI Structural Journal*, V. 93, No. 1, Jan.-Feb., pp. 46-55.

Benmokrane, B., and Rahman, H., eds., 1998, "Durability of Fiber Reinforced Polymer (FRP) Composites for Construction," *Proceedings of the First International Conference (CDCC '98)*, Quebec, Canada, 692 pp.

Benmokrane, B.; Tighiouart, B.; and Chaallal, O., 1996, "Bond Strength and Load Distribution of Composite GFRP Reinforcing Bars in Concrete," *ACI Materials Journal*, V. 93, No. 3, May-June, pp. 246-253.

Boyle, H. C., and Karbhari, V. M., 1994, "Investigation of Bond Behavior Between Glass Fiber Composite Reinforcements and Concrete," *Journal of Polymer-Plastic Technology Engineering*, V. 33, No. 6, pp. 733-753.

Branson, D. E., 1977, *Deformation of Concrete Structures*, McGraw-Hill Book Co., New York, N.Y., pp. 546.

Brown, V., 1997, "Sustained Load Deflections in GFRP-Reinforced Concrete Beams," *Proceedings of the Third International Symposium on Non-Metallic (FRP) Reinforcement for Concrete Structures (FRPRCS-3)*, Japan Concrete Institute, Sapporo, Japan, V. 2, pp. 495-502.

Brown, V., and Bartholomew, C., 1996, "Long-term Deflections of GFRP-Reinforced Concrete Beams," *Proceedings of the First International Conference on Composites in Infrastructure (ICCI-96)*, Tucson, Ariz., pp. 389-400.

CAN/CSA-S6-00, 2000, "Canadian High Bridge Design Code," Clause 16.8.6, Canadian Standard Association (CSA) International, Toronto, Ontario, Canada, 734 pp.

Challal, O., and Benmokrane, B., 1993, "Pullout and Bond of Glass-Fiber Rods Embedded in Concrete and Cement Grout," *Materials and Structures*, V. 26, pp. 167-175.

Clarke, J., and Sheard, P., 1998, "Designing Durable FRP Reinforced Concrete Structures," *Proceedings of the First International Conference on Durability of Composites for Construction*, B. Benmokrane, and H. Rahman, eds., Sherbrooke, Quebec, pp. 13-24.

Conrad, J. O.; Bakis, C. E.; Boothby, T. E.; and Nanni, A., 1998, "Durability of Bond of Various FRP Rods in Concrete," *Proceedings of the First International Conference on Durability of Composites for Construction*, B. Benmokrane, and H. Rahman, eds., Sherbrooke, Quebec, Canada, pp. 299-310.

Coomarasamy, A., and Goodman, S., 1997, "Investigation of the Durability Characteristics of Fiber Reinforced Polymer (FRP) Materials in Concrete Environment," *American Society for Composites—Twelfth Technical Conference*, Dearborn, Mich.

Curtis, P. T., 1989, "The Fatigue Behavior of Fibrous Composite Materials," *Journal of Strain Analysis*, V. 24, No. 4, pp. 235-244.

Dally, J. W., and Riley, W. F., 1991, *Experimental Stress Analysis*, Third Edition, McGraw Hill, New York, N.Y.

Devalapura, R. K.; Greenwood, M. E.; Gauchel, J. V.; and Humphrey, T. J., 1996, *Advanced Composite Materials in Bridges and Structures*, M. M. El-Badry, ed., Canadian Society for Civil Engineering, Montreal, Quebec, pp. 107-116.

Dolan, C. W.; Rizkalla, S.; and Nanni, A., eds., 1999, *Fiber-Reinforced-Polymer Reinforcement for Reinforced Concrete Structures*, SP-188, American Concrete Institute, Farmington Hills, Mich., 1182 pp.

Dowden, D. M., and Dolan, C. W., 1997, "Comparison of Experimental Shear Data With Code Predictions For FRP Prestressed Beams," *Proceedings of the Third International Symposium on Non-Metallic (FRP) Reinforcement for Concrete Structures (FRPRCS-3)*, Japan Concrete Institute, Sapporo, Japan, V. 2, pp. 687-694.

Ehsani, M. R., 1993, "Glass-Fiber Reinforcing Bars," *Alternative Materials for the Reinforcement and Prestressing of Concrete*, J. L. Clarke, Blackie Academic & Professional, London, England, pp. 35-54.

Ehsani, M. R.; Saadatmanesh, H.; and Tao, S., 1995, "Bond of Hooked Glass Fiber Reinforced Plastic (GFRP) Reinforcing Bars to Concrete," *ACI Materials Journal*, V. 92, No. 4, July-Aug., pp. 391-400.

Ehsani, M. R.; Saadatmanesh, H.; and Tao, S., 1996a, "Design Recommendation for Bond of GFRP Rebars to Concrete," *Journal of Structural Engineering*, V. 122, No. 3, pp. 247-257.

Ehsani, M. R.; Saadatmanesh, H.; and Tao, S., 1996b, "Bond Behavior and Design Recommendations for Fiber-Glass Reinforcing Bars," *Proceedings of the First International Conference on Composites in Infrastructure (ICCI-96)*, Tucson, Ariz., pp. 466-476.

El-Badry, M., ed., 1996, "Advanced Composite Materials in Bridges and Structures (ACMBS-II)," *Proceedings of the Second International Conference*, Montreal, Canada, 1027 pp.

Eurocode Provisions, 1999, "Interim Guidance on the Design of Reinforced Concrete Structures Using Fibre Composite Reinforcement," SETO, Institution of Structural Engineers.

Faza, S. S., 1991, "Bending and Bond Behavior and Design of Concrete Beams Reinforced with Fiber Reinforced Plastic Rebars," PhD dissertation, West Virginia University, Morgantown, W.Va., pp. 213.

Faza, S. S., and GangaRao, H. V. S., 1990, "Bending and Bond Behavior of Concrete Beams Reinforced with Plastic Rebars," *Transportation Research Record* 1290, pp. 185-193.

Faza, S. S., and GangaRao, H. V. S., 1993a, "Theoretical and Experimental Correlation of Behavior of Concrete Beams Reinforced with Fiber Reinforced Plastic Rebars," *Fiber-Reinforced-Plastic Reinforcement for Concrete Structures*, SP-138, A. Nanni and C. W. Dolan, eds., American Concrete Institute, Farmington Hills, Mich., pp. 599-614.

Faza, S. S., and GangaRao, H. V. S., 1993b, "Glass FRP Reinforcing Bars for Concrete," *Fiber-Reinforced-Plastic (FRP) Reinforcement for Concrete Structures: Properties and Applications, Developments in Civil Engineering*, V. 42, A. Nanni, ed., Elsevier, Amsterdam, pp. 167-188.

Freimanis, A. J.; Bakis, C. E.; Nanni, A.; and Gremel, D., 1998, "A Comparison of Pullout and Tensile Behaviors of FRP Reinforcement for Concrete," *Proceedings of the Second International Conference on Composites in Infrastructure (ICCI-98)*, Tucson, Ariz., V. 2, pp. 52-65.

GangaRao, H. V. S., and Vijay, P. V., 1997a, "Design of Concrete Members Reinforced with GFRP Bars," *Proceed-*

ings of the Third International Symposium on Non-Metallic (FRP) Reinforcement for Concrete Structures (FRPRCS-3), Japan Concrete Institute, Sapporo, Japan, V. 1, pp. 143-150.

GangaRao, H. V. S., and Vijay, P. V., 1997b, "Aging of Structural Composites under Varying Environmental Conditions," *Non-Metallic (FRP) Reinforcement for Concrete Structures, FRPRCS-3*, V. 2, Japan Concrete Institute, Tokyo, pp. 91-98.

Gao, D.; Benmokrane, B.; and Masmoudi, R., 1998a, "A Calculating Method of Flexural Properties of FRP-Reinforced Concrete Beam: Part 1: Crack Width and Deflection," *Technical Report*, Department of Civil Engineering, University of Sherbrooke, Sherbrooke, Quebec, Canada, 24 pp.

Gao, D.; Benmokrane, B.; and Tighiouart, B., 1998b, "Bond Properties of FRP Rebars to Concrete," *Technical Report*, Department of Civil Engineering, University of Sherbrooke, Sherbrooke, Quebec, Canada, 27 pp.

Gentry, T. R.; Bank, L. C.; Barkatt, A.; and Prian, L., 1998, "Accelerated Test Methods to Determine the Long-Term Behavior of Composite Highway Structures Subject to Environmental Loading," *J. Composites Technology & Research*, V. 20, No. 1, pp. 38-50.

Gergely, P., and Lutz, L. A., 1973, "Maximum Crack width in Reinforced Concrete Flexural Members," *Causes, Mechanism and Control of Cracking in Concrete*, SP-20, R. E. Philleo, ed., American Concrete Institute, Farmington Hills, Mich., pp. 87-117.

Gerritse, A., 1992, "Durability Criteria for Non-Metallic Tendons in an Alkaline Environment," *Proceedings of the First International Conference on Advance Composite Materials in Bridges and Structures (ACMBS-I)*, Canadian Society of Civil Engineers, Sherbrooke, Canada, pp. 129-137.

Hayes, M. D.; Garcia, K.; Verghese, N.; and Lesko, J., 1998, "The Effect of Moisture on the Fatigue Behavior of a Glass/Vinyl Ester Composite," *Proceedings of the Second International Conference on Composites in Infrastructure (ICCI-98)*, Tucson, Ariz., V. 1, pp. 1-12.

Hughes, B. W., and Porter, M. L., 1996, "Experimental Evaluation of Non-Metallic Dowel Bars in Highway Pavements," *Proceedings of the First International Conference on Composites in Infrastructure (ICCI-96)*, Tucson, Ariz., pp. 440-450.

Iyer, S. L., and Sen, R., eds., 1991, "Advanced Composite Materials in Civil Engineering Structures," *Proceedings of the Specialty Conference*, American Society of Civil Engineers, New York, N.Y., 443 pp.

Jaeger, L. G.; Mufti, A.; and Tadros, G., 1997, "The Concept of the Overall Performance Factor in Rectangular-Section Reinforced Concrete Beams," *Proceedings of the Third International Symposium on Non-Metallic (FRP) Reinforcement for Concrete Structures (FRPRCS-3)*, Japan Concrete Institute, Sapporo, Japan, V. 2, pp. 551-558.

Japan Society of Civil Engineers (JSCE) Subcommittee on Continuous Fiber Reinforcement, 1992, *Proceedings of the Utilization of FRP-Rods for Concrete Reinforcement*, Japan Society of Civil Engineers, Tokyo, Japan, 314 pp.

Japan Society of Civil Engineers (JSCE), 1997a, *Proceedings of the Third International Symposium on Non-Metallic*

(FRP) Reinforcement for Concrete Structures (FRPRCS-3), Japan Concrete Institute, Sapporo, Japan, V. 2, pp. 511-518.

Japan Society of Civil Engineers (JSCE), 1997b, "Recommendation for Design and Construction of Concrete Structures Using Continuous Fiber Reinforcing Materials," *Concrete Engineering Series* No. 23, 325 pp.

Kachlakev, D. I., and Lundy, J. R., 1998, "Bond Strength Study of Hollow Composite Rebars with Different Micro Structure," *Proceedings of the Second International Conference on Composites in Infrastructure (ICCI-98)*, Tucson, Ariz., pp. 1-14.

Kage, T.; Masuda, Y.; Tanano, Y.; and Sato, K., 1995, "Long-term Deflection of Continuous Fiber Reinforced Concrete Beams," *Proceedings of the Second International RILEM Symposium on Non-Metallic (FRP) Reinforcement for Concrete Structures (FRPRCS-2)*, Ghent, Belgium, pp. 251-258.

Katz, A., 1998, "Effect of Helical Wrapping on Fatigue Resistance of GFRP," *Journal of Composites for Construction*, V. 2, No. 3, pp. 121-125.

Katz, A.; Berman, N.; and Bank, L. C., 1998, "Effect of Cyclic Loading and Elevated Temperature on the Bond Properties of FRP Rebars," *International Conference on the Durability of Fiber Reinforced Polymer (FRP) Composites for Construction*, Sherbrooke, Canada, pp. 403-413.

Katz, A.; Berman, N.; and Bank, L. C., 1999, "Effect of High Temperature on the Bond Strength of FRP Rebars," *Journal of Composites for Construction*, V. 3, No. 2, pp. 73-81.

Katz, A., 2000, "Bond to Concrete of FRP Rebars after Cyclic Loading," *Journal of Composites for Construction*, V. 4, No. 3, pp. 137-144.

Keesler, R. J., and Powers, R. G., 1988, "Corrosion of Epoxy Coated Rebars—Keys Segmental Bridge—Monroe County," *Report* No. 88-8A, Florida Dept. of Transportation, Materials Office, Corrosion Research Laboratories, Gainesville, Fla.

Kobayashi, K., and Fujisaki, T., 1995, "Compressive Behavior of FRP Reinforcement in Non-prestressed Concrete Members," *Proceedings of the Second International RILEM Symposium on Non-Metallic (FRP) Reinforcement for Concrete Structures (FRPRCS-2)*, Ghent, Belgium, pp. 267-274.

Kumahara, S.; Masuda, Y.; and Tanano, Y., 1993, "Tensile Strength of Continuous Fiber Bar Under High Temperature," *International Symposium on Fiber-Reinforced-Plastic Reinforcement for Concrete Structures*, SP-138, A. Nanni and C. W. Dolan, eds., American Concrete Institute, Farmington Hills, Mich., pp. 731-742.

Litherland, K. L.; Oakley, D. R.; and Proctor, B. A., 1981, "The Use of Accelerated Aging Procedures to Predict the Long Term Strength of GRC Composites," *Cement and Concrete Research*, V. 11, No. 3, pp. 455-466.

Mallick, P. K., 1988, *Fiber Reinforced Composites, Materials, Manufacturing, and Design*, Marcell Dekker, Inc., New York, N.Y., 469 pp.

Mandell, J. F., 1982, "Fatigue Behavior of Fiber-Resin Composites," *Developments in Reinforced Plastics*, Applied Science Publishers, London, England, V. 2, pp. 67-107.

Mandell, J. F., and Meier, U., 1983, "Effects of Stress Ratio Frequency and Loading Time on the Tensile Fatigue of Glass-Reinforced Epoxy," *Long Term Behavior of Composites*, ASTM STP 813, American Society for Testing and Materials, West Conshohocken, Pa., pp. 55-77.

Masmoudi, R.; Benmokrane, B.; and Challal, O., 1996, "Cracking Behavior of Concrete Beams Reinforced with FRP Rebars," *Proceedings of the First International Conference on Composites in Infrastructure (ICCI-96)*, Tucson, Ariz., pp. 374-388.

Meier, U., 1992, "Carbon Fiber Reinforced Polymers: Modern Materials in Bridge Engineering," *Structural Engineering International, Journal of the International Association for Bridge and Structural Engineering*, V. 2, No. 1, pp. 7-12.

Michaluk, C. R.; Rizkalla, S.; Tadros, G.; and Benmokrane, B., 1998, "Flexural Behavior of One-Way Concrete Slabs Reinforced by Fiber Reinforced Plastic Reinforcement," *ACI Structural Journal*, V. 95, No. 3, May-June, pp. 353-364.

MIL-17, 1999, *Guidelines for Characterization of Structural Materials, Composite Materials Handbook*, V. 1, Rev. E, June 1999.

Mindess, S., and Young, F. J., 1981, *Concrete*, Prentice Hall Inc., Englewood Cliffs, N. J., 671 pp.

Mutsuyoshi, H.; Uehara, K.; and Machida, A., 1990, "Mechanical Properties and Design Method of Concrete Beams Reinforced with Carbon Fiber Reinforced Plastics," *Transaction of the Japan Concrete Institute*, Japan Concrete Institute, Tokyo, Japan, V. 12, pp. 231-238.

Nagasaka, T.; Fukuyama, H.; and Tanigaki, M., 1993, "Shear Performance of Concrete Beams Reinforced with FRP Stirrups," *Fiber-Reinforced-Plastic Reinforcement for Concrete Structures*, SP-138, A. Nanni and C. W. Dolan, eds., American Concrete Institute, Farmington Hills, Mich., pp. 789-811.

Nanni, A., ed., 1993a, "Fiber-Reinforced-Plastic (FRP) Reinforcement for Concrete Structures: Properties and Applications," *Developments in Civil Engineering*, Elsevier, V. 42, 450 pp.

Nanni, A., 1993b, "Flexural Behavior and Design of Reinforced Concrete Using FRP Rods," *Journal of Structural Engineering*, V. 119, No. 11, pp. 3344-3359.

Nanni, A.; Al-Zahrani, M.; Al-Dulaijan, S.; Bakis, C. E.; and Boothby, T. E., 1995, "Bond of FRP Reinforcement to Concrete—Experimental Results," *Proceedings of the Second International RILEM Symposium on Non-Metallic (FRP) Reinforcement for Concrete Structures (FRPRCS-2)*, Ghent, Belgium, pp. 135-145.

Nanni, A.; Bakis, C. E.; and Boothby, T. E., 1995, "Test Methods for FRP-Concrete Systems Subjected to Mechanical Loads: State of the Art Review," *Journal of Reinforced Plastics and Composites*, V. 14, pp. 524-588.

Nanni, A., and Dolan, C. W., eds., 1993, *Fiber-Reinforced-Plastic Reinforcement for Concrete Structures*, SP-138, American Concrete Institute, Farmington Hills, Mich., 977 pp.

Nanni, A.; Nenninger, J.; Ash, K.; and Liu, J., 1997, "Experimental Bond Behavior of Hybrid Rods for Concrete

Reinforcement," *Structural Engineering and Mechanics*, V. 5, No. 4, pp. 339-354.

Nanni, A.; Rizkalla, S.; Bakis, C. E.; Conrad, J. O.; and Abdelrahman, A. A., 1998, "Characterization of GFRP Ribbed Rod Used for Reinforced Concrete Construction," *Proceedings of the International Composites Exhibition (ICE-98)*, Nashville, Tenn., pp. 16A/1-6.

National Research Council, 1991, "Life Prediction Methodologies for Composite Materials," *Committee on Life Prediction Methodologies for Composites*, NMAB-460, National Materials Advisory Board, Washington, D.C., 66 pp.

Neale, K.W., and Labossiere, P., eds., 1992, "Advanced Composite Materials in Bridges and Structures," *Proceedings of the First International Conference (ACMBS-I)*, Sherbrooke, Canada, 705 pp.

Noritake, K.; Kakihara, R.; Kumagai, S.; and Mizutani, J., 1993, "Technora, an Aramid FRP Rod," *Fiber-Reinforced-Plastic (FRP) Reinforcement for Concrete Structures: Properties and Applications, Developments in Civil Engineering*, V. 42, A. Nanni, ed., Elsevier, Amsterdam, pp. 267-290.

Odagiri, T.; Matsumoto, K.; and Nakai H., 1997, "Fatigue and Relaxation Characteristics of Continuous Aramid Fiber Reinforced Plastic Rods," *Third International Symposium on Non-Metallic (FRP) Reinforcement for Concrete Structures (FRPRCS-3)*, Japan Concrete Institute, Tokyo, Japan, V. 2, pp. 227-234.

Okamoto, T.; Matsubara, S.; Tanigaki, M.; and Jasuo, K., 1993, "Practical Application and Performance of PPC Beams Reinforced with Braided FRP Bars," *Proceedings Fiber-Reinforced-Plastic Reinforcement for Concrete Structures*, SP-138, A. Nanni, and C. W. Dolan, eds., American Concrete Institute, Farmington Hills, Mich., pp. 875-894.

Okamoto, T.; Nagasaka, T.; and Tanigaki, M., 1994, "Shear Capacity of Concrete Beams Using FRP Reinforcement," *Journal of Structural Construction Engineering*, No. 455, pp. 127-136.

Orangun, C.; Jirsa, J. O.; and Breen, J. E., 1977, "A Reevaluation of Test Data on Development Length and Splices," *ACI JOURNAL*, *Proceedings* V. 74, No. 3, Mar., pp. 114-122.

Plecnik, J., and Ahmad, S. H., 1988, "Transfer of Composite Technology to Design and Construction of Bridges," *Final Report to USDOT*, Contract No. DTRS 5683-C000043.

Pleimann, L. G., 1987, "Tension and Bond Pullout Tests of Deformed Fiberglass Rods," *Final Report for Marshall-Vega Corporation*, Marshall, Arkansas, Civil Engineering Department, University of Arkansas, Fayetteville, Ark., pp. 5-11.

Pleimann, L. G., 1991, "Strength, Modulus of Elasticity, and Bond of Deformed FRP Rods," *Proceedings of the Specialty Conference on Advanced Composite Materials in Civil Engineering Structures*, Material Engineering Division, American Society of Civil Engineers, pp. 99-110.

Porter, M. L., and Barnes, B. A., 1998, "Accelerated Aging Degradation of Glass Fiber Composites," *2nd International Conference on Composites in Infrastructure*, V. II, H. Saadatmanesh and M. R. Eshani, eds., University of Arizona, Tucson, Ariz. pp. 446-459.

Porter, M. L.; Hughes, B. W.; Barnes, B. A.; and Viswanath, K. P., 1993, "Non-Corrosive Tie Reinforcing and Dowel Bars for Highway Pavement Slabs," *Report No. HR-343*, Iowa Highway Research Board and Iowa Department of Transportation, Ames, Iowa.

Porter, M. L.; Mehus, J.; Young, K. A.; O'Neil, E. F.; and Barnes, B. A., 1997, "Aging for Fiber Reinforcement in Concrete," *Non-Metallic (FRP) Reinforcement for Concrete Structures (FRPRCS-3)*, V. 2, Japan Concrete Institute, Tokyo, pp. 59-66.

Portland Cement Association (PCA), 1990, "Concrete Floors on Ground," revised edition, Skokie, Ill., 36 pp.

Post-Tensioning Institute, 1983, *Design and Construction of Post-Tensioned Slabs on Grade*, Phoenix, Ariz.

Priestley, M. N.; Seible, F.; and Calvi, G. M., 1996, *Seismic Design and Retrofit of Bridges*, John Wiley and Sons, New York, N.Y., 704 pp.

Rahman, A. H., and Kingsley, C. Y., 1996, "Fatigue Behavior of a Fiber-Reinforced-Plastic Grid as Reinforcement for Concrete," *Proceedings of the First International Conference on Composites in Infrastructure (ICCI-96)*, H. Saadatmanesh and M. R. Ehsani, eds., Tucson, Ariz., pp. 427-439.

Rahman, H.; Adimi, R.; and Crimi, J., 1997, "Fatigue Behavior of a Carbon FRP Grid Encased in Concrete," *Proceedings of the Third International Symposium on Non-Metallic (FRP) Reinforcement for Concrete Structures (FRPRCS-3)*, Japan Concrete Institute, Sapporo, Japan, V. 2, pp. 219-226.

Rahman, A. H.; Kingsley, C. Y.; and Crimi, J., 1996, "Durability of FRP Grid Reinforcement," *Advanced Composite Materials in Bridges and Structures*, M. M. El-Badry, ed., Canadian Society for Civil Engineering, Montreal, Quebec, pp. 681-690.

Rizkalla, S. H., 1997, "A New Generation of Civil Engineering Structures and Bridges," *Proceedings of the Third International Symposium on Non-Metallic (FRP) Reinforcement for Concrete Structures (FRPRCS-3)*, Sapporo, Japan, V. 1, pp. 113-128.

Rostasy, F. S., 1997, "On Durability of FRP in Aggressive Environments," *Non-Metallic (FRP) Reinforcement for Concrete Structures (FRPRCS-3)*, V. 2, Japan Concrete Institute, Tokyo, pp. 107-114.

Roylance, M., and Roylance, O., 1981, "Effect of Moisture on the Fatigue Resistance of an Aramid-Epoxy Composite," *Organic Coatings and Plastics Chemistry*, American Chemical Society, Washington, D.C., V. 45, pp. 784-788.

Saadatmanesh, H., and Ehsani, M. R., eds., 1998, "Fiber Composites in Infrastructure," *Proceedings of the Second International Conference on Composites in Infrastructure (ICCI-98)*, Tucson, Ariz.

Saadatmanesh, H., and Tannous, F. E., 1999a, "Relaxation, Creep, and Fatigue Behavior of Carbo Fiber-Reinforced Plastic Tendons," *ACI Materials Journal*, V. 96, No. 2, Mar.-Apr., pp. 143-153.

Saadatmanesh, H., and Tannous, F. E., 1999b, "Long-Term Behavior of Aramid Fiber-Reinforced Plastic Tendons," *ACI Materials Journal*, V. 96, No. 3, May-June, pp. 297-305.

- Sakashita, M.; Masuda, Y.; Nakamura, K.; Tanano, H.; Nishida, I.; and Hashimoto, T., 1997, "Deflection of Continuous Fiber Reinforced Concrete Beams Subjected to Loaded Heating," *Proceedings of the Third International Symposium on Non-Metallic (FRP) Reinforcement for Concrete Structures (FRPRCS-3)*, Japan Concrete Institute, Tokyo, Japan, V. 2, pp. 51-58.
- Santoh, N., 1993, "CFCC (Carbon Fiber Composite Cable)," *Fiber-Reinforced-Plastic (FRP) Reinforcement for Concrete Structures: Properties and Applications, Developments in Civil Engineering*, A. Nanni, ed., V. 42, Elsevier, Amsterdam, pp. 223-247.
- Sasaki, I.; Nishizaki, I.; Sakamoto, H.; Katawaki, K.; and Kawamoto, Y., 1997, "Durability Evaluation of FRP Cables by Exposure Tests," *Non-Metallic (FRP) Reinforcement for Concrete Structures (FRPRCS-3)*, V. 2, Japan Concrete Institute, Tokyo, pp. 131-137.
- Scheibe, M., and Rostasy, F. S., 1998, "Stress-Rupture Behavior of AFRP Bars in Concrete and Under Natural Environment," *Second International Conference on Composites in Infrastructure*, V. II, H. Saadatmanesh and M. R. Eshani, eds., University of Arizona, Tucson, Ariz., pp. 138-151.
- Seki, H.; Sekijima, K.; and Konno, T., 1997, "Test Method on Creep of Continuous Fiber Reinforcing Materials," *Proceedings of the Third International Symposium on Non-Metallic (FRP) Reinforcement for Concrete Structures (FRPRCS-3)*, Sapporo, Japan, V. 2, pp. 195-202.
- Sen, R.; Shahawy, M.; Sukumar, S.; and Rosas, J., 1998a, "Effect of Tidal Exposure on Bond of CFRP Rods," *Second International Conference on Composites in Infrastructure*, V. II, H. Saadatmanesh and M. R. Eshani, eds., University of Arizona, Tucson, Ariz., pp. 512-523.
- Sen, R.; Shahawy, M.; Rosas, J.; and Sukumar, S., 1998, "Durability of Aramid Pretensioned Elements in a Marine Environment," *ACI Structural Journal*, V. 95, No. 5, Sept.-Oct., pp. 578-587.
- Sippel, T. M., and Mayer, U., 1996, "Bond Behavior of FRP Strands under Short-Term, Reversed and Cyclic Loading," *Proceedings of the Second International Conference on Advanced Composite Materials in Bridges and Structures (ACMBS-2)*, M. M. El-Badry, ed., Canadian Society for Civil Engineering, Montreal, Quebec, pp. 837-844.
- Sonobe, Y.; Fukuyama, H.; Okamoto, T.; Kani, N.; Kobayashi, K.; Masuda, Y.; Matsuzaki, Y.; Mochizuki, S.; Nagasaka, T.; Shimizu, A.; Tanano, H.; Tanigaki, M., and Tenshigawara, M., 1997, "Design Guidelines of FRP Reinforced Concrete Building Structures," *Journal of Composites for Construction*, V. 1, No. 3, pp. 90-113.
- Tadros, G.; Tromposch, E.; and Mufti, A., 1998, "University Drive/Crowchild Trail Bridge Superstructure Replacement," *Second International Conference on Composites in Infrastructure (ICCI-98)*, Tucson, Ariz., V. 1, pp. 693-704.
- Taerwe, L., ed., 1995, "Non-Metallic (FRP) Reinforcement for Concrete Structures," *Proceedings of the Second International RILEM Symposium (FRPRCS-2)*, Ghent, Belgium, 714 pp.
- Taerwe, L., 1997, "FRP Activities in Europe: Survey of Research and Applications," *Proceedings of the Third International Symposium on Non-Metallic (FRP) Reinforcement for Concrete Structures (FRPRCS-3)*, Sapporo, Japan, V. 1, pp. 59-74.
- Takewaka, K., and Khin, M., 1996, "Deterioration of Stress-Rupture of FRP Rods in Alkaline Solution Simulating as Concrete Environment," *Advanced Composite Materials in Bridges and Structures*, M. M. El-Badry, ed., Canadian Society for Civil Engineering, Montreal, Quebec, pp. 649-664.
- Tamura, T., 1993, "FiBRA," *Fiber-Reinforced-Plastic (FRP) Reinforcement for Concrete Structures: Properties and Applications, Developments in Civil Engineering*, V. 42, A. Nanni, ed., Elsevier, Amsterdam, pp. 291-303.
- Tannous, F. E., and Saadatmanesh, H., 1999, "Durability of AR-Glass Fiber Reinforced Plastic Bars," *Journal of Composites for Construction*, V. 3, No. 1, pp. 12-19.
- Theriault, M., and Benmokrane, B., 1998 "Effects of FRP Reinforcement Ratio and Concrete Strength on Flexural Behavior of Concrete Beams," *Journal of Composites for Construction*, V. 2, No. 1, pp. 7-16.
- Tighiouart, B.; Benmokrane, B.; and Gao, D., 1998, "Investigation of Bond in Concrete Member With Fiber Reinforced Polymer (FRP) Bars," *Construction and Building Materials Journal*, Dec. 1998, p. 10.
- Tokyo Rope, 2000, "CFCC, Carbon Fiber Composite Cable," Product Circular No. 991-2T-SA, Tokyo Rope Manufacturing Co., Tokyo (<http://www.tokyoropeco.jp/>).
- Tomosawa, F., and Nakatsuji, T., 1996, "Evaluation of the ACM Reinforcement Durability by Exposure Test," *Advanced Composite Materials in Bridges and Structures*, M. M. El-Badry, ed., Canadian Society for Civil Engineering, Montreal, Quebec, pp. 699-706.
- Tomosawa, F., and Nakatsuji, T., 1997, "Evaluation of the ACM Reinforcement Durability by Exposure Test," *Non-Metallic (FRP) Reinforcement for Concrete Structures (FRPRCS-3)*, V. 2, Japan Concrete Institute, Tokyo, pp. 139-146.
- Tudos, F., and David, P. K., 1996, "Comments on the Interpretation of Temperature Dependence of Processes in Polymer," *Journal of Thermal Analysis*, Proceedings of the 1995 Symposium on Thermal Analysis, John Wiley & Sons Ltd., Chichester, England, V. 47, No. 2, pp. 589-593.
- Uomoto, T., 2000, "Durability of FRP as Reinforcement for Concrete Structures," *Proceedings of the 3rd International Conference on Advanced Composite Materials in Bridges and Structures, ACMBS-3*, J. L. Humar and A. G. Razaqpur, eds., Canadian Society for Civil Engineering, Montreal, Quebec, pp. 3-17.
- Uppuluri, V. S.; Bakis, C. E.; Nanni, A.; and Boothby, T. E., 1996, "Analysis of the Bond Mechanism in FRP Reinforcement Rods: The Effect of Rod Design and Properties," *Proceedings of the Second International Conference on Advanced Composite Materials in Bridges and Structures (ACMBS-II)*, Montreal, Canada, pp. 893-900.
- Vijay, P. V., and GangaRao, H. V. S., 1996, "Unified Limit State Approach Using Deformability Factors in Concrete

Beams Reinforced with GFRP Bars,” *Proceedings of the Fourth Materials Engineering Conference*, pp. 657-665.

Vijay, P. V., and GangaRao, H. V. S., 1998, “Creep Behavior of Concrete Beams Reinforced with GFRP Bars,” *Proceedings of the First International Conference (CDCC 1998), Durability of Fiber Reinforced Polymer (FRP) Composites for Construction*, pp. 661-667.

Vijay, P. V., and GangaRao, H. V. S., 1999, “Accelerated and Natural Weathering of Glass Fiber Reinforced Plastic Bars,” *Fiber Reinforced Polymer Reinforcement for Reinforced Concrete Structures*, SP-188, C. W. Dolan, S. H. Rizkalla, and A. Nanni, eds., American Concrete Institute, Farmington Hills, Mich., pp. 605-614.

Vijay, P. V.; GangaRao, H. V. S.; and Kalluri, R., 1998, “Hygrothermal Response of GFRP Bars under Different Conditioning Schemes,” *Proceedings of the First International Conference (CDCC 1998)*, Sherbrooke, Canada, pp. 243-252.

Wang, C. K., and Salmon, C. G., 1992, *Reinforced Concrete Design*, 5th Edition, Harper Collins Publication Inc., pp. 1030.

Wang, J., 1998, “Determination of the Shear Resistance of Concrete Beams and Slabs Reinforced with Fibre Reinforced Plastics,” MS thesis, Carleton University, Ottawa, Canada.

Wang, N., and Evans, J. T., 1995, “Collapse of Continuous Fiber Composite Beam at Elevated Temperatures,” *Composites*, V. 26, No. 1, pp. 56-61.

White, T. D., ed., 1992, “Composite Materials and Structural Plastics in Civil Engineering Construction,” *Proceedings of the Materials Engineering Congress*, American Society of Civil Engineers, New York, N.Y., pp. 532-718.

Wu, W.-P., 1990, “Thermomechanical Properties of Fiber Reinforced Plastics (FRP) Bars,” PhD dissertation, West Virginia University, Morgantown, W.Va., 292 pp.

Yamaguchi, T.; Kato, Y.; Nishimura, T.; and Uomoto, T., 1997, “Creep Rupture of FRP Rods Made of Aramid, Carbon and Glass Fibers,” *Proceedings of the Third International Symposium on Non-Metallic (FRP) Reinforcement for Concrete Structures (FRPRCS-3)*, Japan Concrete Institute, Sapporo, Japan, V. 2, pp. 179-186.

Zhao, W.; Maruyama, K.; and Suzuki, H., 1995, “Shear Behavior of Concrete Beams Reinforced by FRP Rods as Longitudinal and Shear Reinforcement,” *Proceedings of the Second International RILEM Symposium on Non-Metallic (FRP) Reinforcement for Concrete Structures (FRPRCS-2)*, Ghent, Belgium, pp. 352-359.

Zhao, W.; Pilakoutas, K.; and Waldron, P., 1997, “FRP Reinforced Concrete Beams: Calculations For Deflection,” *Proceedings of the Third International Symposium on Non-Metallic (FRP) Reinforcement for Concrete Structures (FRPCS-3)*, Japan Concrete Institute, Sapporo, Japan, V. 2, pp. 511-518.

PART 5—DESIGN EXAMPLES

EXAMPLE 1—BEAM DESIGN EXAMPLE

A simply supported, normalweight concrete beam with $f'_c = 4000$ psi (27.6 MPa) is needed in a medical facility to support an MRI unit. The beam is an interior beam. The beam is to be designed to carry a service live load of $w_{LL} = 400$ lb/ft (5.8 kN/m) and a superimposed service dead load of $w_{SDL} = 208$ lb/ft (3.0 kN/m) over a span of $l = 11$ ft (3.35 m). The beam deflection should not exceed $l/240$, which is the limitation for long-term deflection. Due to construction restriction, the depth of the member should not exceed 14 in. (356 mm).

Table E1.1—Manufacturer’s reported GFRP bar properties

Tensile strength, f_{fu}^*	90,000 psi	620.6 MPa
Rupture strain, ϵ_{fu}^*	0.014	0.014
Modulus of elasticity, E_f	6,500,000 psi	44,800 MPa

GFRP reinforcing bars are selected to reinforce the beam; material properties of the bars (as reported by the bar manufacturer) are shown in Table E1.1.

The design procedure presented hereafter is equally applicable to other CFRP and AFRP bars.

Procedure	Calculation in U.S. units	Calculation in S.I. units
<p>Step 1—Estimate the appropriate cross-sectional dimensions of the beam. An initial value for the depth of a simply supported reinforced concrete beam can be estimated from Table 8.2 of the ACI 318-95 Building Code.</p> $h = \frac{l}{16}$ <p>Recognizing that the lower stiffness of GFRP reinforcing bars will require greater depth than steel-reinforced concrete for deflection control, a larger overall height is used.</p> <p>The depth of the member is limited to 14 in. max (356 mm)</p> <p>An effective depth of the section is estimated using 1-1/2 in. clear cover</p> $\text{Estimated } d = h - \text{cover} - d_{b,\text{shear}} - \frac{d_b}{2}$	$h = \frac{(11 \text{ ft}) \left(\frac{12 \text{ in.}}{\text{ft}} \right)}{16} = 8.25 \text{ in.}$ <p>Try $h = 12$ in. < 14 in. max</p> <p>Assuming #5 bars for main = $(5/8)" = 0.625$ in. Assuming #3 bars for shear = $(3/8)" = 0.375$ in. Cover = 1.5 in.</p> <p>A minimum width of approximately 7 in. is required when using 2 #5 or 2 #6 bars with #3 stirrups Try $b = 7$ in.</p> $\text{Estimated } d = 12 - 1.5 - 0.375 - \frac{0.625}{2} = 9.81 \text{ in.}$	$h = \frac{(3.35 \text{ m})}{16} = 0.209 \text{ m}$ <p>Try $h = 305$ mm < 356 mm</p> <p>Assuming 2φ16 mm bars for main Assuming φ9.5 mm bars for shear Cover = 38 mm</p> <p>A minimum width of approximately 7 in. is required when using 2φ16 or 2φ19 bars with φ9.5 stirrups Try $b = 0.178$ m</p> $\text{Estimated } d = 0.305 \times 1000 - 38 - 9.5 - \frac{16}{2} = 250 \text{ mm}$
<p>Step 2—Compute the factored load The uniformly distributed dead load can be computed including the self-weight of the beam</p> $w_{DL} = w_{SDL} + w_{SW}$ <p>Compute the factored uniform load and ultimate moment</p> $w_u = 1.4w_{DL} + 1.7w_{LL}$ $M_u = \frac{w_u l^2}{8}$	$w_{DL} = 208 \frac{\text{lb}}{\text{ft}} + \frac{(7 \text{ in.})(12 \text{ in.})}{\left(\frac{12 \text{ in.}}{\text{ft}} \right)^2} (150 \text{ pcf}) = 295.5 \frac{\text{lb}}{\text{ft}}$ $w_u = 1.4 \left(295.5 \frac{\text{lb}}{\text{ft}} \right) + 1.7 \left(400 \frac{\text{lb}}{\text{ft}} \right) = 1094 \frac{\text{lb}}{\text{ft}}$ $M_u = \frac{\left(1094 \frac{\text{lb}}{\text{ft}} \right) (11 \text{ ft})^2}{8} \cdot \frac{1 \text{ kip}}{1000 \text{ lb}} = 16.5 \text{ kip} \cdot \text{ft}$	$w_{DL} = (3.0 \text{ kN/m}) + (0.178 \text{ m}) (0.305 \text{ m}) (24 \text{ kN/m}^3) = 4.3 \text{ kN/m}$ $w_u = 1.4(4.3 \text{ kN/m}) + 1.7(5.8 \text{ kN/m}) = 15.88 \text{ kN/m}$ $M_u = \frac{(15.88 \text{ kN/m})(3.35 \text{ m})^2}{8} = 22.3 \text{ kN} \cdot \text{m}$
<p>Step 3—Compute the design rupture stress of the FRP bars The beam will be located in an interior conditioned space. Therefore, for glass FRP bars, an environmental reduction factor (C_E) of 0.80 is as per Table 7.1.</p> $f_{fu} = C_E f_{fu}^*$	$f_{fu} = (0.80)(90 \text{ ksi}) = 72 \text{ ksi}$	$f_{fu} = (0.80)(620.6 \text{ MPa}) = 496 \text{ MPa}$
<p>Step 4—Determine the area of GFRP bars required for flexural strength Find the reinforcement ratio required for flexural strength by trial and error using Eq. (8-1), (8-4c), and (8-5). Assume an initial amount of FRP reinforcement</p> $\rho_f = \frac{A_f}{b \cdot d}$	<p>Try 2 #5 bars</p> $\rho_f = \frac{(0.625 \text{ in.}^2)}{(7 \text{ in.})(9.81 \text{ in.})} = 0.009$	<p>Try 2φ16 bars</p> $\rho_f = \frac{(400 \text{ mm}^2)}{(178 \text{ mm})(250 \text{ mm})} = 0.009$

Procedure	Calculation in U.S. units	Calculation in S.I. units
$f_f = \left[\sqrt{\frac{(E_f \epsilon_{cu})^2}{4} + \frac{0.85 \beta_1 f'_c}{\rho_f} E_f \epsilon_{cu} - 0.5 E_f \epsilon_{cu}} \right]$ $M_n = \rho_f f_f \left(1 - 0.59 \frac{\rho_f f_f}{f'_c} \right) b d^2$ <p>Compute the balanced FRP reinforcement ratio</p> $\rho_{fb} = 0.85 \frac{f'_c}{f_{fu}} \beta_1 \frac{E_f \epsilon_{cu}}{E_f \epsilon_{cu} + f_{fu}}$ <p>Compute the strength reduction factor</p> $\phi = \frac{\rho_f}{2 \rho_{fb}} \text{ for } \rho_{fb} < \rho_f \leq 1.4 \rho_{fb}$ <p>Check $\phi M_n \geq M_u$</p>	$f_f = \sqrt{\frac{[6500(0.003)]^2 + 0.85(0.85)(4)}{4} \frac{(0.009)}{(0.009)}} \frac{(0.009)}{\sqrt{(6500)(0.003) - 0.5(6500)(0.003)}}$ $f_f = 70.3 \text{ ksi}$ $M_n = (0.009)(70.3) \left(1 - 0.59 \frac{(0.009)(70.3)}{4} \right) (7)(9.81)^2$ $M_n = 384 \text{ kip} \cdot \text{in.} = 32 \text{ kip} \cdot \text{ft}$ $\rho_{fb} = 0.85 \frac{4}{72} (0.85) \frac{(6500)(0.003)}{(6500)(0.003) + 72} = 0.0086$ $\phi = \frac{0.009}{2(0.0086)} = 0.522$ $\phi M_n = (0.522)(32 \text{ kip} \cdot \text{ft})$ $\phi M_n = 16.7 \text{ kip} \cdot \text{ft} \geq M_u = 16.5 \text{ kip} \cdot \text{ft}$	$f_f = \sqrt{\frac{[44,800(0.003)]^2 + 0.85(0.85)(27.6)}{4} \frac{(0.009)}{(0.009)}} \frac{(0.009)}{\sqrt{(44,800)(0.003) - 0.5(44,800)(0.003)}}$ $f_f = 482.6 \text{ MPa}$ $M_n = (0.009)(482.6) \left(1 - 0.59 \frac{(0.009)(482.6)}{27.6} \right) (178)(250)^2$ $M_n = 43.7 \text{ kN} \cdot \text{m}$ $\rho_{fb} = 0.85 \frac{(27.6)}{(496)} (0.85) \cdot \frac{(44,800)(0.003)}{(44800)(0.003) + (496)} = 0.0086$ $\phi = \frac{0.009}{2(0.0086)} = 0.522$ $\phi M_n = (0.522)(43.7 \text{ kN} \cdot \text{m})$ $\phi M_n = 22.8 \text{ kN} \cdot \text{m} \geq M_u = 22.3 \text{ kN} \cdot \text{m}$
<p>Step 5—Check the crack width. Compute the stress level in the FRP bars under dead load plus live load.</p> $M_{DL} = \frac{\omega_{DL} \dot{f}^2}{8}$ $M_{LL} = \frac{\omega_{LL} \dot{f}^2}{8}$ $M_{DL+LL} = M_{DL} + M_{LL}$ $n_f = \frac{E_f}{E_c} = \frac{E_f}{57,000 \sqrt{f'_c}} \text{ (U.S.)}$ $n_f = \frac{E_f}{E_c} = \frac{E_f}{4750 \sqrt{f'_c}} \text{ (SI)}$ $k = \sqrt{(\rho_f n_f)^2 + 2 \rho_f n_f} - \rho_f n_f$ $f_f = \frac{M_{DL+LL}}{A_d(1 - k/3)}$ <p>Define the effective tension area of concrete.</p> $\beta = \frac{h - kd}{d(1 - k)}$ $d_c = h - d$ $A = \frac{2d_c b}{\text{No. bars}}$ <p>Compare the crack width from Eq. (8-9) using the recommended value of $k_b = 1.2$ for deformed FRP bars</p> $w = \frac{2200}{E_f} \beta k_b f_f^3 \sqrt{d_c A} \text{ (US)}$ $w = \frac{2.2}{E_f} \beta k_b f_f^3 \sqrt{d_c A} \text{ (SI)}$	$M_{DL} = \frac{295.5(11)^2}{8} \cdot \frac{1 \text{ kip}}{1000 \text{ lb}} = 4.47 \text{ kip} \cdot \text{ft}$ $M_{LL} = \frac{400(11)^2}{8} \cdot \frac{1 \text{ kip}}{1000 \text{ lb}} = 6.05 \text{ kip} \cdot \text{ft}$ $M_{DL+LL} = 4.47 + 6.05 = 10.5 \text{ kip} \cdot \text{ft}$ $n_f = \frac{6,500,000 \text{ psi}}{57,000 \sqrt{4000 \text{ psi}}} = 1.8$ $k = \sqrt{[(0.009)(1.8)]^2 + 2(0.009)(1.8)} - 0.009(1.8) = 0.164$ $f_f = \frac{(10.5 \text{ kip} \cdot \text{ft})(12 \text{ in./ft})}{(0.62 \text{ in.}^2)(9.81 \text{ in.})(1 - 0.164/3)} = 22.2 \text{ ksi}$ $\beta = \frac{12 \text{ in.} - (0.164)(9.81 \text{ in.})}{(9.81 \text{ in.})(1 - 0.164)} = 1.267$ $d_c = (12 \text{ in.}) - (9.81 \text{ in.}) = 2.2 \text{ in.}$ $A = \frac{2(2.2 \text{ in.})(7 \text{ in.})}{2} = 15.4 \text{ in.}^2$ $w = \frac{2200}{6500 \text{ ksi}} (1.267)(1.2)(22.2 \text{ ksi}) \sqrt[3]{(2.2 \text{ in.})(15.4 \text{ in.}^2)}$ $w = 37 \text{ mils} > 28 \text{ mils n.g.}$	$M_{DL} = \frac{4.3(3.35)^2}{8} = 6.03 \text{ kN} \cdot \text{m}$ $M_{LL} = \frac{5.8(3.35)^2}{8} = 8.14 \text{ kN} \cdot \text{m}$ $M_{DL+LL} = 6.03 + 8.14 = 14.17 \text{ kN} \cdot \text{m}$ $n_f = \frac{44,800 \text{ MPa}}{4750 \sqrt{27.6 \text{ MPa}}} = 1.8$ $k = \sqrt{[(0.009)(1.8)]^2 + 2(0.009)(1.8)} - 0.009(1.8) = 0.164$ $f_f = \frac{14.17 \times 10^6 \text{ N} \cdot \text{mm}}{(400 \text{ mm}^2)(250 \text{ mm})(1 - 0.164/3)} = 149.9 \text{ MPa}$ $\beta = \frac{305 \text{ mm} - (0.164)(250 \text{ mm})}{(250 \text{ mm})(1 - 0.164)} = 1.263$ $d_c = 305 \text{ mm} - 250 \text{ mm} = 55 \text{ mm}$ $A = \frac{2(55 \text{ mm})(178 \text{ mm})}{2} = 9790 \text{ mm}^2$ $w = \frac{2.2}{44,800 \text{ MPa}} (1.263)(1.2)(149.9 \text{ MPa}) \sqrt[3]{(55 \text{ mm})(9790 \text{ mm}^2)}$ $w = 0.90 \text{ mms} > 0.71 \text{ mm n.g.}$

Procedure	Calculation in U.S. units	Calculation in S.I. units
<p>Crack width limitation controls the design. Try larger amount of FRP reinforcement.</p> $\rho_f = \frac{A_f}{b \cdot d}$ <p>Estimated $d = h - \text{cover} - d_{b, \text{shear}} - \frac{d_b}{2}$</p> <p>Calculate the new capacity.</p> $f_f = \left(\sqrt{\frac{(E_f \epsilon_{cu})^2}{4} + \frac{0.85 \beta_1 f'_c}{\rho_f} E_f \epsilon_{cu} - 0.5 E_f \epsilon_{cu}} \right)$ $M_n = \rho_f f_f \left(1 - 0.59 \frac{\rho_f f_f}{f'_c} \right) b d^2$ <p>$\phi = 0.7$ for $\rho_f \geq 1.4 \rho_{fb}$</p> <p>Check $\phi M_n \geq M_u$</p> $k = \sqrt{(\rho_f n_f)^2 + 2 \rho_f n_f} - \rho_f n_f$ $f_f = \frac{M_{DL+LL}}{A_f d (1 - k/3)}$ $\beta = \frac{h - kd}{d(1 - k)}$ $d_c = h - d$ $A = \frac{2 d_c b}{\text{No. bars}}$ $w = \frac{2200}{E_f} \beta k_b f_f^3 \sqrt{d_c A} \quad (\text{US})$ $w = \frac{2.2}{E_f} \beta k_b f_f^3 \sqrt{d_c A} \quad (\text{SI})$	<p>Note that it is possible to use bars with smaller diameters to mitigate cracking. For example, using three No. 4 bars will result in approximately the same area of FRP and nearly the same effective depth; however, the width of the member should be increased.</p> <p>To maintain $b = 7.0$ in. Try 2#6 $\rightarrow A_f = 0.88$ in.²</p> $\rho_f = \frac{(0.88 \text{ in.}^2)}{(7 \text{ in.})(9.75 \text{ in.})} = 0.0129$ <p>Estimated $d = 12 - 1.5 - 0.375 - \frac{0.75}{2} = 9.75$ in.</p> $f_f = \frac{\sqrt{\frac{[6500(0.003)]^2}{4} + \frac{0.85(0.85)(4)}{(0.0129)}}}{\sqrt{(6500)(0.003) - 0.5(6500)(0.003)}}$ $f_f = 57.1 \text{ ksi}$ $M_n = (0.0129)(57.1) \left(1 - 0.59 \frac{(0.0129)(57.1)}{4} \right) (7)(9.75)^2$ $M_n = 436.9 \text{ kip} \cdot \text{in.} = 36.4 \text{ kip} \cdot \text{ft}$ <p>$\rho_f = 0.0129 > 1.4 \rho_{fb} = 0.012 \rightarrow \phi = 0.7$</p> <p>$\phi M_n = (0.7)(36.4 \text{ kip} \cdot \text{ft})$</p> <p>$\phi M_n = 25.5 \text{ kip} \cdot \text{ft} \geq M_u = 16.5 \text{ kip} \cdot \text{ft}$</p> $k = \sqrt{[(0.0129)(1.8)]^2 + 2(0.0129)(1.8)} - 0.0129(1.8)$ $k = 0.194$ $f_f = \frac{(10.5 \text{ kip} \cdot \text{ft})(12 \text{ in./ft})}{(0.88 \text{ in.}^2)(9.75 \text{ in.})(1 - 0.194/3)} = 15.7 \text{ ksi}$ $\beta = \frac{12 \text{ in.} - 0.194(9.75 \text{ in.})}{(9.75 \text{ in.})(1 - 0.194)} = 1.286$ $d_c = (12 \text{ in.}) - (9.75 \text{ in.}) = 2.25 \text{ in.}$ $A = \frac{2(2.25 \text{ in.})(7 \text{ in.})}{2} = 15.75 \text{ in.}^2$ $w = \frac{2200}{6500 \text{ ksi}} (1.286)(1.2)(15.7 \text{ ksi}) \sqrt[3]{(2.25 \text{ in.})(15.75 \text{ in.}^2)}$ <p>$w = 27$ mils < 28 mils OK</p>	<p>Note that it is possible to use bars with smaller diameters to mitigate cracking. For example, using three No. 4 bars will result in approximately the same area of FRP and nearly the same effective depth; however, the width of the member should be increased.</p> <p>To maintain $b = 0.178$ mm Try 2#19 $\rightarrow A_f = 567$ mm²</p> $\rho_f = \frac{(567 \text{ mm}^2)}{(178 \text{ mm})(248 \text{ mm})} = 0.0129$ <p>Estimated $d = 305 - 38 - 9.5 - \frac{19}{2} = 248$ mm</p> $f_f = \frac{\sqrt{[44,800(0.003)]^2 + \frac{0.85(0.85)(27.6)}{(0.0129)}}}{\sqrt{(44,800)(0.003) - 0.5(44,800)(0.003)}}$ $f_f = 393.5 \text{ MPa}$ $M_n = (0.0129)(393.5) \left(1 - 0.59 \frac{(0.0129)(393.5)}{27.6} \right) (178)(248)^2$ $M_n = 4.95 \times 10^7 \text{ N} \cdot \text{mm} = 49.5 \text{ kN} \cdot \text{m}$ <p>$\rho_f = 0.0129 > 1.4 \rho_{fb} = 0.012 \rightarrow \phi = 0.7$</p> <p>$\phi M_n = (0.7)(49.5 \text{ kN} \cdot \text{m})$</p> <p>$\phi M_n = 34.7 \text{ kN} \cdot \text{m} \geq M_u = 22.3 \text{ kN} \cdot \text{m}$</p> $k = \sqrt{[(0.0129)(1.8)]^2 + 2(0.0129)(1.8)} - 0.0129(1.8)$ $k = 0.194$ $f_f = \frac{14.17 \times 10^{-6} \text{ N} \cdot \text{mm}}{(567 \text{ mm}^2)(248 \text{ mm})(1 - 0.194/3)} = 107.7 \text{ MPa}$ $\beta = \frac{305 \text{ mm} - 0.194(248 \text{ mm})}{248 \text{ mm} - 0.194(248 \text{ mm})} = 1.285$ $d_c = (305 \text{ mm}) - (248 \text{ mm}) = 57 \text{ mm}$ $A = \frac{2(57 \text{ mm})(178 \text{ mm})}{2} = 10,146 \text{ mm}^2$ $w = \frac{2.2}{44,800 \text{ MPa}} (1.285)(1.2)(107.7 \text{ MPa}) \sqrt[3]{(57 \text{ mm})(10,146 \text{ mm}^2)}$ <p>$w = 0.68$ mm < 0.71 mm OK</p>
<p>Step 6—Check the long-term deflection of the beam Compute the gross moment of inertia for the section.</p> $I_g = \frac{bh^3}{12}$ <p>Calculate the cracked section properties and cracking moment</p> $f_r = 7.5 \sqrt{f'_c} \quad (\text{US})$ $f_r = 0.62 \sqrt{f'_c} \quad (\text{SI})$ $M_{cr} = \frac{2 \cdot f_r \cdot I_g}{h}$ $I_{cr} = \frac{bd^3}{3} k^3 + n_f A_f d^2 (1 - k)^2$	$I_g = \frac{(7 \text{ in.})(12 \text{ in.})^3}{12} = 1008 \text{ in.}^4$ $f_r = 7.5 \sqrt{4000} = 474 \text{ psi}$ $M_{cr} = \frac{2(474.34)(1008)}{12} = 79,689 \text{ lb} \cdot \text{in.} = 6.6 \text{ kip} \cdot \text{ft}$ $I_{cr} = \frac{(7)(9.75)^3}{3} (0.194)^3 + 1.8(0.88)(9.75)^2 (1 - 0.194)^2$ $I_{cr} = 114 \text{ in.}^4$	$I_g = \frac{(178 \text{ mm})(305 \text{ mm})^3}{12} = 4.209 \times 10^8 \text{ mm}^4$ $f_r = 0.62 \sqrt{27.6} = 3.25 \text{ MPa}$ $M_{cr} = \frac{2(3.25)(4.209 \times 10^8)}{305} = 8.97 \times 10^6 \text{ N} \cdot \text{mm} = 8.97 \text{ kN} \cdot \text{m}$ $I_{cr} = \frac{(178)(248)^3}{3} (0.194)^3 + 1.8(567)(248)^2 (1 - 0.194)^2$ $I_{cr} = 4.74 \times 10^7 \text{ mm}^4$

Procedure	Calculation in U.S. units	Calculation in S.I. units
<p>Compute the reduction coefficient for deflection using the recommended $\alpha_b = 0.50$</p> $\beta_d = \alpha_b \left[\frac{E_f}{E_s} + 1 \right]$ <p>Compute the deflection due to dead load plus live load</p> $(I_e)_{DL+LL} = \left(\frac{M_{cr}}{M_{DL+LL}} \right)^3 \beta_d I_g + \left[1 - \left(\frac{M_{cr}}{M_{DL+LL}} \right)^3 \right] I_{cr}$ $(\Delta_i)_{DL+LL} = \frac{5M_{DL+LL} \ell^2}{48E_c(I_e)_{DL+LL}}$ <p>Compute the deflection due to dead load alone and live load alone.</p> $(\Delta_i)_{DL} = \frac{w_{DL}}{w_{DL+LL}} (\Delta_i)_{DL+LL}$ $(\Delta_i)_{LL} = \frac{w_{LL}}{w_{DL+LL}} (\Delta_i)_{DL+LL}$ <p>Compute the multiplier for long-term deflection using a $\xi = 2.0$ (recommended by ACI 318 for a duration of more than 5 years)</p> $\lambda = 0.60\xi$ <p>Compute the long-term deflection for 20% sustained live load and compare to long-term deflection limitations</p> $\Delta_{LT} = (\Delta_i)_{LL} + \lambda[(\Delta_i)_{DL} + 0.20(\Delta_i)_{LL}]$ <p>Check Δ_{LT}</p> $\Delta_{LT} \leq \frac{l}{240}$	$\beta_d = 0.50 \left[\frac{6500 \text{ ksi}}{29,000 \text{ ksi}} + 1 \right] = 0.61$ $(I_e)_{DL+LL} = \left(\frac{6.6}{10.5} \right)^3 (0.61)(1008) + \left[1 - \left(\frac{6.6}{10.5} \right)^3 \right] (114)$ $(I_e)_{DL+LL} = 240.7 \text{ in.}^4$ $(\Delta_i)_{DL+LL} = \frac{5(10.5 \text{ kip} \cdot \text{ft})(11 \text{ ft})^2 \left(12 \frac{\text{in.}}{\text{ft}} \right)^3}{48(3605 \text{ ksi})(240.7 \text{ in.}^4)}$ $= 0.26 \text{ in.}$ $(\Delta_i)_{DL} = \frac{292 \frac{\text{lb}}{\text{ft}}}{292 \frac{\text{lb}}{\text{ft}} + 400 \frac{\text{lb}}{\text{ft}}} (0.26 \text{ in.}) = 0.11 \text{ in.}$ $(\Delta_i)_{LL} = \frac{400 \frac{\text{lb}}{\text{ft}}}{292 \frac{\text{lb}}{\text{ft}} + 400 \frac{\text{lb}}{\text{ft}}} (0.26 \text{ in.}) = 0.15 \text{ in.}$ $\lambda = 0.60(2.0) = 1.2$ $\Delta_{LT} = (0.15 \text{ in.}) + 1.2[(0.11 \text{ in.}) + 0.20(0.15 \text{ in.})] = 0.32 \text{ in.}$ $0.32 \text{ in.} \leq \frac{(11 \text{ ft}) \left(12 \frac{\text{in.}}{\text{ft}} \right)}{240} = 0.55 \text{ in. OK}$	$\beta_d = 0.50 \left[\frac{44,800 \text{ MPa}}{200,000 \text{ MPa}} + 1 \right] = 0.61$ $(I_e)_{DL+LL} = \left(\frac{8.97}{14.17} \right)^3 (0.61)(4.209 \times 10^8) + \left[1 - \left(\frac{8.97}{14.17} \right)^3 \right] (4.74 \times 10^7)$ $(I_e)_{DL+LL} = 1.01 \times 10^8 \text{ mm}^4$ $(\Delta_i)_{DL+LL} = \frac{5(14.17 \times 10^6 \text{ N} \cdot \text{mm})(3350 \text{ mm})^2}{48(2.49 \times 10^4 \text{ mm})(1.01 \times 10^8 \text{ mm}^4)}$ $= 6.6 \text{ mm}$ $(\Delta_i)_{DL} = \frac{4.3 \text{ kN/m}}{4.3 \text{ kN/m} + 5.8 \text{ kN/m}} (6.6 \text{ mm}) = 2.8 \text{ mm}$ $(\Delta_i)_{LL} = \frac{5.8 \text{ kN/m}}{4.3 \text{ kN/m} + 5.8 \text{ kN/m}} (6.6 \text{ mm}) = 3.8 \text{ mm}$ $\lambda = 0.60(2.0) = 1.2$ $\Delta_{LT} = (3.8 \text{ mm}) + 1.2[(2.8 \text{ mm}) + 0.20(3.8 \text{ mm})] = 8 \text{ mm}$ $8 \text{ mm} < \frac{3350 \text{ mm}}{240} = 14 \text{ mm OK}$
<p>Step 7—Check the creep rupture stress limits Compute the moment due to all sustained loads (dead load plus 20% of the live load)</p> $M_s = \frac{w_{DL} + 0.20w_{LL}}{w_{DL} + w_{LL}} M_{DL+LL}$ <p>Compute the sustained stress level in the FRP bars</p> $f_{f,s} = \frac{M_s}{A_f d(1 - k/3)}$ <p>Check the stress limits given in Table 8.2 for glass FRP bars</p> $f_{f,s} \leq 0.20 f_{fu}$	$M_s = \frac{292 \frac{\text{lb}}{\text{ft}} + 0.20 \left(400 \frac{\text{lb}}{\text{ft}} \right)}{292 \frac{\text{lb}}{\text{ft}} + 400 \frac{\text{lb}}{\text{ft}}} 10.5 \text{ kip} \cdot \text{ft} = 5.7 \text{ kip} \cdot \text{ft}$ $f_{f,s} = \frac{(5.7 \text{ kip} \cdot \text{ft})(12)}{(0.88 \text{ in.}^2)(9.75 \text{ in.})(1 - 0.194/3)} = 8.52 \text{ ksi}$ $8.52 \text{ ksi} \leq 0.20(72 \text{ ksi}) = 14.4 \text{ ksi}$	$M_s = \frac{4.3 \text{ kN/m} + 0.20(5.8 \text{ kN/m})}{4.3 \text{ kN/m} + 5.8 \text{ kN/m}} 14.17 \text{ kN} \cdot \text{m} = 7.66 \text{ kN} \cdot \text{m}$ $f_{f,s} = \frac{7.66 \times 10^6 \text{ N} \cdot \text{mm}}{(567 \text{ mm}^2)(248 \text{ mm})(1 - 0.194/3)} = 58.2 \text{ MPa}$ $58.2 \text{ MPa} \leq 0.20(496) = 99.2 \text{ MPa}$

Procedure	Calculation in U.S. units	Calculation in S.I. units
<p>Step 8—Design for shear</p> <p>Determine the factored shear demand at a distance d from the support</p> $V_u = \frac{w_u l}{2} - w_u d$	$V_u = \frac{\left(1088 \frac{\text{lb}}{\text{ft}}\right)(11 \text{ ft})}{2} - \left(1088 \frac{\text{lb}}{\text{ft}}\right)\left(\frac{9.75 \text{ in.}}{12 \frac{\text{in.}}{\text{ft}}}\right) = 5.1 \text{ kips}$	$V_u = \frac{(15.88 \text{ kN/m})(3.35 \text{ m})}{2} - (15.88 \text{ kN/m})(0.248) = 22.7 \text{ kN}$
<p>Compute the shear contribution of the concrete for an FRP reinforced member</p> $V_{c,f} = \frac{\rho_f E_f}{90 \beta_{1c} \sqrt{f'_c}} 2 \sqrt{f'_c} b d \text{ (US)}$ $V_{c,f} = \frac{\rho_f E_f}{90 \beta_{1c} \sqrt{f'_c}} \frac{\sqrt{f'_c}}{6} b d \text{ (SI)}$	$V_{c,f} = \frac{0.0129(6500 \text{ ksi}) 2 \sqrt{4000 \text{ psi}}}{90(0.85)(4 \text{ ksi})} (7 \text{ in.})(9.75 \text{ in.}) = 2.37 \text{ kips}$	$V_{c,f} = \frac{0.0129(44,800 \text{ MPa}) \sqrt{27.6 \text{ MPa}}}{90(0.85)(27.6 \text{ MPa})} \frac{\sqrt{27.6 \text{ MPa}}}{6} (178 \text{ mm})(248 \text{ mm}) = 10,580 \text{ N} = 10.58 \text{ kN}$
<p>FRP shear reinforcement will be required. The FRP shear reinforcement will be assumed to be No. 3 closed stirrups oriented vertically. To determine the amount of FRP shear reinforcement required, the effective stress level in the FRP shear reinforcement must be determined. This stress level may be governed by the allowable stress in the stirrup at the location of a bend, which is computed as follows:</p> $f_{fb} = \left(0.05 \frac{r_b}{d_b} + 0.3\right) f_{fu}$	$f_{fb} = \left(0.05 \frac{3(0.375)}{(0.375)} + 0.3\right) (72 \text{ ksi}) = 32.4 \text{ ksi}$	$f_{fb} = \left(0.05 \frac{3(9.5 \text{ mm})}{(9.5 \text{ mm})} + 0.3\right) (496 \text{ MPa}) = 223.2 \text{ MPa}$
<p>The design stress of FRP stirrup is limited to:</p> $f_{fv} = 0.002 E_f \leq f_{fb}$	$f_{fv} = 0.002(6500 \text{ ksi}) = 13 \text{ ksi} \leq 32.4 \text{ ksi}$	$f_{fv} = 0.002(44,800 \text{ MPa}) = 89.6 \text{ MPa} \leq 223.2 \text{ MPa}$
<p>The required spacing of the FRP stirrups can be computed by rearranging Eq. (9-4).</p> $s = \frac{\phi A_f f_{fv} d}{(V_u - \phi V_{c,f})}$	$s = \frac{0.85(2 \times 0.11 \text{ in.}^2)(13 \text{ ksi})(9.75 \text{ in.})}{(5.1 \text{ kips} - 0.85 \times 2.37 \text{ kips})} = 7.6 \text{ in.}$	$s = \frac{0.85(2 \times 71 \text{ mm}^2)(89.6 \text{ MPa})(248 \text{ mm})}{(22,700 \text{ N} - 0.85 \times 10,580 \text{ N})} = 196 \text{ mm}$
<p>Equation (9-7) for minimum amount of shear reinforcement can be rearranged as $s \leq A_{fv} f_{fv} / 50 b_w$ (US) = $A_{fv} f_{fv} / 0.35 b_w$ (SI).</p>	$s \leq (2 \times 0.11 \text{ in.}^2)(13,000 \text{ psi}) / (50)(7 \text{ in.}) = 8.17 \text{ in.}$	$s \leq (2 \times 71 \text{ mm}^2)(89.6 \text{ MPa}) / (0.35)(178 \text{ mm}) = 204 \text{ mm}$
<p>Check maximum spacing limit = $d/2$</p>	$d/2 = 9.75/2 = 4.875 \text{ in.} < 7.6 \text{ in.}$	$d/2 = 248/2 = 124 \text{ mm} < 196 \text{ mm}$

EXAMPLE 2—DEVELOPMENT LENGTH EXAMPLE

An interior simply supported normalweight concrete beam with $b = 9 \text{ in.}$ (229 mm), $h = 16 \text{ in.}$ (406 mm), and $f'_c = 4000 \text{ psi}$ (27.6 MPa) is supported by 8 in. (203 mm) masonry walls on each end and spans 10 ft (3.05 m) (center-to-center of wall) (Fig. E2.1). The beam carries a service live load of $w_{LL} = 2850 \text{ lb/ft}$ (41.6 kN/m) and a service dead load of $w_{SDL} = 1288 \text{ lb/ft}$ (18.8 kN/m) (including the self-weight of the beam). The beam is reinforced with three No. 6 (3φ19) CFRP reinforcing bars for flexure giving a nominal moment capacity of $M_n = 126.7 \text{ kip-ft}$ (171.8 kN.m); material properties of the bars (as reported by the bar manufacturer) are shown in Table E2.1.

The longitudinal reinforcement needs to be detailed after checking the development length; 1.5 in. (38 mm) clear cover is provided and No. 4 (φ13) FRP stirrups are used for shear reinforcement.

Table E2.1—CFRP bar properties reported by the manufacturer

Tensile strength, f_{fu}^*	240 ksi	1655 MPa
Rupture strain, ϵ_{fu}^*	0.012	0.012
Modulus of elasticity, E_f	20,000 ksi	137.9 GPa

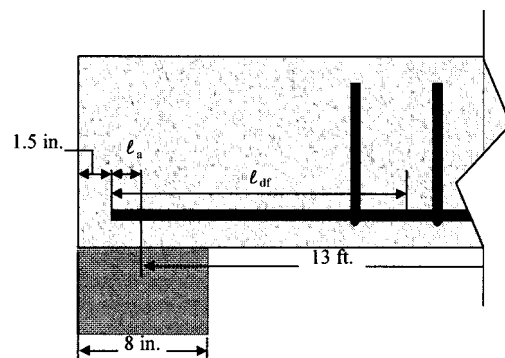
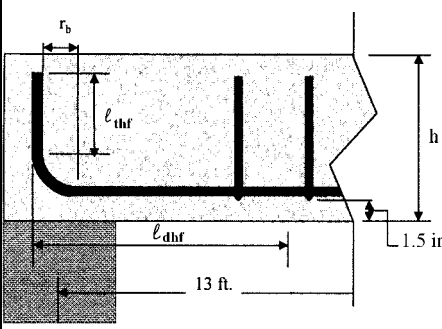


Fig. E2.1—Geometry of the beam near its support.

Procedure	Calculation in U.S. units	Calculation in S.I. units
<p>Step 1—Compute the design material properties of the FRP bars</p>		
<p>The beam will be located in an interior conditioned space. Therefore, using Table 7.1 for CFRP bars, an environmental reduction factor of 1.0 is recommended.</p>		
$f_{fu} = C_E f_{fu}^*$	$f_{fu} = (1.0)(240 \text{ ksi}) = 240 \text{ ksi}$	$f_{fu} = (1.0)(1655 \text{ MPa}) = 1655 \text{ MPa}$
<p>Step 2—Calculate the development length of a straight bar</p>		
<p>The basic development length of a straight bar can be computed as follows:</p>		
$l_{bf} = \frac{d_b f_{fu}}{2700} \text{ U.S. units}$	$l_{bf} = \frac{(0.75 \text{ in.})(240,000 \text{ psi})}{2700} = 67 \text{ in.}$	
$l_{bf} = \frac{d_b f_{fu}}{18.5} \text{ SI units}$		$l_{bf} = \frac{(19 \text{ mm})(1655 \text{ MPa})}{18.5} = 1.7 \text{ m}$
<p>The reinforcement is located in the bottom of the beam, and the cover and spacing are both larger than d_b. Therefore, the multiplication factors on the basic development length are all 1.0, and the development length of a straight bar can be computed as follows:</p>		
$l_{df} = k_m l_{bf}$	$l_{df} = 67 \text{ in.} \times 1.0 = 67 \text{ in.}$	$l_{df} = 1.70 \text{ m} \times 1.0 = 1.70 \text{ m}$
<p>Step 3—Determine the length of bar available for development</p>		
<p>The available development length is the smaller of 1/2 of the span or $1.3M_n/V_u + l_a$. The factored shear demand at the middle of the support needs to be computed.</p>		
$V_u = \frac{(1.4w_{DL} + 1.7w_{LL})l}{2}$	$V_u = \frac{\left[1.4\left(1288 \frac{\text{lb}}{\text{ft}}\right) + 1.7\left(2850 \frac{\text{lb}}{\text{ft}}\right)\right](10 \text{ ft})}{2} = 33.2 \text{ kips}$	$V_u = \frac{[1.4(18.8 \text{ kN/m}) + 1.7(41.6 \text{ kN/m})](3.05 \text{ m})}{2} = 148.0 \text{ kN}$
<p>The distance from the end of the bar to the middle of the support can be found from Fig. E2.1</p>	$l_a = 0.50(8 \text{ in.}) - 1.5 \text{ in.} = 2.5 \text{ in.}$	$l_a = 0.50(203 \text{ mm}) - 38 \text{ mm} = 64 \text{ mm}$
<p>The available development length is computed as the lesser of the following two criteria:</p>		
$\frac{l}{2} + l_a$	$\frac{(10 \text{ ft})\left(12 \frac{\text{in.}}{\text{ft}}\right)}{2} + 2.5 \text{ in.} = 62.5 \text{ in.}$	$\frac{(305 \text{ m})}{2} + 0.064 \text{ m} = 1.59 \text{ m}$
$\frac{1.3M_n}{V_u} + l_a$	$\frac{1.3(126.7 \text{ kip} \cdot \text{ft})\left(12 \frac{\text{in.}}{\text{ft}}\right)}{(33.2 \text{ kip})} + 2.5 \text{ in.} = 62 \text{ in.} \leftarrow$	$\frac{1.3(171.8 \text{ kN} \cdot \text{m})}{(148.0 \text{ kN})} + 0.064 \text{ m} = 1.57 \text{ m} \leftarrow$
	<p style="text-align: center;">Controls</p>	<p style="text-align: center;">Controls</p>
	$l_{df} = 67 \text{ in.} > 62 \text{ in.} \therefore \text{A hooked end will be required}$	$l_{df} = 1.70 \text{ m} > 1.57 \text{ m} \therefore \text{A hooked end will be required}$
<p>Step 4—Determine the development length of a hooked bar</p>		
<p>The basic development length of a hooked bar can be computed as the largest of the following three criteria:</p>		
$l_{bhf} = 4000 \frac{d_b}{\sqrt{f'_c}} \text{ for } f_{fu} \geq 150,000 \text{ psi (U.S.)}$	$l_{bhf} = 4000 \frac{(0.75 \text{ in.})}{\sqrt{4000 \text{ psi}}} = 47 \text{ in.} \leftarrow \text{Controls}$	$l_{bhf} = 330 \frac{(19 \text{ mm})}{\sqrt{27.6 \text{ MPa}}} = 1193 \text{ mm} \leftarrow \text{Controls}$
$l_{bhf} = 330 \frac{d_b}{\sqrt{f'_c}} \text{ for } f_{fu} \geq 1040 \text{ MPa (SI units)}$	$l_{bhf} = 12(0.75 \text{ in.}) = 9 \text{ in.}$	$l_{bhf} = 12(19 \text{ mm}) = 228 \text{ mm}$
$l_{bhf} = 12d_b$	$l_{bhf} = 9 \text{ in.}$	$l_{bhf} = 229 \text{ mm}$
$l_{bhf} = 9 \text{ in. (U.S.)} = 229 \text{ mm (SI)}$	$l_{bhf} = 47 \text{ in.} < 62 \text{ in.}$	$l_{bhf} = 1193 \text{ mm} \leq 1570 \text{ mm}$
<p>Step 5—Determine if the depth of the beam is adequate for the hook</p>		
<p>The geometry of the hook is shown in the following figure:</p>		

Procedure	Calculation in U.S. units	Calculation in S.I. units
 <p>The length of the hook tail and the radius of the bend can be computed as follows:</p> $l_{thf} = 12d_b$ $r_b = 3d_b$ <p>From the geometry shown in the figure, the cover to the end of the hook tail can be determined</p>	$l_{thf} = 12(0.75 \text{ in.}) = 9 \text{ in.}$ $r_b = 3(0.75 \text{ in.}) = 2.25 \text{ in.}$ <p>16 in. {h} - 1.5 in. {cvr} - 0.5 in. {stirrup} - 0.75 in. {long.bar} - 2.25 in. {r_b} - 9 in. {l_thf} = 2.0 in. is adequate to cover the end of the hook tail.</p>	$l_{thf} = 12(19 \text{ mm}) = 228 \text{ mm}$ $r_b = 3(19 \text{ mm}) = 57 \text{ mm}$ <p>381 mm {h} - 38 mm {cvr} - 13 mm {stirrup} - 19 mm {long.bar} - 57 mm {r_b} - 228 mm {l_thf} = 50 mm is adequate to cover the end of the hook tail.</p>

APPENDIX A—TEST METHOD FOR TENSILE STRENGTH AND MODULUS OF FRP BARS

The following is the summary of a test method developed by ACI Committee 440 for tensile strength and modulus of FRP bars. The proposed test method has been submitted to ASTM Subcommittee D-20-18.01, Reinforced Thermosetting Plastics for Approval and Standardization.

This test method is used to determine the tensile properties of FRP bars used in place of steel reinforcing bars in concrete. This test method for obtaining the tensile strength and modulus is intended for use in laboratory tests in which the principal variable is the size or type of FRP bars. The test method focuses on the FRP bar, excluding the performance of the anchorage. Therefore, tests that fail at an anchoring section are disregarded, and the test findings are based on test bars that fail in the test section.

Test specimen

The length of the test bar is defined as the sum of the length of the test section and the lengths of the anchoring sections. The length of the test section is determined from the greater of 4 in. (100 mm) or 40 times the nominal diameter of the FRP bar.

At least five FRP bars are tested. If a bar is found to have failed at an anchoring section, or to have slipped out of an anchoring section, an additional test is performed on a separate bar taken from the same lot.

Test equipment and setup

The testing machine needs to have a loading capacity in excess of the tensile capacity of the test bar and needs to be capable of applying loading at a specific loading rate.

The anchorage needs to be suitable for the geometry of the bar and needs to have the capacity to transmit the loads capable of causing the bar to fail at the test section. The anchorage is constructed so as to transmit loads reliably from the testing machine to the test section, transmitting only axial

loads to the bar, without transmitting either torsion or flexural moment. When mounting the bar on the testing machine, the longitudinal axis of the test specimen should coincide with the imaginary line joining the two anchorages fitted to the testing machine.

Extensometers and strain gages used to measure the elongation of the bar under loading need to be capable of recording all variations in the gage length or elongation during testing with a strain measurement accuracy of at least 10×10^{-6} .

Test method

To determine Young’s modulus and the ultimate strain of the bar, an extensometer or strain gage is mounted in the center of the test section at a distance from the anchorage of at least eight times the nominal diameter of the FRP bar. The extensometer or strain gage needs to be properly aligned with the direction of tension. The gage length when using an extensometer is at least eight times the nominal diameter of the FRP bar.

The rate of loading should be such that the stress in the FRP bar is between 14.5 and 72.5 ksi (100 and 500 MPa) per min. If a strain control type of testing machine is used, the load should be applied to the bar at a fixed rate such that the strain in the FRP bar corresponds to the stress between 14.5 and 72.5 ksi (100 and 500 MPa).

The load is increased until tensile failure, and the strain measurements are recorded until the load reaches at least 60% of the tensile strength.

Calculations

The material properties of the FRP bar are based on at least five FRP bars failing in tension without slipping at the anchorages or rupturing near the anchorages.

The tensile strength is calculated according the equation below with a precision to three significant digits.

$$f_u = F_u/A$$

where

f_u = tensile strength, psi;

F_u = ultimate tensile capacity, lb; and

A = nominal cross-sectional area of test bar, in.².

The tensile stiffness and Young's modulus are calculated from the difference between the load-strain curve values at 20% and 60% of the tensile capacity, obtained from the extensometer or strain gage readings according to the equations below and with a precision to three significant digits. For FRP bars where a tensile strength is given, the values at 20% and 60% of the tensile strength may be used.

$$EA = \Delta F / \Delta \epsilon$$

$$E = \alpha \frac{l}{A}$$

where

EA = tensile stiffness, lb;

E = Young's modulus, psi;

ΔF = difference between the loads at 20% and 60% of the ultimate tensile capacity, lb;

$\Delta \epsilon$ = difference between the strains at 20% and 60% of the ultimate tensile capacity;

α = slope of the load-displacement curve between 20% and 60% of the ultimate capacity, lb/in.; and

l = original gage length, in.

The ultimate strain is the strain corresponding to the tensile strength when the strain gage measurements of the test bar are available up to failure. If extensometer or strain gage measurements are not available up to failure, the ultimate strain can be calculated from the tensile strength and Young's modulus according to the equation below with a precision to three significant digits.

$$\epsilon_u = \frac{F_u}{EA}$$

where ϵ_u = ultimate strain.

APPENDIX B—AREAS OF FUTURE RESEARCH

As pointed out in the body of the document, future research is needed to provide information in areas that are still unclear or are in need of additional evidence to validate performance. The list of topics presented in this appendix has the purpose of providing a summary.

Materials

- Confirmation of normal (Gaussian) distribution to represent the tensile strength of a population of FRP bar specimens.
- Behavior of FRP reinforced member under elevated temperatures.
- Minimum concrete cover requirement for fire resistance.

- Fire rating of concrete members reinforced with FRP bars.
- Effect of transverse expansion of FRP bars on cracking and spalling of concrete cover.
- Creep rupture behavior and endurance times of FRP bars.
- End treatment requirements of saw-cut FRP bars.
- Strength and stiffness degradation of FRP bars in harsh environment.

Flexure/axial force

- Behavior of FRP reinforced concrete compression members.
- Behavior of flexural members with tension and compression FRP reinforcement.
- Design and analysis of concrete non-rectangular sections reinforced with FRP bars.
- Maximum crack width and deflection prediction and control of concrete reinforced with FRP bars.
- Minimum depth of FRP reinforced concrete flexural members for deflection control.
- Long-term deflection behavior of concrete flexural members reinforced with FRP bars.

Shear

- Concrete contribution to shear resistance of members reinforced with FRP bars.
- Failure modes and reinforcement limits of concrete members reinforced with FRP stirrups.
- Use of FRP bars for punching shear reinforcement in two-way systems.

Detailing

- Standardized classification of surface deformation patterns.
- Effect of surface characteristics of FRP bars on bond behavior.
- Lap splices requirement of FRP reinforcement.
- Minimum FRP reinforcement for temperature and shrinkage cracking control.

Structural systems/elements

- Behavior of concrete slabs on ground reinforced with FRP bars.

The design guide specifically indicated that test methods are needed to determine the following properties of FRP bars:

- Bond characteristics and related bond-dependent coefficients.
- Creep rupture and endurance times.
- Fatigue characteristics.
- Coefficient of thermal expansion.
- Durability characterization with focus on alkaline environment and determination of related environmental reduction factor.
- Strength of the bent portion.
- Shear strength.
- Compressive strength.